

1996

# Single cell analysis by capillary electrophoresis with laser-induced native fluorescence detection

Sheri Joanne Lillard  
*Iowa State University*

Follow this and additional works at: <https://lib.dr.iastate.edu/rtd>

 Part of the [Analytical Chemistry Commons](#), [Biochemistry Commons](#), and the [Cell Biology Commons](#)

## Recommended Citation

Lillard, Sheri Joanne, "Single cell analysis by capillary electrophoresis with laser-induced native fluorescence detection " (1996). *Retrospective Theses and Dissertations*. 11160.  
<https://lib.dr.iastate.edu/rtd/11160>

This Dissertation is brought to you for free and open access by the Iowa State University Capstones, Theses and Dissertations at Iowa State University Digital Repository. It has been accepted for inclusion in Retrospective Theses and Dissertations by an authorized administrator of Iowa State University Digital Repository. For more information, please contact [digirep@iastate.edu](mailto:digirep@iastate.edu).

## INFORMATION TO USERS

This manuscript has been reproduced from the microfilm master. UMI films the text directly from the original or copy submitted. Thus, some thesis and dissertation copies are in typewriter face, while others may be from any type of computer printer.

**The quality of this reproduction is dependent upon the quality of the copy submitted.** Broken or indistinct print, colored or poor quality illustrations and photographs, print bleedthrough, substandard margins, and improper alignment can adversely affect reproduction.

In the unlikely event that the author did not send UMI a complete manuscript and there are missing pages, these will be noted. Also, if unauthorized copyright material had to be removed, a note will indicate the deletion.

Oversize materials (e.g., maps, drawings, charts) are reproduced by sectioning the original, beginning at the upper left-hand corner and continuing from left to right in equal sections with small overlaps. Each original is also photographed in one exposure and is included in reduced form at the back of the book.

Photographs included in the original manuscript have been reproduced xerographically in this copy. Higher quality 6" x 9" black and white photographic prints are available for any photographs or illustrations appearing in this copy for an additional charge. Contact UMI directly to order.

# UMI

A Bell & Howell Information Company  
300 North Zeeb Road, Ann Arbor MI 48106-1346 USA  
313/761-4700 800/521-0600



Single cell analysis by capillary electrophoresis  
with laser-induced native fluorescence detection

by

Sheri Joanne Lillard

A dissertation submitted to the graduate faculty  
in partial fulfillment of the requirements for the degree of

DOCTOR OF PHILOSOPHY

Department: Chemistry

Major: Analytical Chemistry

Major Professor: Edward S. Yeung

Iowa State University

Ames, Iowa

1996

**UMI Number: 9626048**

---

**UMI Microform 9626048  
Copyright 1996, by UMI Company. All rights reserved.**

**This microform edition is protected against unauthorized  
copying under Title 17, United States Code.**

---

**UMI**  
**300 North Zeeb Road**  
**Ann Arbor, MI 48103**

Graduate College  
Iowa State University

This is to certify that the Doctoral dissertation of

Sheri Joanne Lillard

has met the dissertation requirements of Iowa State University

Signature was redacted for privacy.

**Major Professor**

Signature was redacted for privacy.

**For the Major Department**

Signature was redacted for privacy.

**For the Graduate College**

## TABLE OF CONTENTS

ACKNOWLEDGMENTS .....	vi
ABSTRACT.....	viii
GENERAL INTRODUCTION.....	1
Dissertation Organization .....	1
Single Cell Analysis.....	1
References.....	2
CHAPTER 1. CAPILLARY ELECTROPHORESIS FOR THE ANALYSIS OF SINGLE CELLS: LASER-INDUCED FLUORESCENCE DETECTION .....	3
INTRODUCTION .....	3
CAPILLARY ELECTROPHORESIS OF SINGLE CELLS.....	4
Preparation of Cell Suspension Solution .....	4
Cell Injection.....	4
Electrokinetic .....	6
Vacuum .....	6
Cell Lysis .....	6
LASER-INDUCED FLUORESCENCE--GENERAL INSTRUMENTATION .....	9
NATIVE FLUORESCENCE.....	10
Insulin in Pancreatic $\beta$ -Cells.....	10
Catecholamines in Adrenal Medullary Cells .....	11
DERIVATIZATION .....	12
Pre-Column Reaction.....	13
Adrenal Medullary Cells.....	13
Neurons .....	14
Helix aspersa .....	14
Aplysia californica.....	14
Erythrocytes .....	15
Post-Column Reaction .....	16
INDIRECT FLUORESCENCE.....	17
Sodium and Potassium.....	18
Lactate and Pyruvate.....	19
FLUORESCENT ENZYME ASSAY.....	19

Erythrocytes .....	20
Lactate Dehydrogenase (LDH) .....	20
Glucose-6-Phosphate Dehydrogenase (G6PDH) .....	21
Lymphocytes and Lymphoblastic Leukemia Cells.....	21
THE FUTURE OF SINGLE-CELL ANALYSIS BY CE-LIF.....	22
Present Limitations .....	22
Further Improvements.....	23
Multiplexing.....	23
Automation .....	23
Future Directions .....	23
ACKNOWLEDGMENT.....	24
REFERENCES .....	24

CHAPTER 2. SEPARATION OF HEMOGLOBIN VARIANTS IN SINGLE HUMAN ERYTHROCYTES BY CAPILLARY ELECTROPHORESIS WITH LASER-INDUCED NATIVE FLUORESCENCE DETECTION .....	28
--	----

ABSTRACT.....	28
INTRODUCTION .....	28
EXPERIMENTAL.....	31
RESULTS .....	32
Electrophoretic Separation.....	32
Effect of Cell Suspension Solution .....	44
Capillary Life .....	44
CONCLUSIONS.....	45
ACKNOWLEDGMENTS .....	46
REFERENCES .....	46

CHAPTER 3. ANALYSIS OF SINGLE ERYTHROCYTES BY INJECTION-BASED CAPILLARY ISOELECTRIC FOCUSING WITH LASER-INDUCED NATIVE FLUORESCENCE DETECTION .....	48
---	----

ABSTRACT.....	48
INTRODUCTION .....	49
EXPERIMENTAL.....	51
RESULTS .....	52
Hemoglobin Separations.....	52
Linearity of the pH Gradient.....	56
CONCLUSIONS.....	67



ACKNOWLEDGMENTS .....	68
REFERENCES .....	68
CHAPTER 4. MONITORING EXOCYTOSIS AND RELEASE OF SEROTONIN FROM INDIVIDUAL MAST CELLS BY CAPILLARY ELECTROPHORESIS WITH LASER-INDUCED NATIVE FLUORESCENCE DETECTION .....	70
ABSTRACT.....	70
INTRODUCTION .....	71
EXPERIMENTAL.....	72
Separation and Detection .....	72
Reagents.....	73
Mast Cell Isolation.....	74
Single Cell Injection and CE Procedure .....	74
RESULTS AND DISCUSSION .....	75
Cell Viability and Adhesion.....	75
Mast Cell Degranulation.....	76
Serotonin LOD and Bulk Release Study .....	81
Introduction of SDS for Cell Lysis .....	81
Single Cell Exocytosis .....	82
Single Granule Detection.....	92
Protein Contents.....	96
CONCLUSIONS.....	96
ACKNOWLEDGMENTS .....	99
REFERENCES .....	101
SUPPORTING INFORMATION .....	104
GENERAL SUMMARY .....	149

## ACKNOWLEDGMENTS

There are many people to whom I am indebted for helping me to achieve this degree. First, I would like to thank Dr. Yeung for his support as my major professor and advisor. He always has encouraged independence, perseverance, and excellence in my graduate research, and I am deeply grateful for the opportunity to have worked in his lab. I would also like to acknowledge my committee members, Professors Sam Houk, Richard Honzatko, Dennis Johnson and Pat Thiel, for their time and input in my oral examinations and this thesis. Finally, I would like to thank Professor Mike McCloskey, Department of Zoology and Genetics, for teaching me both the cell isolation technique and the biology relevant to the mast cell paper.

From San Diego State University, I would like to thank my undergraduate advisor, Professor Bill Tong. I appreciate the undergraduate research experience in his lab, learning about using lasers in analytical chemistry, and his guidance in my applications to graduate school. Somehow, he convinced me to move myself and my family from sunny San Diego to Iowa. Some people thought I was crazy to do so, but when I think about the experience I have had and the influence I have felt working in Ed Yeung's lab, I know that I made the right decision.

To all the past and present members of the Yeung group with whom I have worked, I extend my gratitude. Especially to Dave McGregor, Chris Smith, Leslie Waits, Qifeng Xue and Weihong Tan. I appreciate their support during stressful times such as written and oral prelims, bad results, and grant applications. I would also like to thank Wendy Nelson, for talking to me about research, grad school and life, and for helping me to keep a positive outlook on my graduate career and future. These friendships have made graduate school worthwhile and fun!

To my entire family, I could never acknowledge all that they have done for me, and can only make a dent in it here. I thank my parents, Joanne and Ron, for all the love and support they have given me. They provided countless hours of babysitting during my junior

and senior years at SDSU, without which I probably would not have graduated. I also thank my sister Lori, my grandparents, and my in-laws, for their continuous encouragement.

Finally, I dedicate this dissertation to my husband Randy and my son Jason. They are the reason I kept trying when I felt like quitting, and to them I am forever indebted. Their patience, understanding and love have given me what it takes to succeed. They have endured my hours of studying, long days, nights and over-nighters in the lab, and moody times when things were not quite going right. To Randy, thank you for encouraging everything I have wanted to do in my life for more than 14 years, and for backing it up with all the love and support that I could ever need. To Jason, who once asked me if “all Moms had to do their homework,” thank you for understanding why this is important to me. I am very fortunate to have such great people in my life, and hope that someday I can repay all that they have done for me.

This work was performed at Ames Laboratory under contract no. W-7405-Eng-82 with the U. S. Department of Energy. The United States government has assigned the DOE Report number 1S-T-1791 to this thesis.

**ABSTRACT**

Individual mammalian cells were analyzed by capillary electrophoresis with laser-induced fluorescence detection (CE-LIF). This detection technique was chosen due to its high separation efficiencies, small sample volumes and sensitive detection. Native fluorescence was used, in which the analyte was not tagged with a fluorophore. 275-nm excitation gave attomole ( $\text{amol} = 10^{-18} \text{ mol}$ ) detection limits for the intracellular species of interest. Two projects are described in which hemoglobin (Hb) variants were determined in single red blood cells. In the third experiment, exocytosis and serotonin release were monitored in individual mast cells.

First, single red blood cells, in which Hb molecules exist in their native, tetrameric states were analyzed. Upon injection and lysis of a cell, the tetramers were dissociated on-column into their respective polypeptide chains, separated and detected. Adult (normal and elevated  $A_1$ ) and fetal erythrocytes were analyzed. The amounts of glycosylated and total Hb were found to be uncorrelated.

Second, an injection-based capillary isoelectric focusing technique was developed to separate Hb variants in single cells. Using dilute buffer conditions, the limit of detection (LOD) for Hb was 4 amol. In addition, a linear pH gradient was established along the capillary, which allowed variants differing by as little as 0.025 pI units to be resolved. The identification of variants with unknown pI values was also possible with this system.

Third, the temporal evolution of on-column exocytotic release of serotonin in individual rat peritoneal mast cells (RPMCs) was monitored. The LOD for serotonin was 1.7 amol ( $S/N = 3$ ; rms) with this system. The secretagogue was Polymyxin B sulfate, and was electromigrated into the capillary following injection of a single RPMC. Degranulation was induced and serotonin released, the time courses of which were registered in the electropherograms. Following release, SDS was injected into the capillary to lyse the cell completely and to determine residual serotonin. With this procedure, events that are consistent with released serotonin from single sub-micron granules (250 aL each) were

evident, which, to our knowledge, represent the smallest entities that have been analyzed with CE to date.

## GENERAL INTRODUCTION

### Dissertation Organization

A general introduction precedes four chapters, which are either published papers or submitted manuscripts. The literature review is given in Chapter 1, which has been accepted for publication as a book chapter. Chapter 2 is a paper which has been published in a major chemistry journal. Chapters 3 and 4 are manuscripts which have been submitted to journals. These chapters are followed by a general conclusion. References for each manuscript are at the end of the chapter in which they are cited.

### Single Cell Analysis

Capillary electrophoresis (CE) has become popular for the analysis of individual cells, primarily because of the high separation efficiencies, small sample requirements and sensitive detection methods associated with the technique.<sup>1-3</sup> The challenge of appropriate analytical design has advanced from the fundamental impetus of this application, which is to discover how intracellular constituents relate to one another, and how this compares to the heterogeneous population of cells. More importantly, the purpose is to provide a link between these chemical and statistical relationships and the inception of disease, before the cell undergoes morphological changes.

Quantitation is desirable if one is to demonstrate biologically significant intercellular relationships. However, in situations where absolute quantitation is difficult, determination of relative amounts (or fractions) of components still provides useful information. Single cell analysis is different from what is obtained with a bulk analysis, because intercellular variations are evident. If an intracellular analyte is quantitated by a bulk analysis, the information obtained is an average amount of that component. From this value, deviations from a normal range can be assessed, but only if a large number of cells in the population follow such a trend. In comparison, if cells are analyzed independently from one another, those which lie outside a normal range are immediately apparent. It is this feature--the ability to detect very few abnormal cells within a primarily normal cell population--that makes CE a

very powerful tool for single cell analyses. In addition, such analyses are not limited just to quantitation, but could be expanded to include studies of release, uptake, or intercellular signaling.

#### References

1. Jankowski, J. A.; Tracht, S.; Sweedler, J. V. *Trends Anal. Chem.* **1995**, *14*, 170-176.
2. Yeung, E. S. *Acc. Chem. Res.* **1994**, *27*, 409-414.
3. Hogan, B. L.; Yeung, E. S. *Trends Anal. Chem.* **1993**, *12*, 4-9.

**CHAPTER 1****CAPILLARY ELECTROPHORESIS FOR THE  
ANALYSIS OF SINGLE CELLS: LASER-INDUCED  
FLUORESCENCE DETECTION**

A book chapter accepted by the Handbook of Capillary Electrophoresis<sup>1</sup>

Sheri J. Lillard and Edward S. Yeung

**INTRODUCTION**

In addition to laser-induced fluorescence (LIF), detection schemes for the analysis of intracellular components and monitoring of chemical dynamics with CE also include those based on non-fluorescent detection, such as electrochemical<sup>1-6</sup> and light scattering.<sup>7,8</sup> Recently, a radiochemical detector has been developed<sup>9</sup> and applied to single cell analysis.<sup>10</sup> Mass spectrometry,<sup>11</sup> for which detectability is currently at the level of ten erythrocytes, is also emerging as a detection technique for the analysis of single cells.

Single cell analysis--instrumentation, buffer/separation considerations, cell injection and lysis techniques--in which LIF detection is used, will be emphasized in the remainder of this chapter. Flexible LIF detection schemes provide increased opportunities for retrieving the unique chemical information that resides within each individual cell. Table 1 summarizes the different classes of compounds, as well as the many cell types, that have been studied thus far with adaptations of LIF detection. These are discussed in detail in further sections.

---

<sup>1</sup>Reprinted with permission from *Capillary Electrophoresis for the Analysis of Single Cells: Laser-Induced Fluorescence Detection*, in the *Handbook of Capillary Electrophoresis*, 2nd Ed., Landers, J. P., ed, CRC Press, Boca Raton, Florida, in press, Copyright © CRC Press.



## CAPILLARY ELECTROPHORESIS OF SINGLE CELLS

### Preparation of Cell Suspension Solution

Because extracellular fluid may contain other cell types or potentially interfering compounds, it is necessary to wash the cells of interest to eliminate extracellular matrix. The washing solution must be isotonic for the cells of interest to prevent premature lysing, and chosen carefully to avoid contamination or interferences. It should also be devoid of substances which could promote unwanted secretion of the analyte. A balanced salt<sup>12-14</sup> or phosphate-buffered saline (PBS) solution is generally suitable for both cell washing<sup>15,16</sup> as well as final cell suspension.<sup>15</sup> In the event that high salt concentration is detrimental to the system, an 8% (w/v) glucose solution is isotonic and may be used for human erythrocytes.<sup>17,18</sup>

Typically, a small volume (*ca.* 10  $\mu$ L) of blood or cells is placed in a capped centrifuge tube containing a few mL of wash buffer. The cells are gently shaken, centrifuged, and the supernatant discarded. Another volume of wash buffer is added, and the procedure is repeated about 5 times. After the last volume of supernatant is discarded, the cells are resuspended in an isotonic solution. Depending on the stability of a particular cell type, quite often the cells will remain intact and viable for a few days. If this is the case, the washing procedure should be repeated after overnight storage, to ensure that the contents from any cells which have lysed are removed.

### Cell Injection

Small capillary diameters (i.d. of 5-30  $\mu$ m) simplify injection of mammalian cells, many of which lie within this size range. Under 100-200 $\times$  magnification, both the capillary walls and the cells can be focused within the same plane, which is a necessary condition for

Table 1. Representative cell types and classes of compounds analyzed by CE-LIF

<b>Cell Type</b>	<b>Detection Mode</b>	<b>Separated Components</b>	<b>Ref.</b>
<b>Erythrocytes (human)</b>	Native	Hemoglobin, methemoglobin, carbonic anhydrase	15
	Indirect	Hemoglobin variants	16
		Na, K	17, 36
	Derivatization	Lactate, pyruvate	21
		Hemoglobin, carbonic anhydrase	18, 44
	Enzyme assay	Glutathione	36
Enzyme assay/ particle counting	Lactate dehydrogenase isoenzymes	22	
	Glucose-6-phosphate-dehydrogenase	8	
<b>Adrenal medullary cells (bovine)</b>	Native	Catecholamines	13
	Derivatization	Amines	19
<b>Pancreatic <math>\beta</math>-cells (rat)</b>	Native	Insulin	12
<b>Neurons</b>	Derivatization	Peptides	20
	Derivatization	Amino acids	41, 44
<b>Pheochromocytoma cells (rat)</b>	Derivatization	Amino acids	14
<b>Lymphocytes (human; normal and leukemia cells)</b>	Enzyme assay	Lactate dehydrogenase isoenzymes	23

successful and reproducible cell injection. Capillaries with a 50  $\mu\text{m}$  i.d. have been used for the injection of cell contents from a lysed cell.<sup>19,20</sup> However, for injection of an intact cell, sample dilution and injection control are potential drawbacks of using a larger capillary.

### ***Electrokinetic***

Gilman and Ewing have utilized an electrokinetic cell injection method, which allows a cell to be viewed as it migrates into the capillary by electroosmotic flow.<sup>14</sup> In this system, the cells were placed in a culture dish, into which a platinum wire was inserted. The capillary injection end was attached to a micromanipulator, then positioned near a cell under 200 $\times$  magnification. A voltage of 2 kV was applied, and a cell was migrated into the capillary, taking between 15 and 90 s for injection. The capillary was then moved to a reservoir containing derivatization and lysing reagents, which were subsequently injected electrokinetically and allowed to react. Finally, the capillary was returned to the separation buffer, and electrophoresis resumed.

### ***Vacuum***

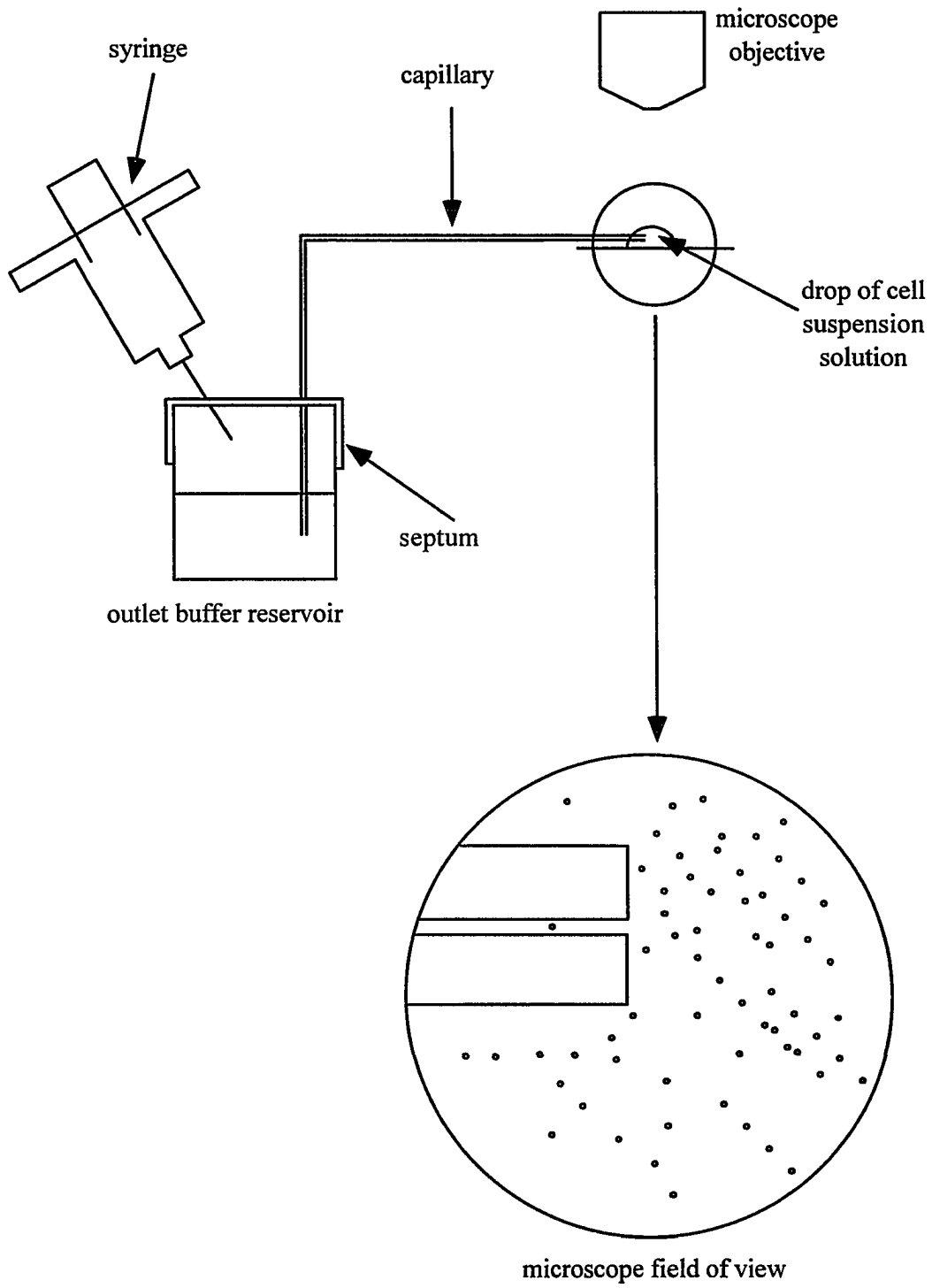
Since most on-column detection schemes do not have restricted access to the capillary outlet, cells may also be drawn into the capillary by creating a partial vacuum.<sup>12-13, 15-18, 21-23</sup>

A typical set-up for this type of cell injection is shown in Figure 1. An air-tight septum is placed over the outlet buffer reservoir, through which the capillary and a syringe are inserted. A drop of cell suspension solution is placed on a microscope slide under *ca.* 100 $\times$  magnification of a light microscope. Guided by a micromanipulator stage with appropriate support (e.g., teflon tubing) to prevent unwanted movement, the inlet end of the capillary is then placed into the droplet. By carefully controlling the pressure of the syringe, one cell can be drawn inside the capillary and visually confirmed. The capillary is then removed from the droplet, returned to the inlet buffer reservoir, and electrophoresis initiated.

### **Cell Lysis**

Cells that are sensitive to differences in osmotic pressure, such as erythrocytes, will lyse within a few seconds after contact is made with the separation buffer. Typical CE buffers have an ionic strength usually less than 100 mM, which is much lower than that inside an

Figure 1. Schematic of single cell injection into a capillary column.



erythrocyte. Once the cell and isotonic zone move away from each other, the cell is lysed, intracellular contents released, and separation is initiated. However, other cell types are considerably more rugged, and will not lyse readily upon differences in buffer ionic strength. For these situations, a harsher procedure is necessary to disrupt the cell membrane quickly.

Gilman and Ewing<sup>14</sup> added digitonin, a lysing agent, into the reagent buffer to facilitate cell lysis. This was introduced into the capillary following the injection of individual PC12 cells. Chang and Yeung<sup>13</sup> found that adrenal medullary cells do not lyse readily upon contact with separation buffer, and required an additional step to expedite lysis. The cell suspension solution was diluted 40× with water on the microscope slide, and the subsequently injected cells lysed upon contact with the separation buffer.

Xue and Yeung<sup>23</sup> have reported that lymphocytes also fall into this category, and a lysing procedure was necessary that did not alter the enzyme activity that was being measured. They found that when a tesla coil was applied to the outside of the capillary in which the cell resided following injection, the external electrical field plus heat produced by the tesla coil disrupted the membrane and released the intracellular components. The procedure used to lyse pancreatic  $\beta$ -cells<sup>12</sup> on column involved electromigration of 0.05% SDS following cell injection.

### **LASER-INDUCED FLUORESCENCE--GENERAL INSTRUMENTATION**

Laser-induced fluorescence is a highly favorable detection scheme for the determination of intracellular components by CE.<sup>24</sup> Limits of detection (LOD) are unparalleled, with the most impressive ranging from zeptomole<sup>25</sup> ( $\text{zmol} = 10^{-21}$  mol) levels to single enzyme molecules.<sup>26</sup> The variety of LIF modes with outstanding detection limits has made this technique a necessary tool to study individual cells. The experimental design for LIF detection is essentially the same whether individual cells or small sample volumes are injected into the capillary, and independent of the LIF mode.

Variable components of the detector set-up which depend on the laser wavelength include lens and mirror materials, and wavelength range and type (cut-off, bandpass or

interference) of emission filters. If the excitation wavelength of interest is not emitted from the laser as a single line, then it is selected by either a prism or an interference filter before reaching the optics for the CE system. The laser beam is then focused with a lens onto the detection window of the capillary. Fluorescence is collected at 90° with a 10-20× microscope objective, passed through appropriate spectral and spatial filters, and detected by a photomultiplier tube (PMT).

To improve sensitivity, Shippy et al. used a slightly different LIF set-up.<sup>20</sup> Their modifications included using a reflective microscope objective for fluorescence collection and photon-counting for detection, with the rest of the components essentially the same as described above.

### NATIVE FLUORESCENCE

The measurement of native fluorescence from biological molecules such as amino acids and proteins is not new,<sup>27</sup> although reports of laser-induced native protein fluorescence applied to capillary electrophoresis are fairly recent.<sup>28-30</sup> This mode of protein detection is based on the aromatic amino acid residues of the protein or peptide. Tryptophan, tyrosine, and to a lesser extent, phenylalanine, are all excited by UV radiation. Tryptophan is the most highly fluorescing, with an excitation maximum around 280-nm that is closely matched with the 275.4-nm line of an argon-ion laser. Protein fluorescence is very sensitive to environmental factors, for example, SDS will render some proteins undetectable by this scheme. Hence, separation conditions, buffer components, and other environmental considerations that could alter protein structure must be considered, especially when applied to the analysis of individual cells.

#### **Insulin in Pancreatic $\beta$ -Cells**

Tryptophan fluorescence usually dominates in the native fluorescence of proteins, however insulin does not contain tryptophan. Its protein fluorescence is derived primarily from the tyrosine residues in this 5.7 kd protein. Tong and Yeung<sup>12</sup> have demonstrated the detection of insulin using 275-nm excitation in single pancreatic  $\beta$ -cells. In this study, the

best detection limit achieved for insulin was 73 amol (S/N = 10) using a poly(ethylene oxide) coated capillary. Thirteen individual  $\beta$ TC3 cells were analyzed, with an average insulin content of  $1.55 \pm 0.74$  fmol found; in a separate batch of nine cells,  $1.89 \pm 1.03$  fmol was found. The insulin amount in this cultured cell line is about 20 - 30% that of normal cells. Intercellular variations were evident, with RSDs of 48% and 54%, respectively, found among the two cell lines. Also, a decreasing trend of insulin amount with time is seen over the course of the experiment. This may be due to basal release of insulin or partial lysis as the experiment proceeds. In addition, the cells do not lyse readily on column, and injection of SDS (as discussed on page 10) is also necessary to lyse an individual cell once it has been injected.

### **Catecholamines in Adrenal Medullary Cells**

Catecholamines are usually detected electrochemically,<sup>5,31</sup> however, their determination by CE with native LIF has been introduced recently.<sup>13</sup> Chang and Yeung have shown that some amines with aromatic or indole groups can be detected by native fluorescence when excited by 275 or 284 nm laser light. Like proteins, native fluorescence of amines is sensitive to environment, especially pH, with higher fluorescence intensity at low pH.<sup>13</sup> Nonetheless, native LIF has high enough sensitivity to detect catecholamines in single adrenal medullary cells.

For several analyzed cells from a given gland, intercellular variation in the amounts of norepinephrine (NE) and epinephrine (E) was evident, however, the ratio of the two remained fairly constant. In addition, the average amounts of NE and E in a single cell varied significantly depending on the source glands, which were obtained from different cows. In one gland the average amounts of NE and E were, respectively,  $19 \pm 9$  and  $55 \pm 30$  fmol; in another gland they were  $72 \pm 30$  and  $380 \pm 150$  fmol. Such differences among cell populations revealed by this method should be useful to neurochemical studies.



## DERIVATIZATION

High sensitivity and low detection limits are the remarkable highlights of laser-induced fluorescence detection. However, many of the most common lasers operate in the visible region (e.g., Ar<sup>+</sup> 488-, 514- and He-Cd 442-nm lines) and do not have wavelengths that allow natural fluorescence of biologically interesting species. More likely, is that such species do not exhibit fluorescent properties at all, which makes derivatization a necessary option to detect low analyte levels.

Frequently, the analytes of interest are amino acids, peptides, or proteins (including enzymes), that contain functional groups for which sensitive fluorogenic reagents have been developed. Naphthalene dicarboxaldehyde (NDA), *o*-phthaldialdehyde (OPA), 3-(4-carboxybenzoyl)-2-quinolinecarboxaldehyde (CBQCA), and fluorescamine, are such examples.<sup>32-34</sup> These reagents are either non-fluorescent prior to reaction or their hydrolysis products do not fluoresce. Both are desirable features when low analyte quantities in small volumes of biological matrices are derivatized. Fluorescein-based tags<sup>25,35</sup> can be used for amines, whereas sulfhydryl groups are reactive with monobromobimane (mBBr).<sup>36</sup> However, since the latter two reagents are usually fluorescent in both reacted and unreacted states, derivatization must occur prior to separation. Furthermore, the electrophoretic peak corresponding to the unreacted label should be well resolved from and should not interfere with the analytes of interest. Other common derivatization reagents include 5-dimethylaminonaphthalene-1-sulfonyl (DANSYL) chloride and fluorescein isothiocyanate (FITC).<sup>37-39</sup>

Another interesting derivatization method uses the cell not as the analyte, but rather as a biosensor.<sup>40</sup> Shear and coworkers positioned live cells near the capillary outlet, and used the cell response to the analyte for detection. Using the calcium indicator fluo-3 in the separation buffer, when a species (e.g., acetylcholine) that caused a change in Ca<sup>+2</sup> concentration eluted upon the cell, fluorescence was measured and related to the analyte concentration.

### **Pre-Column Reaction**

Derivatization methods in which the reaction is allowed to proceed prior to separation in the capillary can be useful for single cells. An advantage of such a scheme is that derivatizing conditions, which are often hydrophobic, do not have to be compatible with the primarily aqueous buffers in CE. Although dilution of intracellular components remains a drawback, successful strategies to apply such schemes to individual cells include performing reactions on isolated single cells,<sup>19-20,41</sup> and utilizing the intact cell as a reaction vessel.<sup>36</sup> Pre-column derivatization possesses several limitations. First, sufficient volumes (> 25 nL) must be available for derivatization. Second, multiple derivatizations for the same molecule can occur, yielding several peaks for each analyte. Third, migration times are for the derivatized product and not the native analyte. As a result, identification and quantitation can be difficult.

### ***Adrenal Medullary Cells***

The development of an on-line preconcentrator was applied to the determination of intracellular components by Hoyt et al.<sup>19</sup> For the analysis of single cells, the preconcentrator was positioned 2-3 mm from the injection end of the capillary, and had a total length of 1-3 mm. The gap at the end was necessary to allow room for the micro-injection pipet. The preconcentrator was constructed from reversed-phase LC packing material immobilized between frits made of 22- $\mu$ m borosilicate glass microspheres. A 250-nL microvial was used, in which an individual cell and phosphate buffer were placed. Subsequently, NDA, NaCN, and phosphate buffer were added to give a final reagent volume of 47 nL, and the cellular contents were derivatized. Thirty nL of derivatized cell supernatant was then injected onto the preconcentrator. The analytes were eluted from the preconcentrator region with 70% acetonitrile (20 s, 10 kV), followed by electrophoresis with the separation buffer. In the derivatized amine contents from a single adrenal medullary cell, a combination of amino acids, biogenic amines, and peptides (i.e., amines which are derivatized by NDA) were found.

## *Neurons*

### *Helix aspersa*

In a study based on the methods developed for open-tubular liquid chromatography (OTLC), Kennedy et al. demonstrated the applicability of this technique to CE.<sup>41</sup> The large neurons of *Helix aspersa* were used in this work, because of the ease with which they can be manipulated. A 500-nL microvial, which was constructed from a capillary melted closed on one end, was used such that one cell was isolated and contained within. NDA and other necessary reagents were added, and allowed to lyse and derivatize the cell.

The NDA-derivatives of an E4 cell from *Helix* were separated using CE. Many peaks were tentatively identified as NDA-amino acids based on migration times. In addition, many unidentified derivatized components were present, which demonstrates the efficiency of derivatization in a complex matrix. In this experiment, only about 20% of the total cell contents was injected onto the column, rather than an entire, intact cell. Hence, the possibility that one can do several CE runs from the contents of one cell is evident. More importantly, this suggests that conditions could be varied in such runs, from which many different classes of compounds could be determined sequentially from one cell.

### *Aplysia californica*

A protocol in which fluorescamine was used as a derivatizing reagent for peptides and amino acids in *Aplysia californica* neuronal cells has been developed recently by Shippy et al.<sup>20</sup> In this system, the absorptivity of labeled arginine was found to be only a factor of two lower with 350-360 nm light, than at the maximum of 405 nm. Hence, the 354-line from a He-Cd laser as the excitation source, plus a reflective microscope objective for fluorescence collection, and photon-counting, provided high-sensitivity detection.

The derivatization procedure utilized small volumes of reagents which were added to a single cell (in 0.50  $\mu$ L artificial seawater) isolated on a glass surface. Subsequently, 5  $\mu$ L fluorescamine (in DMF) was added to the cell, and lysis (confirmed under a microscope) and reaction allowed to proceed. Since the cell was lysed during the derivatization step, an aliquot of the contents from an individual cell ( $\sim$  2 nL) is injected, rather than the intact cell itself. Although the detection of fluorescamine hydrolysis products was evident following

separation, when 20 mM SDS was added to the separation buffer, the number and intensity of such peaks decreased.

Individual identified neurons were analyzed in this study, for which different neurons contained different peptides. There is a similar peak pattern for the different cell types, however, unique peaks are also present for each type. For example, egg-laying hormone (ELH) peptide was identified in a bag cell neuron, by spiking it with an ELH standard. The LOD of tagged ELH was 2.3 nM, which was determined by derivatizing a 10-nM solution of the peptide with fluorescamine. The ability of this scheme to derivatize low concentrations of analytes is significant, and could possibly lead to the assay of cell subsections. Further enhancement is expected if dilution is minimized by performing reactions on-column, or in microvial environments.

### ***Erythrocytes***

The mBBr microderivatization of intracellular thiols was performed by using the cells as individual reaction vessels, each with a 90-fL volume.<sup>36</sup> Monobromobimane was added to a volume of cells, upon which the reagent was able to permeate the cell membrane, react with intracellular thiols, and the larger derivatization product retained inside the membrane following reaction. In this manner, the reaction was contained, excess extracellular reagent could be removed from the cells, and dilution was minimal. The derivatization was macroscopic (i.e., all cells derivatized in the same solution) and pre-column. There is still the issue of unreacted mBBr, some of which was retained by the cellular reaction vessel. However, since this compound migrated well ahead of the intracellular thiols, there was no interference in the CE run from its presence.

The reaction of mBBr with reduced glutathione (a sulfur-containing tripeptide) gave a LOD of 5.9 amol (S/N = 3). The average intracellular mBBr-GSH amount from the analysis of six individual erythrocytes was found to be  $68 \pm 48$  amol per cell. Further experiments in this work revealed that such intracellular derivatization reactions can be manipulated. When diamide, which is known to oxidize glutathione, was added to the cells, reaction with mBBr was prevented and the peak for derivatized GSH disappeared. When dithiothreitol was added subsequently, glutathione was re-reduced and the peak returned.

An on-column scheme was developed by Gilman and Ewing, in which NDA was used to derivatize and detect amines in rat PC12 cells.<sup>14</sup> In this work, a single cell was viewed under a microscope and electrokinetically injected into the capillary, as discussed on page 6. After cell injection, a reagent buffer was electrophoretically introduced (30 s, 2 kV), and allowed to react for 10 min. The reagent buffer consisted of digitonin (for cell lysis), NDA, NaCN, Val-Tyr-Val (internal standard), and ethanol and acetonitrile (from the digitonin and NDA solutions, respectively). To ensure that no sample was lost during transfer of the capillary to the separation buffer vial, reagent buffer was injected a second time (15 s, 2 kV) before electrophoresis. After using the injection end of the capillary as a reaction chamber, electrophoresis was allowed to proceed, and the NDA-derivatized amines were separated and detected using LIF.

NDA-derivatized contents from single PC12 cells, as well as the cell medium, were separated. The identified amines included alanine, glycine, taurine, glutamate and aspartate. In addition, several unidentified peaks were recorded and one cell was found to contain norepinephrine. It was necessary to determine the contribution of cell medium species to the analysis of a single cell, and subtract such contributions. Hence,  $\gamma$ -Glu-Gly was added as an internal standard to the culture medium, to assess the amount of extracellular solution injected with a cell. Although some peaks are present in both cell and background experiments, this method of quantitation and subtraction of cell medium components allows intracellular components to be quantitated.

### **Post-Column Reaction**

Post-column derivatization avoids many of the problems associated with pre-column derivatization. There is minimal sample preparation. In addition, because the sample is unaltered, migration times are those of the native analyte, not a derivatized product. This can lead to improved identification and quantitation. Furthermore, detection of degradation products is less likely to occur because the time between derivatization and detection is minimized. This can be a drawback, however; since the signal is a function of the reaction

rate, the reactor must be optimized for maximum signal and carefully calibrated for quantitative work.

Ewing, et al. recently demonstrated the use of a post-column gap reactor with 10- $\mu\text{m}$  capillaries.<sup>42</sup> Previous post-column derivatization schemes used 50- $\mu\text{m}$  or 25- $\mu\text{m}$  separation capillaries.<sup>43</sup> With a 10- $\mu\text{m}$  capillary, reactors with gaps of 4 to 160  $\mu\text{m}$  were easily constructed. Using OPA/2-mercaptoethanol for derivatization, amino acids and proteins were separated and peak efficiencies of 230,000 theoretical plates were obtained. Mass detection limits of 130 and 5.2 attomoles were obtained for glycine and human transferrin, respectively. This system has also been optimized for use with NDA/2-mercaptoethanol and used for the detection of amino acids in the homogenate of a snail brain as well as hemoglobin in a single human erythrocyte.<sup>44</sup>

In a similar method, Zhang and Yeung have demonstrated OPA post-column derivatization using coaxially connected capillaries for the detection of hemoglobin and carbonic anhydrase in single human erythrocytes.<sup>18</sup> With this system, a LOD of 17 amol was found for glycine. Several amines were determined with all LOD less than 153 amol. Adult (normal and diabetic) and fetal erythrocytes were analyzed with differences in protein composition evident.

### INDIRECT FLUORESCENCE

Fluorescence is sensitive and selective, however, these desired characteristics also inherently limit its applicability as a general detector. In order to expand the number of analytes that may be determined in single cells, it is necessary to include those that do not have a functional group which is conducive to either direct fluorescence or derivatization. This is accomplished by using indirect fluorescence detection, which has been shown to give mass detection limits on the order of 50 amol in CE.<sup>45,46</sup> In this scheme, the background electrolyte (i.e., separation buffer component) fluoresces to give a high detector response. The charge of this electrolyte is chosen to have the same sign as the analytes. When the analyte ions migrate toward the detector, preservation of local charge neutrality necessitates

that they will displace the buffer ions. Since this displacement removes fluorescing ions from the detector region, a negative peak ensues, corresponding to the analyte band.

When indirect LIF is applied to the analysis of single cells, additional factors need to be addressed. Because maintaining a stable fluorophore concentration is crucial for sensitive detection, items that can disturb this equilibrium, such as cell matrix material, (aqueous) intracellular fluid, and injected cell suspension solution, must be controlled. In spite of these additional considerations, both cations and anions have been determined in single red blood cells with indirect fluorescence. The general nature of this detection scheme should eventually lead to the determinations of multiple, structurally dissimilar components in single cells.

### **Sodium and Potassium**

While inorganic ions from particulate matter usually do not represent a threat to detection, it was learned by Li and Yeung that indirect LIF was sensitive enough to sense such contamination, which could, in fact, be near the mass detection limit.<sup>17</sup> The single-cell determinations of Na and K by this method were found to require extensive contamination control, in addition to the other experimental considerations of indirect detection. It was necessary to use plastic (i.e., non-glass) buffer vials and microscope slides, since glass slides were found to release sodium salts even after thorough washings. In addition, they found that prolonged cell storage in low ionic strength solutions resulted in Na and K being exuded from the cell. This was minimized by adjusting the cell preparation such that washing time was reduced, and a fresh batch of cells was prepared every hour. These additional precautions reduced the contamination problem, and allowed reproducible determinations to be made.

After suitable measures for contamination control were taken, the analysis of 49 individual erythrocytes revealed that the average amounts of K and Na were  $10.8 \pm 6.3$  and  $0.33 \pm 0.31$  fmol, respectively. This large deviation is not expected to be caused by experimental error, but instead, these amounts are thought to vary due to cell age.

### **Lactate and Pyruvate**

Lactate and pyruvate are involved in the glycolysis process in the red blood cell, and are converted to each other via an enzymatic reaction. Although they play an important role in metabolic processes, they are difficult to detect at low levels since they do not contain useful functional groups for either direct detection or derivatization.

Indirect LIF allowed sensitive detection of the intracellular anions, lactate and pyruvate.<sup>21</sup> Under optimal conditions, the LOD for lactate was found to be about 20 amol, which is well within the range for single-cell analysis. In this system, the primary interference was caused by excessive cell suspension solution which was injected with the cell. By etching the injection end with HF to ~50  $\mu\text{m}$  o.d., the amount of this solution injected was decreased, thereby improving the stability of the system.

The average amounts of pyruvate and lactate from the analysis of 27 single cells were found to be 2.1 and 1.3 fmol, respectively, with a ratio of 1.6 for pyruvate to lactate. Although this ratio should be independent of cell size, it showed considerable variation among the analyzed cells, which may be due to differing metabolism and enzyme activity.

### **FLUORESCENT ENZYME ASSAY**

Capillary electrophoresis has been used to perform enzymatic analyses by Regnier et al.,<sup>47-49</sup> in which enzyme and substrate were allowed to react on-column, so that a reaction product can be detected with high sensitivity. In this technique, direct fluorescence detection of a product molecule is monitored. In general, the separation buffer contains the substrate molecule(s). The enzyme of interest is injected, electrophoretically migrated a distance through the capillary, and allowed to react. Upon contact with the substrate, product molecules will be formed, and a product molecule zone will migrate past the detector. Sometimes, the enzyme and substrate are allowed to react for a given time without applied potential, in which case, product is accumulated and its location is basically undisturbed. The highlight of this technique is the natural amplification that is exhibited, which is responsible for the extremely high sensitivity of this method. One enzyme molecule can produce thousands of product molecules, which can then be related back to the enzyme activity.



## Erythrocytes

### *Lactate Dehydrogenase (LDH)*

The determination of LDH isoenzymes by an on-column enzyme assay protocol with LIF detection was accomplished by Xue and Yeung for the analysis of single red blood cells.<sup>22</sup> In this work, LIF detection of nicotinamide adenine dinucleotide (NADH) product zones via the enzymatic reaction,  $\text{NADH} + \text{pyruvate} \leftrightarrow \text{NAD}^+ + \text{lactate}$ , catalyzed by LDH, was employed for the measurement of LDH activity. In this experiment, the reverse catalytic reaction was run, and the substrates  $\text{NAD}^+$  and pyruvate were present in the separation buffer at all times. The presence of lactate, pyruvate, and  $\text{NAD}^+$  in the capillary gave a low fluorescence background, hence did not disturb the NADH measurement. For this on-column reaction, a single cell was injected and the intracellular isoenzymes allowed to separate for 1 min at 30 kV. The voltage was turned off, and the enzyme and substrate proceeded to react for 2 min, followed by electrophoresis of the resultant NADH zones. This system exhibits a large (natural) amplification, since the turnover number for LDH is  $\sim 1000/\text{s}$ <sup>50</sup>—which means that 1 enzyme molecule produces  $\sim 1000$  product (i.e., NADH) molecules each second. Such an amplification results in a low LOD of  $1.3 \times 10^{-21}$  mol of LDH.

The separation and detection of LDH isoenzymes was performed for thirty-six single erythrocytes. The average total LDH activity was determined as  $1.36 \pm 0.7$  nIU per cell. Although the variation is large, a positive linear correlation of  $r^2 = 0.64$  was found in the ratio of LDH1/LDH2 activities for 31 cells. Both total enzyme activity, which is probably a function of cell age, as well as relative amounts of specific isoenzymes, which may be elevated/reduced due to disease, are potentially useful measurements for the further investigation of diseases.

### ***Glucose-6-Phosphate Dehydrogenase (G6PDH)***

Tan and Yeung have integrated this type of LIF enzyme assay with light scattering detection,<sup>22</sup> such that the activity of G6PDH, and its concentration could be determined simultaneously.<sup>8</sup> The monitored enzyme reaction was nicotinamide adenine dinucleotide phosphate (NADP<sup>+</sup>) plus glucose-6-phosphate (G6P), catalyzed by G6PDH, to produce the detected fluorescent product NADPH. Anti-G6PDH coated latex particles were also present in the capillary, which, in the presence of the enzyme, agglutinated to produce large particles that were detected by light scattering.

This enzymatic reaction of G6PDH was found to be very pH-dependent, with 7.4 to 8.6 the optimal pH range. A pH of 8.4, plus the use of an Ar<sup>+</sup> laser (350/360 nm excitation) with 420-nm long-pass and 480-nm interference filters for emission, allowed sensitive detection of the NADPH product zones. For the on-column assay, a LOD for G6PDH [via NADPH detection] of 0.1 and 1 zmol was obtained in the absence and presence of antibody-coated particles, respectively. The analysis of 30 individual erythrocytes revealed that the average amount of G6PDH per cell was  $(15 \pm 9) \times 10^{-21}$  mol, and the average total G6PDH activity per cell was  $27 \pm 14$  pIU. These correspond to an intercellular variation of 12× in enzyme activity and 8× in enzyme quantity. Furthermore, by correlating the two measurements, they found that only about 35% of the enzyme in a cell is active. As with most distributions obtained by studying individual cells, such a variation is expected and probably has a partial dependence on the age of the cell.

### **Lymphocytes and Lymphoblastic Leukemia Cells**

The enzyme assay protocol which was developed for the analysis of single erythrocytes,<sup>22</sup> has been applied recently to the study of lymphocytes.<sup>23</sup> The objective of this work was to evaluate the feasibility of LDH activity as a unique marker for leukemia. The same reaction and direction for the production of NADH were used as in the erythrocyte studies.<sup>22</sup> A comparison was made of LDH activities in single normal lymphocytes, and T-

type and B-type lymphoblastic leukemia cells, to search for correlations in isoenzyme ratio with disease state.

The first consideration in this work was the difficulty in lysing individual lymphocytes, as compared to erythrocytes. This was eventually done with the use of a tesla coil, as discussed on page 10. Also, longer separation and incubation times, 3 and 5 min, respectively, were used to improve S/N. The diameters of lymphocytes vary greatly, from 6 to 14  $\mu\text{m}$ ,<sup>51</sup> and as expected, the intracellular LDH activities also showed large variations. The average LDH activities for individual normal, T-type, and B-type cells were found to be 6.3, 5.2, and 5.0 nIU, respectively.

It was hoped that LDH ratios might be used to depict different health and metabolic states, thus LDH4/LDH2 ratios were examined in the studied cells. The average LDH4/LDH2 ratios for T-type and B-type cells were 43% and 73% higher, respectively, than for normal cells. The difference between the leukemia cells is expected, as they have different functions. However, this increase was not observed for every cell studied in a given cell line, which implies that a larger number of cells should be analyzed before deriving conclusions about the presence of disease.

## THE FUTURE OF SINGLE-CELL ANALYSIS BY CE-LIF

### Present Limitations

The specialized information that is obtained from the analysis of intact cells by CE, either in their entirety or as subcellular compartments, is significant and cannot be disputed. However, to become clinically useful, great strides must be taken to increase throughput, i.e. the number of cells that can be analyzed in a given time. The separation step consumes most of the analysis time, but as long as it remains manageable (e.g., *ca.*  $\leq 10$  min), it is not desirable to increase separation speed at the risk of sacrificing separation efficiency. Hence, other ways in which throughput can be increased should be considered.

Also, although current cell injection techniques are functional, both electrokinetic and vacuum-based injection methods suffer from several drawbacks. Even an experienced

experimenter is inherently limited by the nature of present injection methods, which at best take about 10 s and at worst over one minute for the complete cell injection process. Although visual confirmation of the cell inside the capillary is imperative, this adds to the tedious nature of manually injecting individual cells.

## **Further Improvements**

### ***Multiplexing***

The first improvement to cell throughput is that of simultaneously monitoring many capillaries or separation channels. If one can analyze 100 cells simultaneously, then the ability to accumulate and compile meaningful statistics will be accomplished. Plausible multiplexed instrumentation has been developed for the purpose of DNA sequencing,<sup>52,53</sup> however, to apply these to the analysis of individual cells, additional factors remain to be addressed. Most notably, precise and simultaneous individual cell injection into multiple capillaries. Additionally, modifications to the detection apparatus that would permit sensitive detection in capillaries having an i.d. of *ca.* 20- $\mu\text{m}$  are necessary.

### ***Automation***

Improving the speed and ease with which individual cells are introduced into the capillary is necessary, especially if multiplexing is desired. For example, it would not be feasible to manually inject 100 cells into 100 capillaries. Therefore, in addition to monitoring simultaneous separation channels, it will be necessary to automate current injection methods, such that the injection of a single cell and its confirmation can be electrically monitored. This will allow the full benefit of multiplexing to be realized, and the accumulation of cell data to proceed more rapidly. A suitable interface to a flow cytometer may be a viable approach.

## **Future Directions**

The future of single cell analysis by CE-LIF over the next decade should see significant improvements in cell throughput and analysis speed, by the way of automation and multiplexing. It will also encounter a vast increase in the types of cells analyzed, as well as the nature of intracellular components determined, based on creative LIF detection

schemes. The improvement in the production of diode lasers with useful wavelengths for native biomolecules and sensitive derivatizing agents, should lead to more compact and possibly portable devices. In addition to the above, subcellular compartmental analysis, kinetic studies, and multiparametric determinations by CE-LIF should find increased capabilities in the future.

The technology of single-cell analysis will eventually be developed into a practical, clinical tool for the early diagnosis of disease. With automated cell injection, and multiple separation channels with simultaneous detection, a statistically useful number of cells could be analyzed, maybe to find that 1 cell in  $10^6$  that signifies carcinogenesis or HIV infection.

#### ACKNOWLEDGMENT

The Ames Laboratory is operated for the U.S. Department of Energy by Iowa State University under Contract No. W-7405-Eng-82. This work was supported by the Director of Energy Research, Office of Basic Energy Sciences, Division of Chemical Sciences. We thank Professor Andrew G. Ewing for suggestions on parts of this manuscript. S.J.L. thanks the Phillips Petroleum Company for a fellowship.

#### REFERENCES

1. Ewing, A. G.; Mesaro, J. M.; Gavin, P. F. *Anal. Chem.* **1994**, *66*, 527A-537A.
2. Kristensen, H. K.; Lau, Y. Y.; Ewing, A. G. *J. Neurosci. Methods* **1994**, *51*, 183-188.
3. Ewing, A. G. *J. Neurosci. Methods* **1993**, *48*, 215-224.
4. Olefirowicz, T. M.; Ewing, A. G. *Chimia* **1991**, *45*, 106-108.
5. Olefirowicz, T. M.; Ewing, A. G. *J. Neurosci. Methods* **1990**, *34*, 11-15.
6. Olefirowicz, T. M.; Ewing, A. G. *Anal. Chem.* **1990**, *62*, 1872-1876.
7. Rosenzweig, Z.; Yeung, E. S. *Anal. Chem.* **1994**, *66*, 1771-1776.
8. Tan, W.; Yeung, E. S. *Anal. Biochem.* **1995**, *226*, 74-79.
9. Tracht, S. E.; Toma, V.; Sweedler, J. V. *Anal. Chem.* **1994**, *66*, 2382-2389.
10. Jankowski, J. A.; Tracht, S.; Sweedler, J. V. *Trends Anal. Chem.* **1995**, *14*, 170-176.

11. Hofstadler, S. A.; Swanek, F. D.; Gale, D. C.; Ewing, A. G.; Smith, R. D. *Anal. Chem.* **1995**, *67*, 1477-1480.
12. Tong, W.; Yeung, E. S. submitted to *J. Chromatogr.*
13. Chang, H. T.; Yeung, E. S. *Anal. Chem.* **1995**, *67*, 1079-1083.
14. Gilman, S. D.; Ewing, A. G. *Anal. Chem.* **1995**, *67*, 58-64.
15. Lee, T. T.; Yeung, E. S. *Anal. Chem.* **1992**, *64*, 3045-3051.
16. Chapters 2 and 3 of this dissertation.
17. Li, Q.; Yeung, E. S. *J. Capillary Electrophor.* **1994**, *1*, 55-61.
18. Zhang, L. L.; Yeung, E. S. *J. Chromatogr.*, in press.
19. Hoyt Jr., A. M.; Beale, S. C.; Larmann Jr., J. P.; Jorgenson, J. W. *J. Microcol. Sep.*, **1993**, *5*, 325-330.
20. Shippy, S. A.; Jankowski, J. A.; Sweedler, J. V. *Anal. Chim. Acta.* **1995**, *307*, 163-171.
21. Xue, Q.; Yeung, E. S. *J. Chromatogr. A*, **1994**, *661*, 287-295.
22. Xue, Q.; Yeung, E. S. *Anal. Chem.* **1994**, *66*, 1175-1178.
23. Xue, Q.; Yeung, E. S. *J. Chromatogr.*, in press.
24. Yeung, E. S. Optical detectors for capillary electrophoresis, in *Advances in Chromatography*, V. 35, Brown, P. R., and Grushka, E., Eds., Marcel Dekker, New York, pp. 20-31, 1995.
25. Cheng, Y.-F.; Dovichi, N. J. *Science* **1988**, *242*, 562-564.
26. Xue, Q.; Yeung, E. S. *Nature*, **1995**, *373*, 681-683.
27. Steiner, R. F., and Weinryb, I., *Excited States of Proteins and Nucleic Acids*, Plenum Press, New York, 1971.
28. Swaile, D. F.; Sepaniak, M. J. *J. Liq. Chromatogr.* **1991**, *14*, 869-893.
29. Lee, T. T.; Yeung, E. S. *J. Chromatogr.* **1992**, *595*, 319-325.
30. Lee, T. T.; Lillard, S. J.; Yeung, E. S. *Electrophoresis*, **1993**, *14*, 429-438.
31. Wallingford, R. A.; Ewing, A. G. *Anal. Chem.* **1989**, *61*, 98-100.
32. Szulc, M. E.; Krull, I. S. *J. Chromatogr. A*. **1994**, *659*, 231-245.
33. Liu, J.; Hsieh, Y.-Z.; Wiesler, D.; Novotny, M. *Anal. Chem.* **1991**, *63*, 408-412.

34. Pentoney Jr., S. L.; Huang, X.; Burgi, D. S.; Zare, R. N. *Anal. Chem.* **1988**, *60*, 2625-2629.
35. Sweedler, J. V.; Shear, J. B.; Fishman, H. A.; Zare, R. N.; Scheller, R. H. *Anal. Chem.* **1991**, *63*, 496-502.
36. Hogan, B. L.; Yeung, E. S. *Anal. Chem.* **1992**, *64*, 2841-2845.
37. Olefirowicz, T. M.; Ewing, A. G., Detection methods in capillary electrophoresis, in *Capillary Electrophoresis*, Grossman, P. D., and Colburn, J. C., Eds., Academic Press, New York, Chap. 2, 1992.
38. Lawrence, J. F. *J. Chrom. Sci.* **1979**, *17*, 147-151.
39. Ohkura, Y.; Nohta, H. Fluorescence derivatization in high-performance liquid chromatography, in *Advances in Chromatography*, V. 29, Gidding, J. C., Grushka, E., and Brown, P. R., Eds., Marcel Dekker, New York, pp. 221-258, 1989.
40. Shear, J. B.; Fishman, H. A.; Albritton, N. L.; Garigan, D.; Zare, R. N.; Scheller, R. H. *Science* **1995**, *267*, 74-77.
41. Kennedy, R. T.; Oates, M. D.; Cooper, B. R.; Nickerson, B.; Jorgenson, J. W. *Science* **1989**, *246*, 57-63.
42. Gilman, S. D.; Pietron, J. J.; Ewing, A. G. *J. Microcol. Sep.* **1994**, *6*, 373-384.
43. Rose, D. J.; Jorgenson, J. W. *J. Chromatogr.* **1988**, *447*, 117-131.
44. Gilman, S. D.; Ewing, A. G. *Anal. Meth. Instrum.* **1995**, *2*, 133-141.
45. Kuhr, W. G.; Yeung, E. S. *Anal. Chem.* **1988**, *60*, 2642-2646.
46. Yeung, E. S.; Kuhr, W. G. *Anal. Chem.* **1991**, *63*, 275A-282A.
47. Regnier, F. E.; Patterson, D. H.; Harmon, B. J. *Trends. Anal. Chem.* **1995**, *14*, 177-181.
48. Wu, D.; Regnier, F. E. *Anal. Chem.* **1993**, *65*, 2029-2035.
49. Miller, K. J.; Leesong, I.; Bao, J.; Regnier, F. E.; Lytle, F. E. *Anal. Chem.* **1993**, *65*, 3267-3270.
50. Zubay, G. *Biochemistry*, 3rd Ed.; Wm. C. Brown Publishers: Dubuque, IA, p. 209, 1993.
51. Sprent, J.; Tough, D. F. *Science* **1994**, *265*, 1395-1400.

52. Ueno, K.; Yeung, E. S. *Anal. Chem.* **1994**, *66*, 1424-1431.
53. Lu, X.; Yeung, E. S. *Appl. Spectrosc.* **1995**, *49*, 605-609.



**CHAPTER 2****SEPARATION OF HEMOGLOBIN VARIANTS IN SINGLE HUMAN  
ERYTHROCYTES BY CAPILLARY ELECTROPHORESIS WITH LASER-  
INDUCED NATIVE FLUORESCENCE DETECTION**

A paper published in the *Journal of Chromatography*<sup>1</sup>

Sheri J. Lillard, Edward S. Yeung, Roy M. A. Lautamo<sup>2</sup> and David T. Mao<sup>2</sup>

**ABSTRACT**

Single human red blood cells, in which the hemoglobin (Hb) molecules exist in their native, tetrameric states, were analyzed. Upon injection and lysis of a cell, the tetramers were dissociated on-column into their respective polypeptide chains, separated, and detected by laser-induced native fluorescence detection with 275-nm excitation. This technique was applied to the determination of hemoglobin variants as found in adult (normal and elevated Hb A<sub>1</sub>) and fetal erythrocytes. Normal adult cells contained 9.6% and 4.8% glycated  $\beta$ - and  $\alpha$ -chains, respectively. Cells with elevated Hb A<sub>1</sub> gave 30% and 12%. The amounts of glycated Hb and total Hb in a given cell were found to be uncorrelated.

**INTRODUCTION**

The separation of hemoglobin (Hb) variants by CE represents a special challenge due to the similarities among the various hemoglobin molecules which are present in a human

---

<sup>1</sup>Reprinted with permission from *Journal of Chromatography A*, 718 (1995) 397-404.  
Copyright © 1995 Elsevier Science B. V.

<sup>2</sup>J&W Scientific, 91 Blue Ravine Road, Folsom, CA.

erythrocyte. The hemoglobin molecule exists as a tetramer of four polypeptide chains to each of which a heme group is attached. Human hemoglobin has an approximate molecular mass of 65,500 [1]. The main adult component, Hb A<sub>0</sub>, consists of two  $\alpha\beta$  dimers ( $\alpha_2\beta_2$ ) and comprises about 90% of the total hemoglobin content [2]. While genetic variants involve one or more differing amino acids in the protein sequence of one or both types of globin chains, other variants, such as Hb A<sub>1c</sub> arise from a post-translational modification [2]. In fact, Hb A<sub>1c</sub>, which constitutes roughly 5% of the total hemoglobin in normal erythrocytes, only differs from Hb A<sub>0</sub> by one glucose molecule attached to the N-terminal valine of each  $\beta$ -chain [2].

With more than 500 variants known to human hemoglobin [3], there are many hemoglobinopathies for which diagnosis is based on the detection of variants. Examples include the presence of the abnormal variant Hb S in sickle cell anemia [4] or the increased amount of Hb A<sub>2</sub> in  $\beta$ -thalassemia [5]. Hb A<sub>1c</sub> is known to be elevated two- to three-fold in untreated diabetes mellitus, and its monitoring serves to give a measure of long-term blood glucose control [6].

Additionally, Hb A<sub>1c</sub> may also be used to assess relative cell age. The life span of a circulating human erythrocyte is about 120 days [7,8]. Most studies, in which a comparison between a cellular constituent (or property) and cell age is made, utilize a density-gradient centrifugation method, such as that of Murphy [9]. In such a physical separation of cells, the more dense cells are presumed to be older, while the less dense cells correspond to the younger population. Fitzgibbons et al. conducted a study in which Hb A<sub>1a+b</sub> and A<sub>1c</sub> were determined as a function of cell density, and a positive correlation of the amounts was seen [10]. Glycohemoglobins were also determined by Elseweidy et al. [11], in which a dextran 40 density gradient centrifugation method was utilized. Glycohemoglobin amounts in both adult and fetal red blood cells were shown to increase with increasing cell density. Some investigators still question whether density centrifugation can truly separate cells on the basis of age, hence, the validity of correlations of density with cell age have remained somewhat ambiguous [8]. However, the mechanism by which glycohemoglobin is formed [2] makes

this class of compounds a good candidate for the determination of relative cell age in a population of cells, independent of density-based fractionations.

The total hemoglobin content in human erythrocytes is about 450 amol [12], of which Hb A<sub>1c</sub> is about 5% in normal adults, and 2-3 times higher in diabetics. This amount is sufficient to allow determination at the level of a single cell by employing a sensitive detection scheme such as laser-induced native fluorescence [13]. Determinations of single erythrocytes, when compared to a sample of lysed cells in which the average is assessed, allow subtle intercellular differences to be seen, which in turn may give further insights into the aging process.

Although CE has been utilized to efficiently separate hemoglobin variants and/or their corresponding globin chains, the absorption detection methods used with most of these studies would not permit low enough detection limits for single cell analysis [14-19]. Separations of globin chains under denaturing CE conditions, as well as intact genetic variants by cIEF, were demonstrated by Zhu et al. [14,15]. Ferranti et al. also separated normal globin chains by free-zone CE, utilizing a coated capillary [16]. The separation of Hbs A, F, S and C by free zone electrophoresis was demonstrated by Huang et al., in which a neutral, hydrophilic coated capillary was used [17]. Using a dynamic cIEF technique, Molteni et al. have separated Hb A<sub>1c</sub> from A<sub>0</sub> as well as from other variants [18]. Hempe and Craver used a similar cIEF approach to separate hemoglobins, including Hb A<sub>1c</sub> in blood samples [19]. However, they injected only 40-nL sample volumes, instead of filling 25-100% of the capillary length as in normal or dynamic cIEF [15,18].

In this work, we demonstrate a separation scheme based on free-zone electrophoresis for the separation of hemoglobin variants in single human erythrocytes. To our knowledge, this is the first report in which Hb variants were determined in single cells. Previous work involved the separation of Hb A<sub>0</sub> from carbonic anhydrase and methemoglobin in single human erythrocytes [13]. In the surfactant-based system described here, the Hb molecules are denatured on-column into their corresponding polypeptide chains. Hemoglobin variants from single human adults (normal and elevated Hb A<sub>1</sub>) and fetal red blood cells are separated and

identified. Capillary lifetime, as well as the effects of the cell suspension buffer, are also discussed.

### EXPERIMENTAL

The experimental set-up used in this work has been described elsewhere [13]. Briefly, 20- $\mu\text{m}$  I.D., 360- $\mu\text{m}$  O.D. fluorocarbon (FC)-coated experimental capillaries were used (J&W Scientific, Folsom, CA, USA). The total length is 75 cm (65 cm to the detector). A high-voltage power supply (Glassman High Voltage, Whitehorse Station, NJ; EH Series; 0-40 kV) was used for electrophoresis, with an applied voltage of +25 kV at the injection side. The capillary was rinsed with running buffer for *ca.* 1 hr, then equilibrated at +25 kV for an equivalent amount of time before use. The standards were injected hydrodynamically by raising the sample vial to a height of 11 cm relative to the detection end for 30 s. Electropherograms were recorded via a 24-bit A/D interface (ChromPerfect Direct, Justice Innovation, Palo Alto, CA, USA) and stored on a computer. Further peak analysis was performed by Peakfit (Jandel Scientific Software, San Rafael, CA).

An argon-ion laser (Spectra Physics, Mountain View, CA; Model 2045) was used as the excitation source, from which the 275.4-nm line was isolated with a prism. The laser was focused with a 1-cm focal length quartz lens onto the detection window. Two UG-1 color filters (Schott Glass Technologies, Duryea, PA) were used to reject scattered light and placed directly in front of the photomultiplier tube.

All chemicals were obtained from Fisher Scientific (Fair Lawn, NJ), unless otherwise noted. The running buffer for electrophoresis was 50 mM  $\text{H}_3\text{PO}_4$ , and 0.05% (w/v) fluorocarbon surfactant (FC, J&W Scientific, Folsom, CA), adjusted to  $\text{pH } 2.7 \pm 0.1$  with NaOH. Deionized water was used from a Waters Purification System (Millipore, Milford, MA). The buffer was filtered before use with a 0.22  $\mu\text{m}$  cutoff cellulose acetate filter (Costar, Cambridge, MA). Hemoglobin A<sub>0</sub> was purchased from Sigma Chemical (St. Louis, MO).

Normal adult erythrocytes were obtained from a presumably healthy female volunteer. Fetal erythrocytes (cord blood sample), and elevated Hb A<sub>1</sub> samples were drawn into EDTA-tubes and obtained from Mercy Hospital (Des Moines, IA). Phosphate buffered saline (PBS) was comprised of 135 mM NaCl and 20 mM  $\text{NaH}_2\text{PO}_4 \cdot \text{H}_2\text{O}$ ;  $\text{pH } 7.4$ . All cells

were treated the same way prior to injection: 20  $\mu\text{L}$  of whole blood was washed with PBS, centrifuged and the supernatant discarded. This procedure was repeated 5 times, after which the cells were resuspended in 8% (w/v) D-glucose. The cell injection procedure has been described previously [13,20]. Briefly, the injection end of the capillary was aligned by micro-positioners with the cell of interest, as confirmed visually in the field of view of a 100 $\times$  microscope. An air-tight syringe connected to the distal end of the capillary served to draw the cell into the capillary. Once injected, the capillary was placed in the buffer vials to initiate electrophoresis. The osmotic pressure inside the cell causes lysis when the buffer solution was drawn over the cell. If the same cell solution was to be used the following day, the glucose solution was washed away and the cells were suspended in PBS for refrigerated storage overnight.

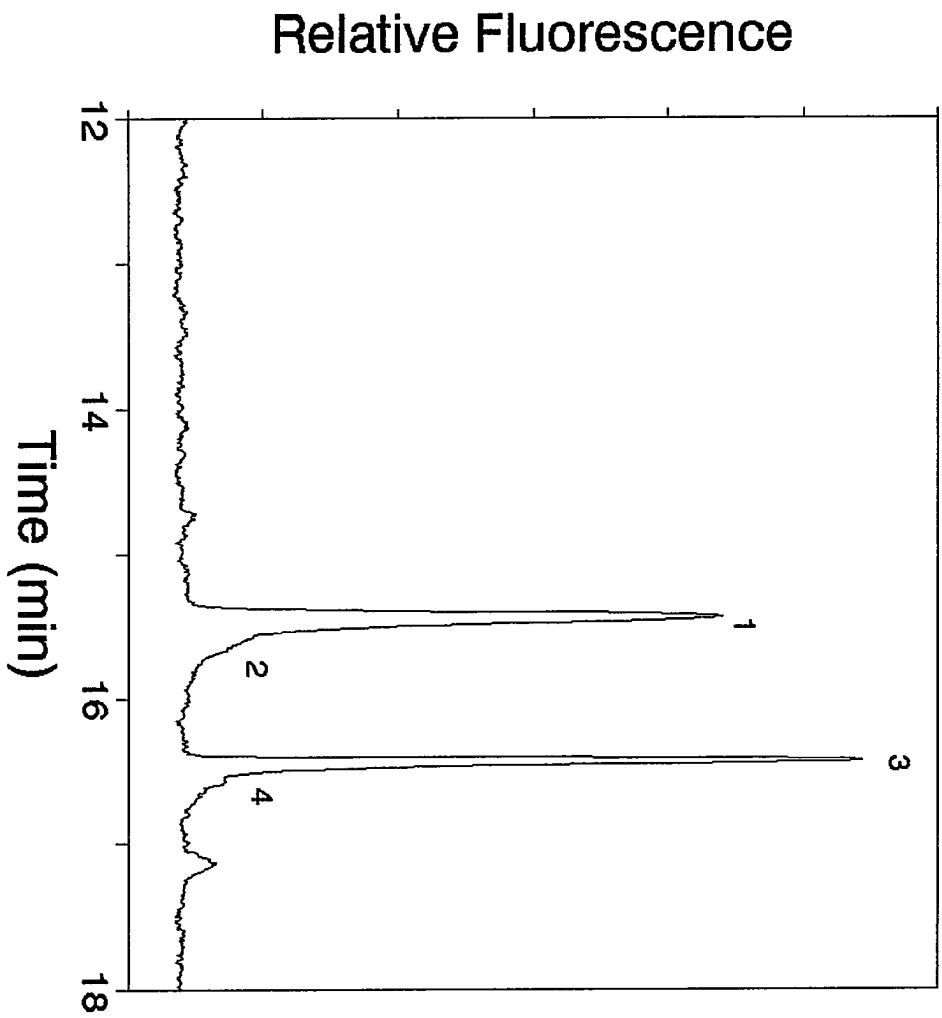
## RESULTS

### Electrophoretic Separation

In this work, a favorable environment for hemoglobin separation is created by an approach which is different from, but as effective as, focusing techniques. In Figure 1, an electropherogram of hemoglobin in single human erythrocytes (normal adult) is shown. The mechanism and important features of the separation are explained as follows. Firstly, a hydrophobic fluorocarbon coating is used, in which protein adsorption to the capillary wall is minimized. This is evident by the extremely narrow peak widths. The half-widths of the  $\beta$  and  $\alpha$  chains, are 0.09 and 0.06 min., respectively.

Secondly, a fluorocarbon surfactant (FC) is also added to the acidic ( $\text{pH} = 2.7 \pm 0.1$ ) running buffer. When a cell is introduced into the capillary, it is initially suspended in an isotonic solution of 8% glucose, hence, the hemoglobin molecules contained within are in their native, tetrameric state. Upon contact with the lower ionic strength running buffer, in which a surfactant is also present, the cell is easily lysed, and the hemoglobin molecules released. When these molecules are then exposed to the acidic, surfactant-containing running buffer, the protein is denatured (i.e., the tetramers are dissociated) and their constituent

Figure 1. Single red blood cell (normal adult). Peak identification: (1)  $\beta$ -, (2)  $\beta$ -glycated-, (3)  $\alpha$ -, and (4)  $\alpha$ -glycated-chains.



polypeptide chains are separated. Thirdly, the running buffer serves to oxidize the heme groups from the ferrous to the ferric state. This was demonstrated by adding Hb A<sub>0</sub> (ferrous) to a solution of running buffer. The color changed from red to brown immediately upon contact; this brown color is evidence that oxidation has taken place. Subsequent determinations of A<sub>0</sub> vs. methemoglobin revealed no differences in migration time (data not shown). Our previous results [13] showed that A<sub>0</sub> and methemoglobin have different electrophoretic mobilities. The simplicity of the electropherograms here confirm that only one form (the latter) exists in this buffer. Although we will continue to use the familiar Hb notation, it is clear that all variants are altered similarly. When the  $\alpha$ - and  $\beta$ -chains of A<sub>0</sub> were detected at 415-nm, a signal decrease of approximately two orders of magnitude was observed, versus 210-nm detection. It is apparent that with our conditions, essentially all heme groups dissociated from the polypeptide chains; the small signal at 415-nm being due to a relatively small number of chains which still contain the heme. We therefore conclude that the compounds which are separated and detected in this work are globin chains without the heme groups.

Although Hb A<sub>1c</sub> ( $\alpha_2(\beta\text{-glucose})_2$ ) is the major glycosylated hemoglobin in human red blood cells, glycosylation may occur at the N-terminus of the  $\alpha$  or  $\beta$  chain, or at the  $\epsilon\text{-NH}_2$  groups of specific lysine residues [2]. Like Hb A<sub>1c</sub>, these glycohemoglobins are also elevated in diabetics. In most cases, four peaks are evident in the adult erythrocytes studied. The first and third peaks correspond to the  $\beta$  and  $\alpha$  chains, respectively, while we can assign the second and fourth peaks to the  $\beta$ - and  $\alpha$ -glycosylated chains, respectively. Because any glycosylated polypeptide chain only differs from its respective unglycosylated form by one sugar molecule, it is expected that the glycosylated and unglycosylated chains will migrate very close to one another. Because Hb A<sub>1c</sub> is known to be the major glycosylated component, with glycosylation on the  $\beta$ -chain, this implies that peak 2 corresponds to the  $\beta$ -glycosylated chains, and peak 4 to the  $\alpha$ -glycosylated ones. The average amounts of  $\beta$ - and  $\alpha$ -glycosylated chains are 9.6% and 4.8%, respectively, of the total Hb.



Figure 2 shows the separation of Hb in a single adult erythrocyte containing an elevated amount of fast Hb ( $A_1 = A_{1a} + A_{1b} + A_{1c}$ , all of which are glycosylated at the  $\beta$ -N-terminus). This blood sample was independently assayed by the hospital, and was found to contain 16.2% fast Hb (i.e., Hb  $A_1$ ). The fact that peaks 2 and 4 are substantially larger in Figure 2 compared to Figure 1 is positive confirmation of our peak assignments. From our single-cell determinations, the relative  $\beta$ - and  $\alpha$ -glycosylated fractions were found to be 30% and 12%, respectively. Differences between the two types of assays may be explained as follows. Firstly, the fast Hb assay constitutes an average, whereas values from individual cells will display the heterogeneity of the cell population. Thus, the effects of glucose (or sugar) exposure can be seen, probably reflecting the cell age. Secondly, there can be additional glycohemoglobin chains present in peak 2, other than those of the fast Hbs. This would also give rise to a higher observed amount over the assayed value.

Structural differences in the hemoglobin variants give rise to unique information from the electropherograms. Approximately 80% of the total hemoglobin in the fetal erythrocyte is hemoglobin F ( $\alpha_2\gamma_2$ ), with about 10% of Hb F existing as the acetylated metabolite, F<sub>1</sub> ( $\alpha_2(\gamma\text{-acetyl})_2$ ) [21]. It is also known that there are two structural genes for the  $\gamma$  chain, as residue 136 may either be glycine ( $G_\gamma$ ) or alanine ( $A_\gamma$ ). At birth, these are present in the ratio of 3  $G_\gamma$ :1  $A_\gamma$  [21]. Figure 3 shows the separation of hemoglobins from a single fetal erythrocyte. The first peak corresponds to the  $\gamma$ -chains while the second one is probably a variant of Hb F, since it appears in neither the A<sub>0</sub> standard sample nor the adult cells. The total Hb F content (Peaks 1 + 2) is 78%, of which peak 2 is 9%. Therefore, we have identified peak 2 tentatively as Hb F<sub>1</sub>, which agrees with the literature value, rather than a genetic variant. As with the glycosylated chains, the acetylated chain migrates very close to the unacetylated form. Peak 3 corresponds to the  $\beta$  chain, and is present at about 22%. Because the  $\beta$  and both of the  $\gamma$  peaks only correspond to one variant each, the percentages of the globin chains are considered equal to the percentage of the intact variant. Finally, the fourth peak corresponds to the alpha chain, as in all other electropherograms. The peak identities in Figure 3 were confirmed by coinjections of hemoglobin standards (A, A<sub>2</sub>, S, F), as compared

Figure 2. Single red blood cell (diabetic adult; i.e., elevated Hb A<sub>1</sub>). Peak identification: (1)  $\beta$ -, (2)  $\beta$ -glycated-, (3)  $\alpha$ -, and (4)  $\alpha$ -glycated-chains.

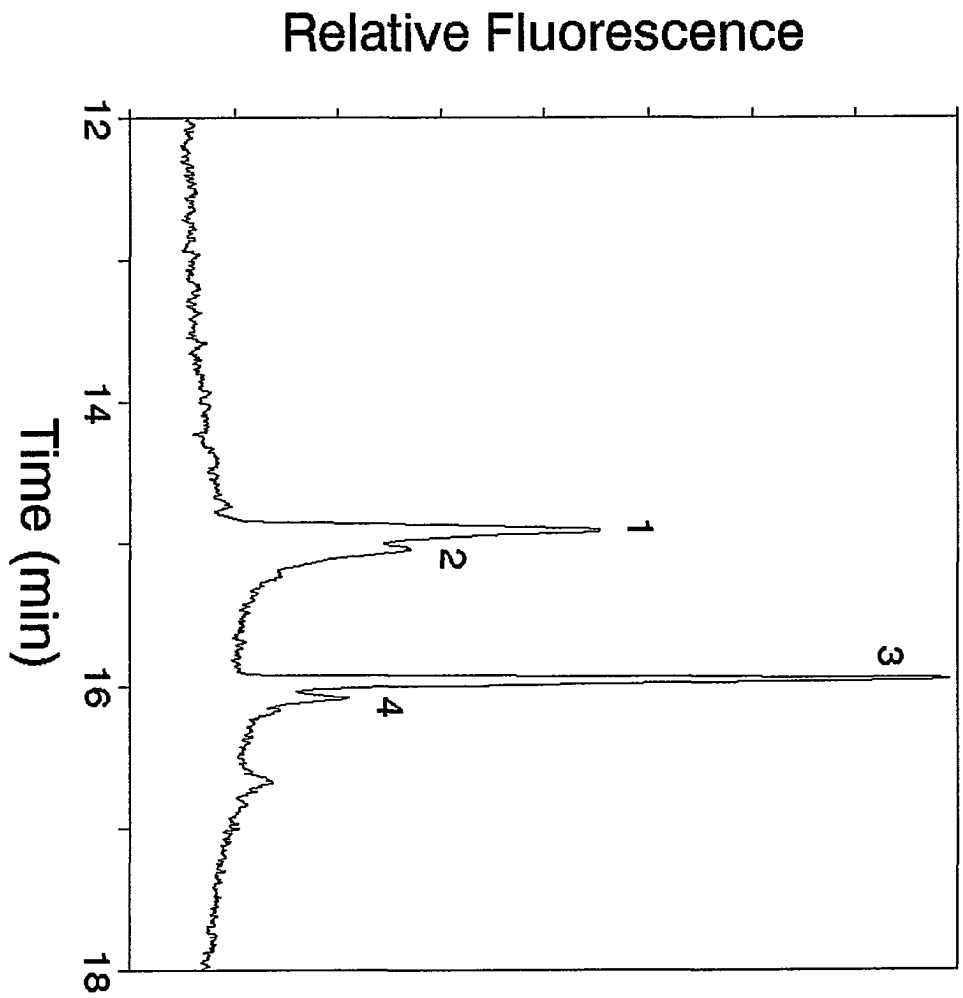
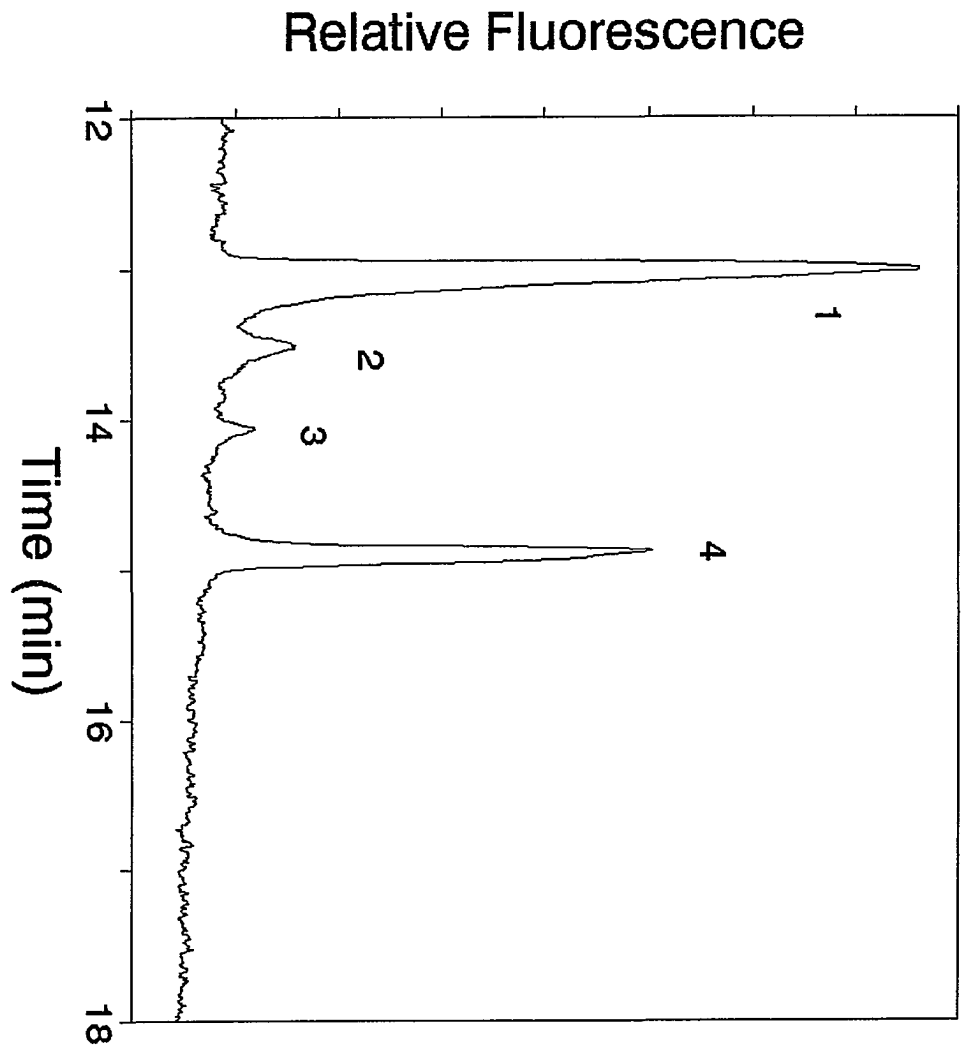


Figure 3. Single fetal red blood cell. Peak identification: (1)  $\gamma$ -, (2)  $\gamma$ -acetyl-, (3)  $\beta$ -, and (4)  $\alpha$ -chains.

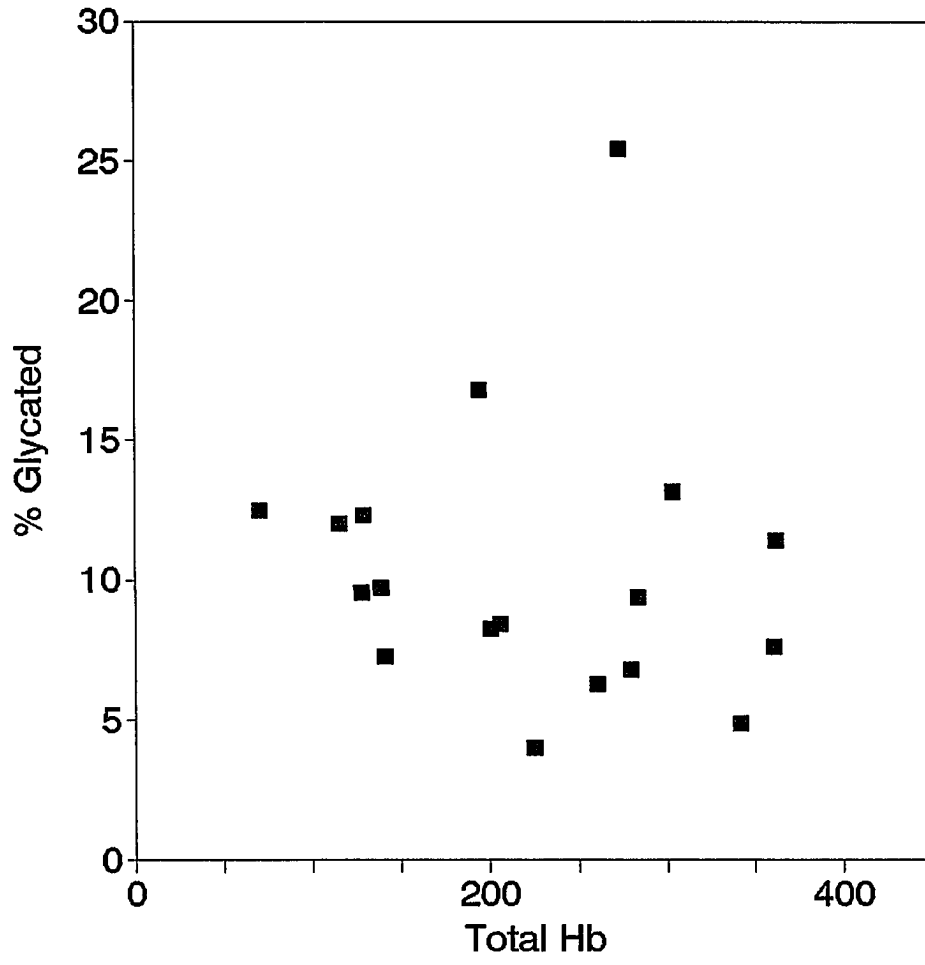


to clinical samples with known Hb C and G variants (200-nm absorption detection; data not shown). The assignments given to the peaks from single cells are consistent with those of the standards. It is interesting to note that the migration order of the globin chains in this work is reversed compared to other reports [14,16], under seemingly similar conditions. The elution order appears to depend on the specific composition of the buffer components. When a sample of Helena Hb standard was pretreated by (a) dilution in water, (b) acidified acetone to remove the heme groups with dilution in water, or (c) dissolution in 7 M urea and 0.2% FC, no changes in the electropherograms were observed. When a polyacrylamide (PA) coated capillary was used in conjunction with a pH 3.0 phosphate buffer, the elution order was again identical even though the resolution becomes poorer. However, when 7 M urea was added to our running buffer (either PA or FC coated columns), the elution order was reversed (i.e. became identical to ref. 14 and 16). We further found that adding urea changed the pH of the buffer from 3.0 to 4.15 (apparent value). Since the pK of the carboxyl groups is around 4.5, the reversed elution order is not unexpected. Finally, the results of ref. 16 (without urea) are probably due to a higher than expected pH in the running buffer.

Because all the hemoglobin subfractions in the fetal cell presumably contain the normal  $\alpha$ -chain, it is expected that its peak area should be the highest. This is what is seen for lysed [cord blood] erythrocytes using 210-nm absorption detection (data not shown). With native LIF detection, the fluorescence efficiency of the polypeptide chains depends on the aromatic amino acid residues, primarily tryptophan. The number of tryptophan, tyrosine, and phenylalanine residues are, respectively, 3, 4, and 7 for the  $\gamma$ -chain, 2, 3, and 7 for the  $\beta$ -chain, and 1, 3, and 6 for the  $\alpha$ -chain [23]. This is the primary reason the peak corresponding to  $\gamma$  (Figure 3) is larger than that of  $\alpha$ .

In Figure 4, the amount of glycosylated Hb (measured as glycosylated  $\beta$ -chain amount) is plotted against total Hb, for the adult cells. These amounts are shown to be uncorrelated with each other. As a cell ages, the amount of glycosylated hemoglobin is increased, however, the amount of total hemoglobin is not decreased. This means that total hemoglobin content is not a function of cell age, and as a cell circulates, loss of hemoglobin occurs by another mechanism. We note that there is a large variation in the amounts of total hemoglobin from

Figure 4. Correlation between the fraction of glycated  $\beta$ -chain and the total Hb in different red blood cells in a normal adult.





cell to cell. This is consistent with our earlier study [13], and confirms that the intercellular variations, in this study and in the earlier study, are not due to artifacts of either experiment.

### **Effect of Cell Suspension Solution**

The primary concern, when choosing a cell-suspension solution, is one that is isotonic, such that the integrity of the cells is maintained during storage. The PBS solution in which the cells are washed normally serves this purpose well. However, with our system, the high salt concentration (135 mM NaCl) caused severe broadening and distortions in peak shape in the electropherograms. In the separations of Hb A<sub>0</sub> chains as a function of solvent, the  $\beta$ -chain peak half-width increased from  $0.087 \pm 0.005$  to  $0.181 \pm 0.007$  min for 8% glucose and PBS, respectively; the  $\alpha$ -chain peak half-width increased from  $0.055 \pm 0.004$  to  $0.202 \pm 0.011$  min. This effect is likely due to localized heating (due to the high salt concentration) or disturbance of the capillary coating/surfactant equilibrium by the same matrix. Another possibility is that a reverse stacking effect is occurring; the more slowly traveling molecules speed up when the running buffer is contacted, thus broadening the zones. Satow et al. also reported a similar effect of severe peak broadening for samples containing high salt concentrations [22].

### **Capillary Life**

The fluorocarbon capillary coating has been shown to be extremely rugged. One capillary can be used for several months, with regeneration possible should the separation efficiency start to degrade. Electroosmotic flow does change from one capillary to another, and changes gradually as a function of use, as evident in the migration times in Figure 1-3. Normalization of the migration times based on standards is a solution, but is not implemented here because of the simplicity of the electropherograms. Several things become apparent when the capillary starts to break down. Normally, the alpha and beta chain peaks of Hb A<sub>0</sub> (a standard) are approximately equal in peak height. When the coating begins to degrade, the beta peak becomes very short and broadens, while the alpha peak always remains sharp and at a constant height.

When this phenomenon occurs, the column can be regenerated in one of two ways. Firstly, the capillary can be flushed with a higher percentage surfactant buffer (e.g., 1% FC) for more than one hour, as recommended by the manufacturer for 50- $\mu$ m capillaries. However, in our experience, this did not seem to be effective for small I.D. capillaries. Alternatively, we have found that filling the capillary with the running buffer (50 mM phosphate, pH 2.7, 0.05% FC-surfactant) and leaving that inside (without flow) for several hours to several days seems to regenerate the capillary. When poor resolution developed in one capillary, precluding its further use, it was stored for more than one month filled with the running buffer. After this length of time, with static-regeneration, it was put to use again, with acceptable performance.

With this combination of coating and buffer, it seems that an important factor towards good performance is letting the surfactant molecules diffuse to coat the capillary wall on their own—without the influence of pressure or potential, as is typically used to equilibrate capillaries. Naturally, this results in a much slower equilibration, but its effectiveness seems to outweigh the time it takes to regenerate the column. It does not take weeks, however, to regenerate a capillary. In most cases, several hours, or overnight, is sufficient time to allow the performance to return to normal.

## CONCLUSIONS

This separation system, in which hemoglobin molecules are denatured on-column to their respective polypeptide chains has shown to be an effective technique for the separation of hemoglobin variants in single human erythrocytes. Fetal, normal adult and elevated Hb A<sub>1</sub> adult red blood cells were analyzed, with the corresponding (oxidized) polypeptide chains determined at the attomole level. Glycated Hb fractions were identified, and confirmation was made by noting the overall increase in diabetic cells versus normal ones. In a given cell, the amount of glycated chains was found to be uncorrelated with total hemoglobin amount. It is concluded that loss of hemoglobin from a cell is independent of cell age, since glycated-Hb is known to increase with the length of time the cell is in circulation. The 20- $\mu$ m capillaries

that were used in this study are still in the development stages, thus one would expect even better performance once reproducible manufacturing protocols are implemented.

### ACKNOWLEDGMENTS

The authors wish to thank Ms. Carol Deal Eilers at Mercy Hospital in Des Moines, Iowa, for donation of and assistance with the fetal and diabetic blood samples. In addition, we would like to acknowledge Phillips Petroleum Co. for a graduate fellowship. The Ames Laboratory is operated for the U.S. Department of Energy by Iowa State University under Contract No. W-7405-Eng-82. This work was supported by the Director of Energy Research, Office of Basic Energy Sciences, Division of Chemical Sciences.

### REFERENCES

1. R. E. Dickerson and I. Geis, *Hemoglobin*, 1983, Benjamin/Cummings, Menlo Park, p. 21.
2. H. F. Bunn in D. F. H. Wallach (Editor), *The Function of Red Blood Cells: Erythrocyte Pathobiology*, 1981, Alan R. Liss, New York, pp. 223-239.
3. H. G. Bunn and B. G. Forget, *Hemoglobin: Molecular, Clinical and Genetic Aspects* (1986), pp. 381-451, W. B. Saunders, Philadelphia.
4. H. F. Bunn, B. G. Forget and H. M. Ranney, *Hemoglobinopathies*, 1977, W. B. Saunders, Philadelphia, p. 131.
5. H. F. Bunn, B. G. Forget and H. M. Ranney, *Hemoglobinopathies*, 1977, W. B. Saunders, Philadelphia, p. 2.
6. H. F. Bunn, K. H. Gabbay and P. M. Gallop, *Science*, 200 (1978) 21-27.
7. P. M. Ness and J. M. Stengle in D. M. Surgenor (Editor), *The Red Blood Cell*, 1974, Academic Press, New York, v. 1, pp. 22-24.
8. M. R. Clark, *Physiol. Reviews*, 68 (1988) 503-554.
9. J. Murphy, *J. Lab. Clin. Med.*, 82 (1973) 334-341.
10. J. F. Fitzgibbons, R. D. Koler and R. T. Jones, *J. Clin. Invest.*, 58 (1976) 820-824.

11. M. M. Elseweidy, M. Stallings and E. C. Abraham, *J. Lab. Clin. Med.*, 102 (1983) 628-636.
12. R. B. Pennell in D. M. Surgenor (Editor), *The Red Blood Cell*, Academic Press, New York, v. 1, pp. 100-101.
13. T. T. Lee and E. S. Yeung, *Anal. Chem.*, 64 (1992) 3045-3051.
14. M. Zhu, R. Rodriguez, T. Wehr and C. Siebert, *J. Chromatogr.*, 608 (1992) 225-237.
15. M. Zhu, T. Wehr, V. Levi, R. Rodriguez, K. Shiffer and Z. A. Cao, *J. Chromatogr.*, 652 (1993) 119-129.
16. P. Ferranti, A. Malorni, P. Pucci, S. Fanali, A. Nardi and L. Ossicini, *Anal. Biochem.*, 194 (1991) 1-8.
17. T. L. Huang, P. C. H. Shieh and N. Cooke, *J. High Resol. Chrom.*, 17 (1994) 676-678.
18. S. Molteni, H. Frischknecht and W. Thormann, *Electrophoresis*, 15 (1994) 22-30.
19. J. M. Hempe and R. D. Craver, *Clin. Chem.*, 40 (1994) 2288-2295.
20. B. L. Hogan and E. S. Yeung, *Anal. Chem.*, 64 (1992) 2841-2845.
21. H. Lehmann and R. G. Huntsman, *Man's Haemoglobins*, 1974, North Holland Publishing Co., Oxford, p. 61.
22. T. Satow, A. Machida, K. Funakushi and R. Palmieri, *J. High Resol. Chrom.*, 14 (1991) 276-279.
23. H. Lehmann and P. A. M. Kynoch, *Human Haemoglobin Variants and Their Characteristics* (1976), pp. 13-19, North Holland Publishing Co., Amsterdam.

**CHAPTER 3****ANALYSIS OF SINGLE ERYTHROCYTES BY  
INJECTION-BASED CAPILLARY ISOELECTRIC FOCUSING  
WITH LASER-INDUCED NATIVE FLUORESCENCE DETECTION**

A paper submitted to the Journal of Chromatography

Sheri J. Lillard and Edward S. Yeung

**ABSTRACT**

A modified version of capillary isoelectric focusing (cIEF) was developed to separate hemoglobin variants contained within single human erythrocytes. Laser-induced native fluorescence with 275-nm excitation was used to detect the separated hemoglobins. In this method, baseline fluctuations were minimized and detection sensitivity was improved by using dilute solutions of anolyte, catholyte, and carrier ampholytes (with methylcellulose). Since electroosmotic flow was used for mobilization of the focused bands, separation and detection were integrated into a single step. The capillary was first filled with only ampholyte solution, and the cell (or standard) was injected as in capillary zone electrophoresis. The ~ 90 fL injection volume for individual cells is  $7 \times 10^4$ -times lower than those previously reported. Adult (normal and elevated A<sub>1</sub>), sickle (heterozygous), and fetal erythrocytes were analyzed, with the amounts of hemoglobins A<sub>0</sub>, A<sub>1c</sub>, S and F determined. The pH gradient for cIEF was linear ( $r^2 = 0.9984$ ), which allowed tentative identification of Hb F<sub>ac</sub>. Variants differing by as little as 0.025 pI units were resolved.

## INTRODUCTION

Capillary isoelectric focusing (cIEF) is a high-resolution mode of capillary electrophoresis (CE), in which amphoteric species (e.g., proteins) are separated according to their isoelectric points (pI). Several modes of cIEF now exist, however, the basic mechanism remains the same. The pH gradient is obtained by filling the capillary with carrier ampholytes—amphoteric substances which are neutral over a specified pH range. Acid is placed in the anodic (injection side) buffer vial, and base in the cathodic vial. Upon application of the electric field, a pH gradient is established along the capillary. Proteins migrate to the point at which pH equals pI and stop (i.e., focus). The focused bands are then detected, usually by a mobilization step in which they are swept toward the detector.

The high efficiency of this technique is well suited for the determination of hemoglobin (Hb) variants. Due to the difficulty in separating Hb by CE, most high resolution Hb separations are done by cIEF. However, there are a few reports in which Hb has been separated by capillary zone electrophoresis. The determination of globin chains using coated capillaries and denaturing conditions has been performed starting from Hb solutions [1-4] as well as from individual erythrocytes [5]. Intact Hb variants have been separated by reducing electroosmotic flow (EOF) with a coated capillary [6], as well as with uncoated capillaries using Tris, borate or barbital buffers [3,7].

Highly efficient separations of Hb variants by conventional cIEF have been demonstrated [1-2,8-15]. In these examples, the ampholytes are mixed with the sample, and the entire capillary is filled with protein. Typically, coated capillaries are used to eliminate EOF, so that when the proteins focus, they remain stationary. Subsequent mobilization is then necessary to sweep the zones past the detector. Cathodic [1-2,8-9], anodic [11,16], or pressure [16] mobilization steps are common when EOF is zero. In some cases, EOF is sufficient to focus and mobilize proteins in a single step. This has been demonstrated both in coated capillaries, in which EOF is reduced [9,14,17], and in bare fused-silica capillaries [18,19]. When bare capillaries are used, the addition of a dynamic polymer coating (e.g., methylcellulose) helps to reduce electroosmotic flow, as well as to prevent adsorption of proteins to the capillary wall.

Detection for conventional cIEF is typically based on on-line absorbance, however, laser-induced fluorescence (LIF) was used by Shimura and Kasai for the detection of labeled peptides [20]. Foret et al. have used a combination of hydrodynamic flow and EOF to mobilize and elute Hb variants into a fraction collector, for subsequent analysis by mass spectrometry (MS) [13]. Pawliszyn et al. have developed concentration gradient detectors [21-24] in combination with short capillaries. They have extended this detection scheme to allow imaging of the focused bands with a CCD camera [25]. Recently, they have developed an imaging detector for cIEF based on fluorescence [26], and a similar method for the absorption imaging of Hb [15].

The cIEF conditions in the reports described above provide efficient separations of Hb variants for sample volumes  $> 100$  nL. However, such volumes preclude the analysis of single mammalian cells, which are around 1 pL in volume. Lower injection volumes are necessary, and several reports have demonstrated the use of sample volumes substantially less than the entire volume of the capillary. One mode of cIEF was developed by Thormann et al., in which only a fraction of the capillary is filled with sample [27-30]. This method, termed dynamic cIEF, utilizes an uncoated capillary and a polymeric additive, hence, EOF mobilization. Hemoglobins were successfully separated with this method. Smaller volumes ( $\sim 40$  nL) of Hb variants were injected and separated by Hempe and Craver [31]. However, the lowest injection volume reported thus far is 6.5 nL for the separation of RNase proteins by Chen and Wiktorowicz [32]. Both reports [31,32] utilized coated capillaries, relying on a combination of EOF and pressure to mobilize the proteins. Naturally, injection-based cIEF depends on the favorable mobility of the analyte, such that it reaches the focusing zone ( $\text{pH} = \text{pI}$ ) before mobilization carries the zone beyond the detection window.

In this work, we report a separation scheme based on cIEF in which a single red blood cell (i.e.,  $\sim 90$  fL) is injected. To our knowledge, this represents the lowest volume for a sample in cIEF. Native LIF detection is used to determine hemoglobin variants in normal, diabetic, and sickle adult erythrocytes, as well as fetal (cord blood) erythrocytes.

## EXPERIMENTAL

The experimental instrumentation used in this work has been described previously [5]. Briefly, a 21- $\mu\text{m}$  I.D., 360- $\mu\text{m}$  O.D. bare capillary was used (Polymicro Technologies, Phoenix, AZ), with a total length of 40 cm (30 cm to detector). Electrophoresis was driven by a high-voltage power supply (Glassman High Voltage, Whitehorse Station, NJ; EH Series; 0-40 kV). The applied voltage was +24 kV at the injection end, and was constant during the entire separation (i.e., focusing and mobilization). Before each run, the capillary was rinsed with 20 mM NaOH for 5 min, then rinsed (5 min) and filled with the ampholyte mixture. The ampholyte solution consisted of 0.5% Ampholine, pH 5.0-8.0 (Pharmacia, Uppsala, Sweden) and 0.1% methylcellulose, 25 cp (Aldrich, Milwaukee, WI). A 24-bit A/D interface (ChromPerfect Direct, Justice Innovation, Palo Alto, CA) was used to record electropherograms which were stored on a computer.

The 275.4-nm line of an argon-ion laser (Spectra Physics, Mountain View, CA; Model 2045) was isolated with a prism and used as the excitation source. The laser was focused with a 1-cm focal length quartz lens onto the capillary. Fluorescence was collected with a 10 $\times$  microscope objective (Edmund Scientific, Barrington, NJ) and passed through two UG-1 color filters (Schott Glass Technologies, Duryea, PA) onto a photomultiplier tube.

Unless otherwise noted, all chemicals were obtained from Fisher Scientific (Fair Lawn, NJ). The anolyte and catholyte were 1 mM  $\text{H}_3\text{PO}_4$  and 2 mM NaOH, respectively. Before each run they were prepared fresh from stock solutions of 10 mM  $\text{H}_3\text{PO}_4$  and 1 M NaOH, and filtered with 0.22- $\mu\text{m}$  cutoff cellulose acetate filters (Costar, Cambridge, MA).

Hemoglobin  $\text{A}_0$  standard (Sigma Chemical, St. Louis, MO) was injected hydrodynamically by raising the sample vial to a height of 11 cm relative to the detection end for 10 s ( $\sim 0.14$  nL injected volume). Sickel-Trol sickle cell hemoglobin controls (normal adult and sickle cell erythrocyte suspensions) were purchased from Dade International (Miami, FL). Fetal (cord blood sample) and adult (elevated  $\text{A}_1$ ) erythrocytes were obtained from Mercy Hospital (Des Moines, IA). All cells were washed in the same way prior to injection: 10  $\mu\text{L}$  of whole blood or erythrocyte suspensions were washed with phosphate



buffered saline (PBS), which consisted of 135 mM NaCl and 20 mM  $\text{NaH}_2\text{PO}_4$ ; pH 7.4. The cells were then centrifuged and the supernatant discarded. This procedure was repeated at least 5 times, with the cells finally suspended in a solution of PBS.

The procedure for injecting individual cells is the same as described previously [5]. Because high salt concentration can be detrimental to cIEF, approximately 200  $\mu\text{L}$  of 8% (w/v) glucose was placed on a microscope slide. The inlet end of the capillary was inserted into this drop, then 10  $\mu\text{L}$  of cell solution (PBS) was placed on the slide near the capillary tip. A septum was placed over the outlet buffer vial to create an air-tight seal, into which a syringe needle was inserted. By applying gentle suction, one cell was injected and visually confirmed under the microscope. Following cell injection, the inlet end of the capillary was immersed in its buffer vial and electrophoresis initiated.

## RESULTS

### Hemoglobin Separations

The distinction between our cIEF protocol and others is the amount of sample injected into the capillary. Most previous reports have used absorption detection, where limitations in detectability have influenced the development of separation conditions. With less sensitive detection, a greater amount of sample must be introduced into the capillary (whether it is filled or injected). The separation mechanism depends critically on the integrity of the pH gradient and the ability of the ampholytes to buffer and focus the proteins. Therefore, it is not surprising that significantly altering the injected sample amount would require manipulation of the separation conditions.

In cIEF methods published thus far, anolyte and catholyte concentrations are at least 10 mM  $\text{H}_3\text{PO}_4$  and 10 mM NaOH, respectively. These are typically used in conjunction with ampholyte concentrations of  $> 1\%$  [1-2,8-12,31], although lower concentrations [10-13,19,32] have been used. Likewise, when methylcellulose (MC) is used as an additive in either coated or uncoated capillaries, typical concentrations are greater than 0.2% [9,12,31-32], although 0.1% MC has been used [12,19]. When uncoated capillaries were used at near

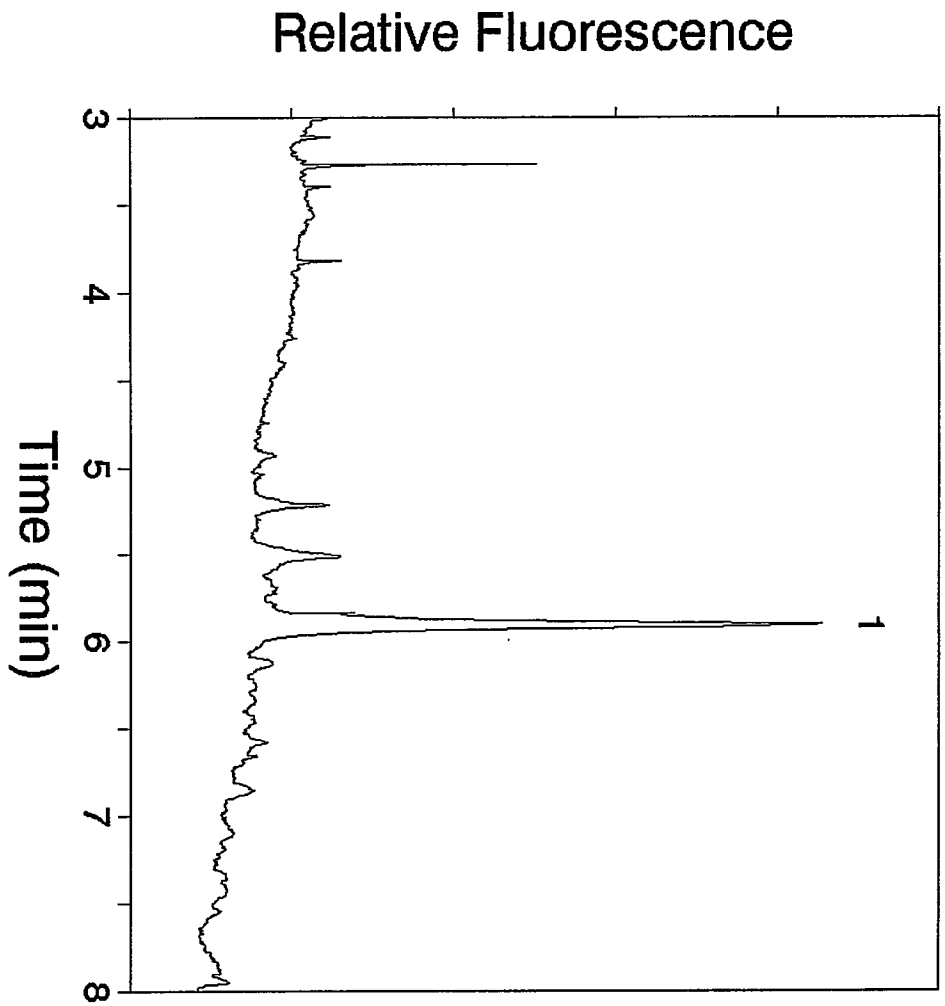
neutral pH, it was found that significant protein adsorption caused the pH gradient to deviate from linearity with decreasing MC concentration [12].

The above observations are probably indicative of the higher analyte concentrations used. Anolyte and catholyte concentrations must also be sufficient to allow a stable pH gradient to be formed. Furthermore, a certain level of ampholytes must be present to maintain the pH gradient, and to buffer and focus higher concentrations of proteins.

Native LIF detection of Hb from single red blood cells has been demonstrated previously for CE [5,33]. However, typical concentrations of ampholytes and MC in cIEF presented detection problems. For example, when 0.4% MC-25 and 1% Ampholine (pH 5-8) were used with anolyte and catholyte concentrations of 10 mM  $\text{H}_3\text{PO}_4$  and 20 mM NaOH, respectively, good separations of the variants from standard samples were seen (data not shown). However, baseline instability did not allow the detection sensitivity required for the analysis of single cells. When the concentration of the ampholyte mixture was decreased to 0.1% MC-25 and 0.5% Ampholine to improve detectability (with identical anolyte and catholyte), peak integrity was compromised and often even double peaks were seen for  $A_0$ . With the lower concentration of ampholytes in the capillary, hence, lower buffering capacity, 10 mM  $\text{H}_3\text{PO}_4$  may have been sufficient to partially dissociate the Hb molecules, which were also present in low amounts.

In order to retain detection sensitivity, 0.1% MC-25 and 0.5% Ampholine were chosen as our final ampholyte mixture. However, to prevent Hb dissociation, the anolyte and catholyte concentrations were decreased to 1 mM  $\text{H}_3\text{PO}_4$  and 2 mM NaOH, respectively. Anolyte and catholyte were prepared fresh before each run, to ensure that the pH of these solutions remained consistent despite the low buffering capacity. In Figure 1, an electropherogram for Hb  $A_0$  (standard) is shown in which these dilute conditions are used. The injected amount is about 290 amol, which is less than the 450 amol of Hb in an individual erythrocyte [34]. Since this is about 10,300 $\times$  less Hb injected than previously reported [31], it is reasonable that higher MC and ampholyte concentrations are not necessary to successfully focus such low amounts of Hb.

Figure 1. Hemoglobin A<sub>0</sub> standard (peak 1),  $2 \times 10^{-6}$  M (0.14 nL injection). LOD is  $3 \times 10^{-8}$  M, or 4 amol (S/N = 2).



This dilute system was then applied to the analysis of individual erythrocytes containing different types of Hb variants. At least two single cell runs were performed for each cell type to confirm the peak patterns, however, only the data from the electropherograms displayed here were analyzed. Figure 2 is the analysis of a normal adult erythrocyte. Figure 3 is the separation of Hb A<sub>0</sub> and A<sub>1c</sub> from a patient containing elevated Hb A<sub>1</sub>. This sample was independently assayed by the hospital to give an A<sub>1</sub> value of 16.4%. We have identified peak 2 as A<sub>1c</sub>, and determined it to be 12% of the total Hb (i.e., peaks 1 + 2). This differs from the hospital assay because Hb A<sub>1</sub> is comprised of several glycosylated forms of Hb, of which A<sub>1c</sub> is the major component. Also, it is expected that the amount of a component determined in single cells will deviate from the average (bulk) value.

Other types of human red blood cells were also studied with these conditions. A single sickle cell was analyzed and is shown in Figure 4. This type of cell is heterozygous for the sickle trait, which means that the cell produces both Hb S and A<sub>0</sub> in approximately equal amounts. Our analysis revealed the amounts of Hb S and A<sub>0</sub> to be 44.7% and 55.3%, respectively. Figure 5 shows the Hb separation from a single fetal (cord blood sample) erythrocyte in which Hb F and A<sub>0</sub> (peaks 1 and 2, respectively) were identified. Linearity of the pH gradient is described in the following section, and is shown in Figure 6. Based on this linear regression, peak 3 was tentatively identified as acetylated fetal hemoglobin (Hb F<sub>ac</sub>) with a calculated pI of 6.914, compared to a literature value of 6.911 [31]. In Fig. 5, total Hb F (i.e., peaks 1 + 3) is 73.3%, of which F<sub>ac</sub> is 12.4%. Hb A<sub>0</sub> comprised 26.7% of the total Hb in this cell, which is in agreement with literature values.

### **Linearity of the pH Gradient**

The linearity of the pH gradient is shown in Figure 6 (solid line). It was determined by plotting relative migration times (vs. A<sub>0</sub>) of the Hb variants in single cells as a function of literature values of pI [31]. The relative migration times of S, F, A<sub>0</sub> and A<sub>1c</sub> were 0.926, 0.976, 1.000 and 1.014, respectively. Linear regression analysis revealed respective pI values of 7.209 (7.207), 7.054 (7.060), 6.979 (6.974) and 6.935 (6.936); parenthetical quantities are

Figure 2. Single red blood cell (normal adult). Peak 1 is Hb A<sub>0</sub>.

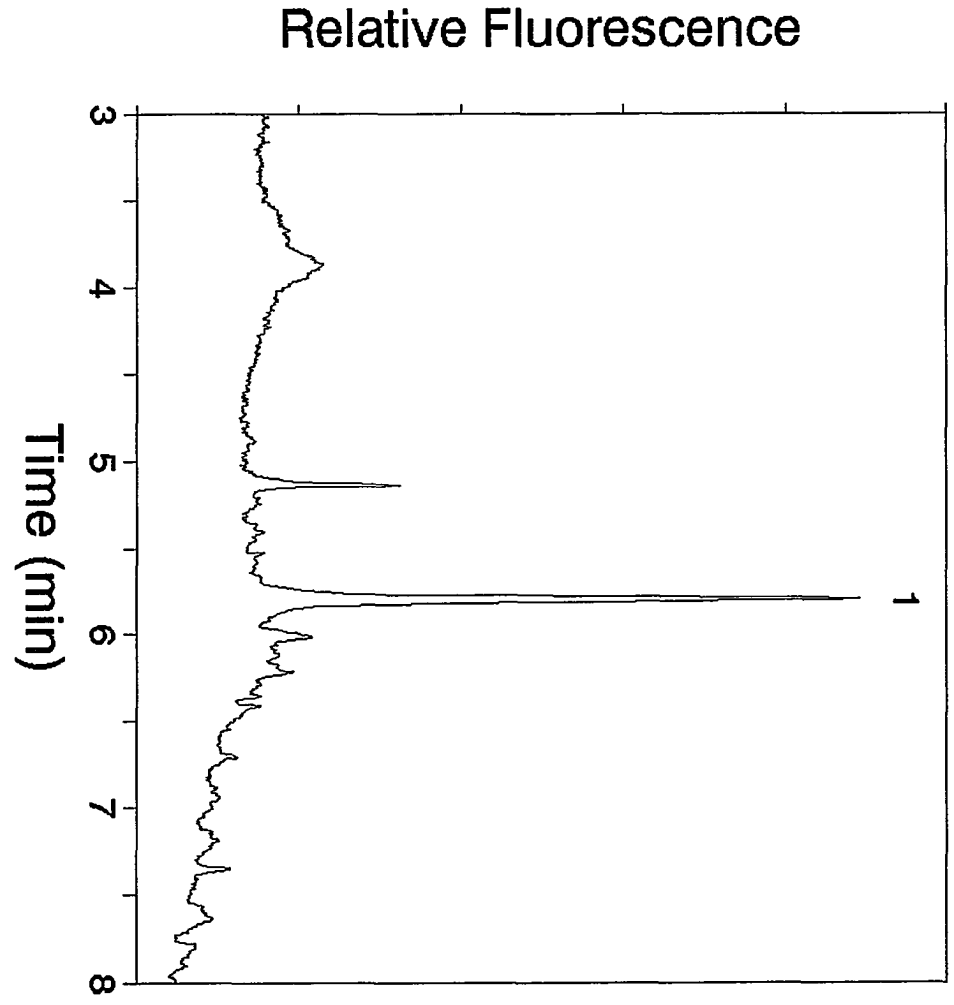


Figure 3. Single red blood cell (elevated  $A_1$ ). Hb peak identification: (1)  $A_0$ , (2)  $A_{1c}$ .



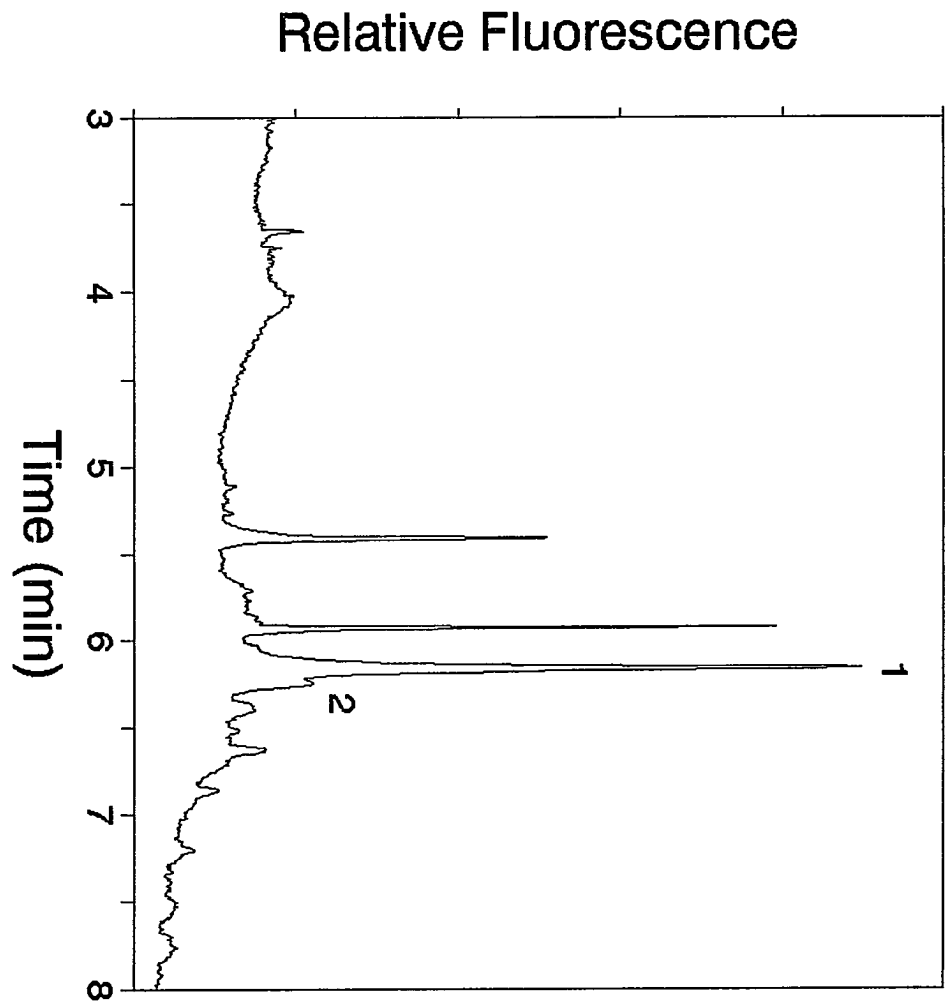


Figure 4. Single sickle red blood cell. Hb peak identification: (1) S, (2) A<sub>0</sub>.

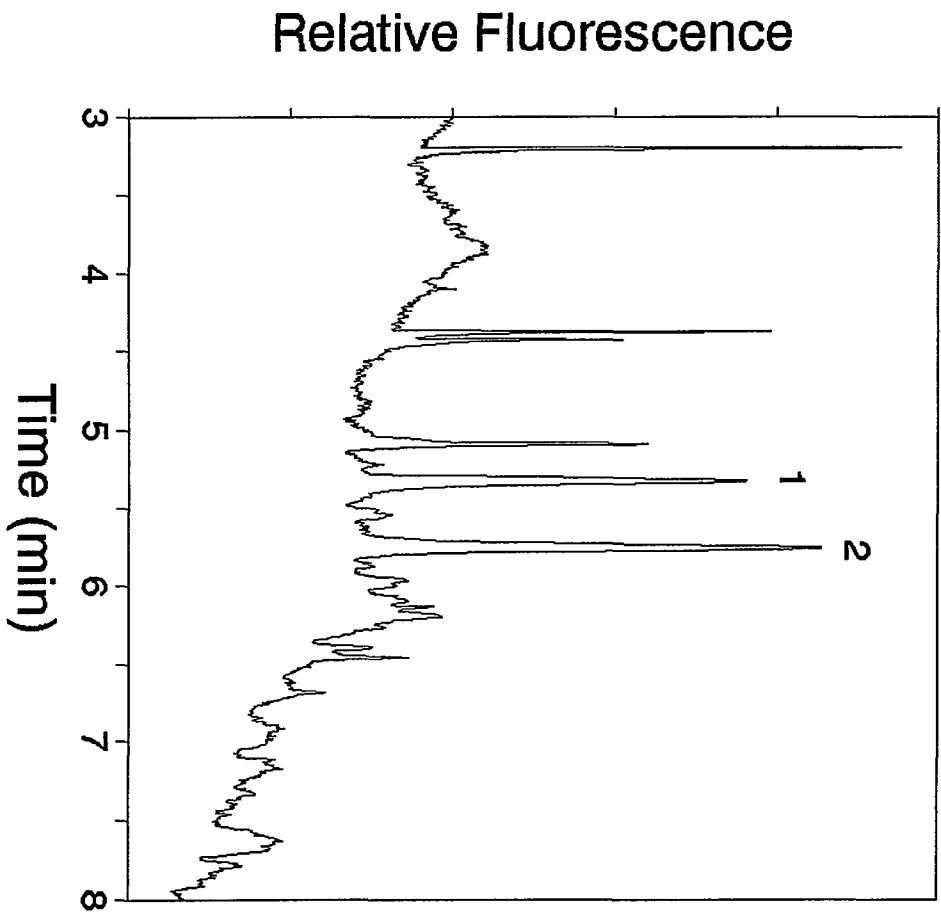


Figure 5. Single fetal red blood cell. Hb peak identification: (1) F, (2) A<sub>0</sub>, (3) F<sub>ac</sub>.

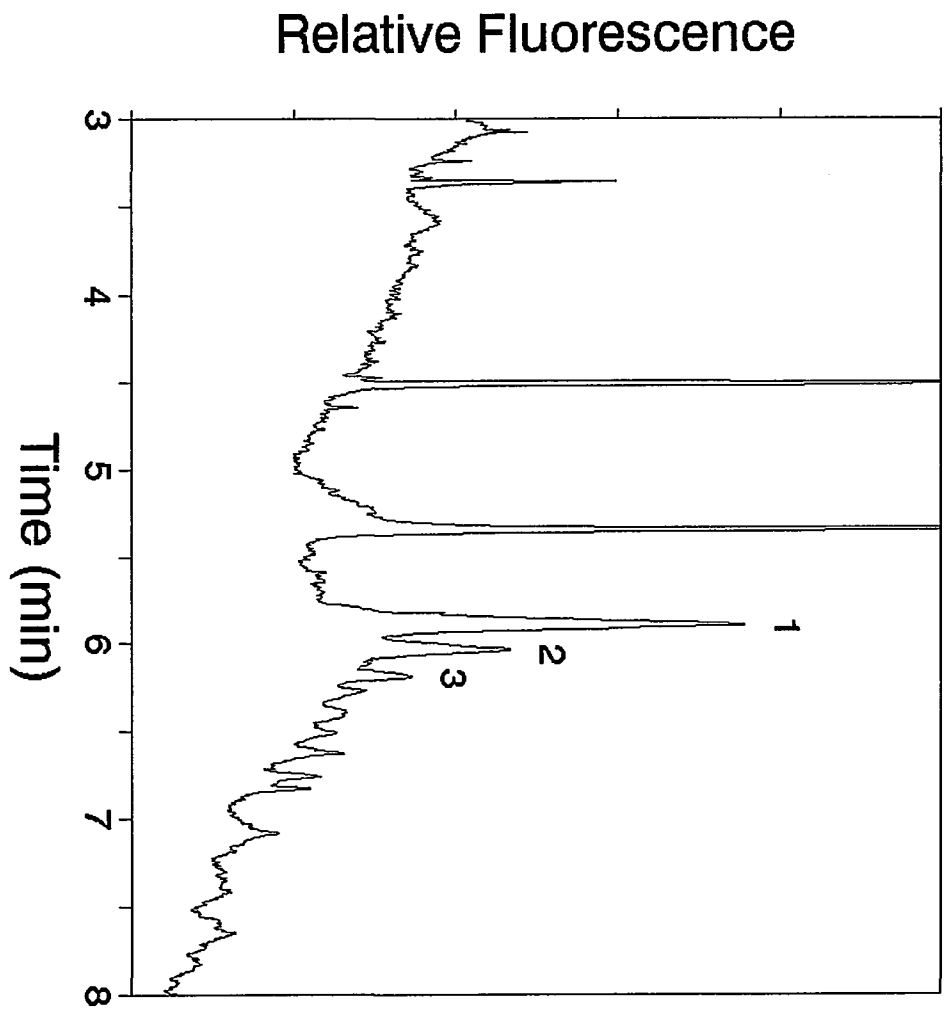
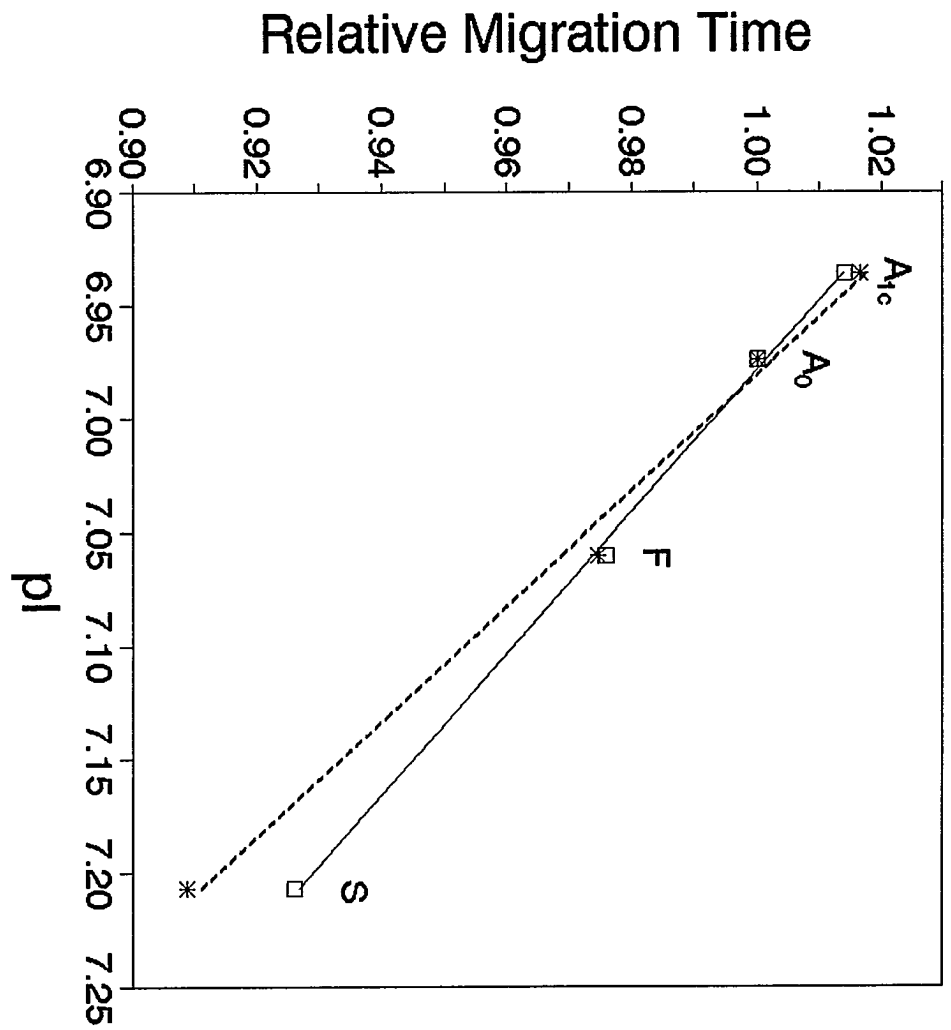


Figure 6. Linearity of pH gradient. Relative migration times (vs. Hb A<sub>0</sub>) are plotted as a function of literature pI values [31]. Dilute buffer conditions (solid line) are described in the Experimental section and gave  $r^2 = 0.9984$ . Concentrated (dashed line) buffer conditions gave  $r^2 = 0.9932$ , and are as follows: anolyte, 10 mM H<sub>3</sub>PO<sub>4</sub>; catholyte, 20 mM NaOH; ampholyte mixture, 0.4% methylcellulose (25 cp) with 1% Ampholine (pH 5-8); 50 μm-I.D. capillary.



the referenced isoelectric points [31]. A correlation coefficient ( $r^2$ ) of 0.9984 was found using dilute conditions. As mentioned in the previous section, the pI of Hb F<sub>ac</sub> was determined to be 6.914 (6.911) by this linearity plot. It is interesting to note that a peak occurs around 5.25 ( $\pm 0.15$ ) min in every electropherogram. The relative migration time of this peak is 0.884, with a calculated pI of 7.341. Hb A<sub>2</sub> has a pI of 7.411 [31], however it is unlikely that the peak is A<sub>2</sub>. Its concentration is only about 3% in normal red cells, and in all cells analyzed the concentration of this component was much greater than that. Also, all other Hb variants determined with this system had a calculated pI within 0.006 pI units of the literature value. Because the difference between A<sub>2</sub> and our unknown peak is 0.07 pI units, this peak is not assigned as A<sub>2</sub> and remains unidentified at this time.

The linearity of a gradient with more concentrated buffer conditions and hemolysate samples (instead of single cells) is also plotted in Fig. 6 (dashed line). The correlation coefficient of this system is 0.9932. Comparing the two plots, it is apparent that more concentrated conditions lead to a steeper gradient. With such a gradient, resolution is improved because for the same  $\Delta$ pI, there is a greater difference in migration times. However, detection is compromised and these conditions do not allow Hb in individual cells to be determined.

## CONCLUSIONS

In this work we have developed an injection-based cIEF method well suited for the analysis of very small sample volumes, such as individual cells. By diluting all buffer components, baseline stability was improved and attomole detection limits were reached, which were necessary to determine Hb in a single cell. Adult (normal and diabetic), fetal and sickle erythrocytes were analyzed. A linear pH gradient ( $r^2 = 0.9984$ ) served to confirm the peak identities for Hb S, F, A<sub>0</sub> and A<sub>1c</sub>. In addition, it allowed identification of Hb F<sub>ac</sub> in a single fetal erythrocyte. The performance of the system is sufficient to determine analytes with a pI difference as low as 0.025, and may be used to identify proteins with unknown isoelectric points.



### ACKNOWLEDGMENTS

The authors thank Ms. Carol Deal Eilers at Mercy Hospital in Des Moines, IA for providing the diabetic and cord blood samples. The Ames Laboratory is operated for the U.S. Department of Energy by Iowa State University under Contract No. W-7405-Eng-82. This work was supported by the Director of Energy Research, Office of Basic Energy Sciences, Division of Chemical Sciences.

### REFERENCES

1. M. Zhu, R. Rodriguez, T. Wehr and C. Siebert, *J. Chromatogr.*, 608 (1992) 225-237.
2. M. Zhu, T. Wehr, V. Levi, R. Rodriguez, K. Shiffer and Z. A. Cao, *J. Chromatogr. A*, 652 (1993) 119-129.
3. M. Castagnola, I. Messana, L. Cassiano, R. Rabino, D. V. Rossetti and B. Giardina, *Electrophoresis*, 16 (1995) 1492-1498.
4. P. Ferranti, A. Malorni, P. Pucci, S. Fanali, A. Nardi and L. Ossicini, *Anal. Biochem.*, 194 (1991) 1-8.
5. S. J. Lillard, E. S. Yeung, R. M. A. Lautamo and D. T. Mao, *J. Chromatogr.*, 718 (1995) 397-404.
6. T.-L. Huang, P. C.-H. Shieh and N. Cooke, *J. High Resol. Chromatogr.*, 17 (1994) 676-678.
7. A. Sahin, Y. R. Laleli and R. Ortancil, *J. Chromatogr.*, 709 (1995) 121-125.
8. M. Zhu, R. Rodriguez and T. Wehr, *J. Chromatogr.*, 559 (1991) 479-488.
9. X.-W. Yao, D. Wu and F. E. Regnier, *J. Chromatogr.*, 636 (1993) 21-29.
10. Q. Tang, K. Herrata and C. S. Lee, personal communication.
11. M. Conti, C. Gelfi and P. G. Righetti, *Electrophoresis*, 16 (1995) 1485-1491.
12. T.-L. Huang, P. C. H. Shieh and N. Cooke, *Chromatographia*, 39 (1994) 543-548.
13. F. Foret, O. Muller, J. Thorne, W. Gotzinger and B. L. Karger, *J. Chromatogr. A*, 716 (1995) 157-166.
14. X.-W. Yao and F. E. Regnier, *J. Chromatogr.*, 632 (1993) 185-193.
15. J. Wu and J. Pawliszyn, *Electrophoresis*, 16 (1995) 670-673.

16. T. J. Nelson, *J. Chromatogr.*, 623 (1992) 357-365.
17. K. G. Moorhouse, C. A. Eusebio, G. Hunt and A. B. Chen, *J. Chromatogr. A*, 717 (1995) 61-69.
18. J. R. Mazzeo and I. S. Krull, *Anal. Chem.*, 63 (1991) 2852-2857.
19. J. R. Mazzeo and I. S. Krull, *J. Chromatogr.*, 606 (1992) 291-296.
20. K. Shimura and K. Kasai, *Electrophoresis*, 16 (1995) 1479-1484.
21. J. Wu and J. Pawliszyn, *Talanta*, 39 (1992) 1281-1288.
22. J. Wu, P. Frank and J. Pawliszyn, *Appl. Spectrosc.*, 46 (1992) 1837-1840.
23. J. Wu and J. Pawliszyn, *J. Chromatogr.*, 608 (1992) 121-130.
24. J. Wu and J. Pawliszyn, *Anal. Chem.*, 64 (1992) 2934-2941.
25. J. Wu and J. Pawliszyn, *Anal. Chim. Acta*, 299 (1995) 337-342.
26. X.-Z. Wu, J. Wu and J. Pawliszyn, *Electrophoresis*, 16 (1995) 1474-1478.
27. W. Thormann, J. Caslavská, S. Molteni and J. Chmelik, *J. Chromatogr.*, 589 (1992) 321-327.
28. S. Molteni and W. Thormann, *J. Chromatogr.*, 638 (1993) 187-193.
29. J. Caslavská, S. Molteni, J. Chmelik, K. Slais, F. Matulik and W. Thormann, *J. Chromatogr. A*, 680 (1994) 549-559.
30. S. Molteni, H. Frischknecht and W. Thormann, *Electrophoresis*, 15 (1994) 22-30.
31. J. M. Hempe and R. D. Craver, *Clin. Chem.*, 40 (1994) 2228-2295.
32. S.-M. Chen and J. E. Wiktorowicz, *Anal. Biochem.*, 206 (1992) 84-90.
33. T. T. Lee and E. S. Yeung, *Anal. Chem.*, 64 (1992) 3045-3051.
34. R. B. Pennell in D. M. Surgenor (Editor), *The Red Blood Cell*, Academic Press, New York, v. 1, pp. 100-101.

**CHAPTER 4****MONITORING EXOCYTOSIS AND RELEASE  
OF SEROTONIN FROM INDIVIDUAL MAST CELLS  
BY CAPILLARY ELECTROPHORESIS WITH  
LASER-INDUCED NATIVE FLUORESCENCE DETECTION**

A paper submitted to Analytical Chemistry

Sheri J. Lillard, Edward S. Yeung and Michael A. McCloskey<sup>1</sup>

**ABSTRACT**

The complex temporal evolution of on-column exocytotic release of serotonin from individual rat peritoneal mast cells (RPMCs) was monitored by using capillary electrophoresis. Laser-induced native fluorescence detection with 275-nm excitation was used, and a detection limit of 1.7 amol (S/N = 3; rms) was obtained for serotonin. A physiological running buffer was used to ensure that the cell remained viable throughout. The secretagogue was Polymyxin B sulfate (Pmx). Following the injection of a single mast cell into the capillary, electromigration of Pmx toward and past the cell induced degranulation and release of serotonin. The time course of release was registered in the electropherograms with sub-second resolution. Subsequent introduction of SDS caused the cell to lyse completely and allowed the residual serotonin to be quantified. The average amount of serotonin observed per RPMC was  $1.6 \pm 0.6$  fmol; the average percentage of serotonin released was  $28 \pm 14\%$ . Events that are consistent with released serotonin from single sub-micron granules (250 aL each) were evident, each of which contained an average amount

---

<sup>1</sup>Department of Zoology and Genetics, Iowa State University, Ames, IA 50011

of  $5.9 \pm 3$  amol. To our knowledge, these represent the smallest entities that have been analyzed with CE to date.

## INTRODUCTION

Serotonin (5-hydroxytryptamine) is an important biogenic amine in both mammalian and non-mammalian signal transduction systems. It has been reported that brain serotonin plays a role in psychiatric syndromes<sup>1</sup> including obsessive-compulsive disorder<sup>2</sup> and depression,<sup>3</sup> as well as suicide.<sup>4</sup> In addition, its presence in peripheral tissues may point to its involvement in other disorders, such as those involving the gastrointestinal tract.<sup>5</sup>

Microscale analytical instrumentation has allowed in vitro analyses of single cells with neurochemical applications. Pihel et al. showed the co-release of serotonin and histamine from individual vesicles in single mast cells using carbon fiber microelectrodes.<sup>6</sup> Tan et al. have demonstrated uptake of serotonin in single astrocytes using fluorescence microscopy with 305-nm excitation from an argon-ion laser.<sup>7</sup> Capillary electrophoresis (CE) has been used for the analysis of single neurons.<sup>8-16</sup> In these studies, intracellular constituents such as amino acids<sup>8-9</sup> and neuropeptides<sup>10</sup> were detected with laser-induced fluorescence (LIF) after chemical derivatization. Electrochemical detection also has been used to detect intracellular components in single neurons after separation by CE.<sup>11-16</sup> Single adrenal medullary cells, as a model system closely resembling neurons, have been studied and amines and catecholamines determined using LIF, with<sup>17</sup> and without<sup>18</sup> fluorescence labeling.

In addition, CE has been used to determine released components from individual cells. By off-column incubation in reserpine, an agent which depletes vesicular dopamine, prior to injection of a single cell, Kristensen et al. have identified dopamine contained in two intracellular compartments of single *Planorbis corneus* nerve cells.<sup>12</sup> The observation of 2 CE peaks corresponds to a two-step lysis and release of dopamine. Recently, Tong and

Yeung have permeabilized individual pancreatic b-cells on-column and measured both the amount of insulin released and the amount which remained in the cell.<sup>19</sup>

Non-cytolytic release of intracellular constituents can occur via exocytosis,<sup>20</sup> which is a very common cellular event. In this secretion process, membranes of secretory granules in the cytoplasm first fuse with the plasma membrane, followed by extrusion of the granules into the extracellular matrix. Mediators (e.g., histamine and serotonin) are then displaced from the granular core. Here we describe on-column exocytotic release from individual mast cells using CE-LIF. In this novel application, we extend CE from its typical use as a separation device to one in which temporal monitoring of a biological event is achieved. A distinct advantage of CE, compared to microelectrode measurements, is that all exocytotic events from the entire cell can be measured. When microelectrodes are used,<sup>6</sup> monitoring is limited by the size of the electrode, hence localized, to a small region of the cell. Also with CE, the cell and its granules are confined within the capillary, such that dilution is minimized and all contents are subsequently detected. In this way, we are able to detect serotonin originating from individual sub-micron granules, which, to our knowledge, are the smallest entities ever determined using CE.

## EXPERIMENTAL SECTION

### Separation and Detection

The experimental instrumentation used in this work has been described previously.<sup>21</sup> A 21- $\mu\text{m}$  I.D., 360- $\mu\text{m}$  O.D. bare fused-silica capillary was used (Polymicro Technologies, Phoenix, AZ), with a total length of 40 cm (30 cm to detector). A high-voltage power supply (Glassman High Voltage, Whitehorse Station, NJ; EH Series; 0-40 kV) was used to drive electrophoresis with an applied voltage of +11 kV at the injection end. Each new capillary was rinsed with deionized water, 20 mM NaOH, and running buffer (10 min each) before use. The column was then equilibrated for 1-2 h before single cell runs were performed.

The 275.4-nm line of an argon-ion laser (Spectra Physics, Mountain View, CA; Model 2045) was isolated with a prism and used as the excitation source. A 1-cm focal

length quartz lens was used to focus the laser onto the capillary. Fluorescence was collected with a 10× microscope objective (Edmund Scientific, Barrington, NJ) and passed through two UG-1 color filters (Schott Glass Technologies, Duryea, PA) onto a photomultiplier tube. An RC-filter, consisting of a 10-K $\Omega$  resistor and a 10- $\mu$ F capacitor, was placed at the PMT output to allow spurious spikes in the electropherogram to be distinguished easily. Electropherograms were recorded at 5 Hz with a 24-bit A/D interface (ChromPerfect Direct, Justice Innovation, Palo Alto, CA) and were stored on a computer. Peak integration was performed with commercial software (Peakfit, Jandel Scientific Software, San Rafael, CA).

### Reagents

Unless otherwise noted, all chemicals were obtained from Fisher Scientific (Fair Lawn, NJ). Cells were suspended in mast cell ringer buffer (MCR), which consisted of 5 mM glucose, 5 mM MgCl<sub>2</sub>, 2 mM CaCl<sub>2</sub>, 2.5 mM KCl, 140 mM NaCl and 10 mM HEPES; pH 7.4. MCR was also used as the CE running buffer and was filtered with a 0.22- $\mu$ m cutoff cellulose acetate filter (Costar, Cambridge, MA) before use. Serotonin hydrochloride standard (Sigma Chemical, St. Louis, MO) was dissolved in deionized water, and injected hydrodynamically by raising the sample vial to a height of 11 cm relative to the detection end for 10 s (~0.14 nL injected volume). Polymyxin B sulfate was purchased from Life Technologies (Grand Island, NY), dissolved in DMSO and diluted to strength in MCR buffer. RPMI buffer consisted of RPMI with 5% fetal bovine serum (both obtained from Life Technologies). Isotonic Percoll was prepared by mixing 20 mL Percoll (Sigma Chemical, St. Louis, MO), 1.8 mL 10× Hank's balanced salt solution (Life Technologies) and 0.2 mL 1 M HEPES. The isotonic Percoll was centrifuged for 20 min (2100 rpm, 10°C) to sediment and remove any Percoll crystals. 20 mL 30% and 15 mL 80% Percoll were prepared by appropriate dilutions of isotonic Percoll in RPMI buffer. The density gradient was poured by laying the 30% Percoll on the 80% and applying 2 mL RPMI buffer to the top. The gradient was stored on ice until used.

### **Mast Cell Isolation**

Peritoneal mast cells (RPMCs) were isolated from male Sprague-Dawley rats. The rats were anesthetized with ether, then decapitated. Approximately 20 mL of Tyrode's buffer [5.5 mM glucose, 137 mM NaCl, 2.7 mM KCl, 1 mM CaCl<sub>2</sub>, 0.45 mM NaH<sub>2</sub>PO<sub>4</sub>, 1 mg/mL bovine serum albumin (Sigma), 10 U/mL heparin (Sigma) and 12 mM HEPES; pH 7.4] was injected into the peritoneal cavity. The rat was inverted about 15 times, an incision was made in the cavity, and the buffer (which contained cells) withdrawn. The buffer was centrifuged for 5 min (1500 rpm, 10°C) and the supernatant discarded. The cells were washed once more in Tyrode's buffer, and the centrifugation repeated. Then the cells were resuspended in ~3 mL RPMI buffer, applied to the Percoll gradient, and centrifuged for 20 min (2200 rpm, 10°C). The supernatant was aspirated and the cells were washed twice in DMEM (Dulbecco's Modified Eagle Medium) containing 10% serum (5 min, 1500 rpm, 10°C). The supernatant was discarded, the cells washed once in MCR (5 min, 1500 rpm, 10°C) and finally suspended in MCR buffer. An aliquot of cells was diluted 10-fold in 0.22% trypan blue (in phosphate buffered saline) and counted using a Brightline Hemacytometer (Hauser Scientific). Average yield was  $\sim 1-2 \times 10^6$  cells/rat.

### **Single Cell Injection and CE Procedure**

The procedure for injecting individual cells is the same as described previously.<sup>21</sup> Approximately 15  $\mu$ L of cell solution (MCR) was placed on a microscope slide and the inlet side of the capillary was inserted. Polyimide coating (~5 mm) was removed from this end of the capillary, such that the location of the cell could be estimated to within ~1 mm. A septum was placed over the outlet buffer vial to create an air-tight seal, into which a syringe needle was inserted. By applying gentle suction, one cell was injected and the process was visually confirmed under the microscope. The application of pressure by pushing some of the extracellular fluid out of the capillary confirmed cell adhesion to the capillary wall. The inlet side of the capillary was then immersed in a buffer vial which contained Polymyxin B sulfate (Pmx) at a final concentration of 50 U/mL in MCR. Electrophoresis was run for 0.5 min to migrate the Pmx zone to the region of the cell, the buffer was switched to one

containing MCR only, and the released serotonin zone was migrated away from the cell for 1 min. Electrophoresis was stopped, the capillary was removed, and 0.1% SDS (Sigma) in MCR was introduced into the capillary to lyse the cell, with visual confirmation through the microscope. The capillary was then returned to the MCR buffer vial (without Pmx) and electrophoresis continued.

## RESULTS AND DISCUSSION

### Cell Viability and Adhesion

The morphology of intact versus degranulated cells differs considerably. Under 100× total magnification, intact cells are round with a smooth and well defined cell membrane. Degranulated cells do not appear smooth; they look roughened and porous following the degranulation process. In several of the single-cell runs that we performed, the degranulated cell (or cell residue) was not visible after the 0.5-min introduction of Pmx and 1-min electromigration. Because the cell was gone, either it lysed prematurely or it moved. Premature lysis is unlikely, since the degranulated cells viewed under a microscope remained unlysed upon prolonged exposure to Pmx. It is more likely that the cell migrated further along the capillary, and as discussed below, we have seen the position of the degranulated cell change between these two steps (in the direction of the detector). Ideally, the cell should be stationary throughout the experiment.

Cell adhesion depends on the capillary surface as well as the condition of the cell. Pretreating the capillary with NaOH at the onset of the experiments aids in cell adsorption to the capillary wall, and if necessary, occasional treatments between runs can help maintain this for a while. However, the longer the time since cell isolation, the less likely the cells are to adhere well to the silica surface of the capillary. Hence, cell viability is critical in all aspects of these experiments.

Once the cells are isolated, they remain viable for several hours in MCR. Although they would last longer in 5-10% serum, interference from native protein fluorescence necessitates that our cell suspension solution be free of extra protein. How long the cells last can vary from batch to batch. We have found evidence of spontaneous degranulation in the



cell suspension in as little as 3 h, and have used cells from other batches as long as 24 h following isolation. During the cell isolation procedure, higher concentrations of serum in the wash buffers seem to prolong cell viability. In addition, such factors as the health state or age of the rat may also affect how long the cells last following isolation.

### **Mast Cell Degranulation**

Degranulation of rat peritoneal mast cells is very dramatic when the cells are exposed to the proper secretagogue. Compounds such as 48/80<sup>22</sup> and Pmx<sup>23</sup> have been known for quite some time to degranulate mast cells. Calcium ionophore A23187 also has been used to induce release of histamine and serotonin.<sup>24</sup> We performed preliminary studies with a microscope and video camera, which revealed that both 48/80 (10  $\mu\text{g}/\text{mL}$ ) and Pmx (100 U/mL) induce rapid degranulation over a period of about 10 s. Video data were collected using Pmx-induced secretion, and images from these are included as Supporting Information, Fig. S1A through S1X. A total of 24 images were taken at 0.5 s intervals, from which the degranulation process is clearly visible.

Six of the series of video images are shown in Fig. 1. Even though these are spaced at 2 s intervals, the main features and typical time dependence of exocytosis are visible. In the initial frame, all cells were in their native state. In subsequent frames, black spots representing sub-micron granules can be seen developing at the cell perimeters. The number of spots increased with time up to and including the last frame, after which further development was not evident. Exocytosis for each cell was not synchronous, although all events started within a 2-s time interval. One cell in the image (bottom left) did not exhibit any change, presumably because it was not viable. Even based on a simple count, different cells released different numbers of granules. For example, the cell in the center appears to release significantly less than the others. The released granules can stay attached to the cell membrane, despite the fact that Pmx wash solution is flowing past them throughout, or become detached from the cell in the 0.2 s time scale (Fig. S2A through S2F, taken at 1/15 s intervals).

Figure 1. Time evolution of exocytosis in mast cells stimulated by Pmx. Photos are taken at 2 s intervals. See text for details.

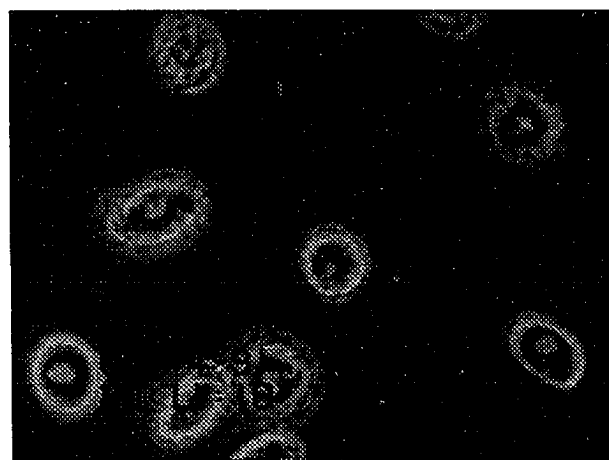
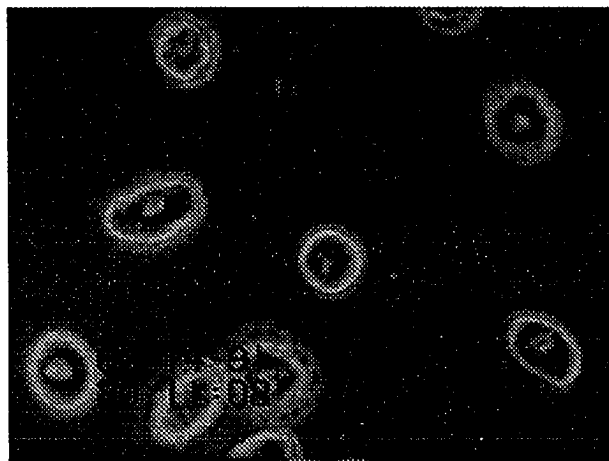
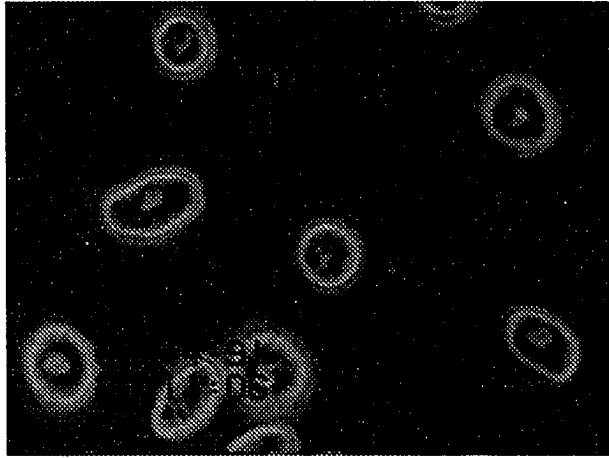
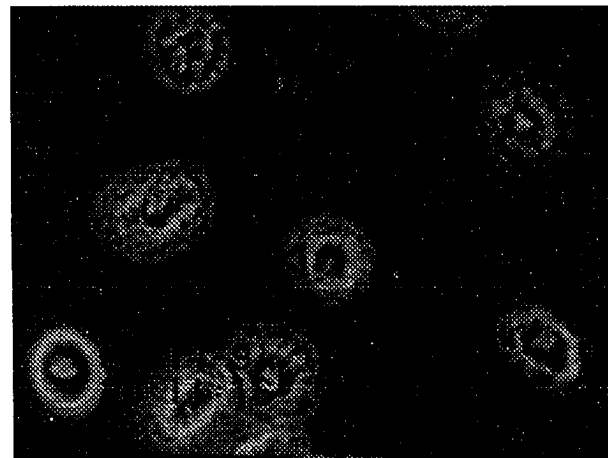
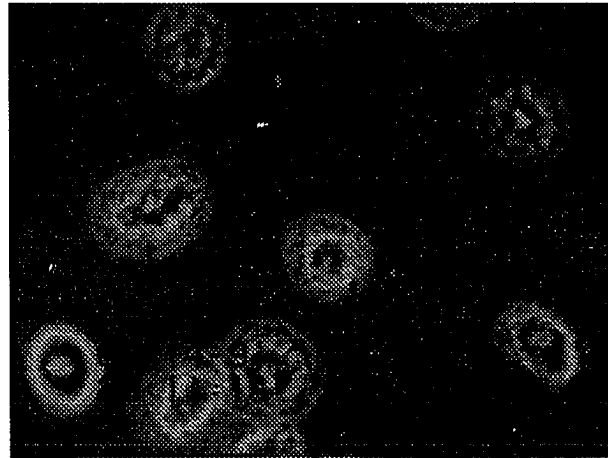
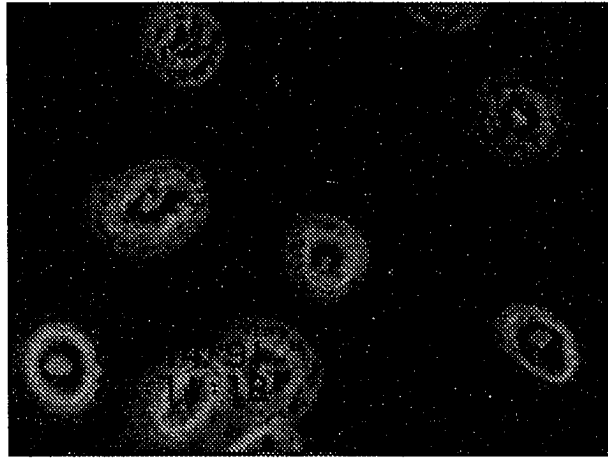


Figure 1. (continued)



### **Serotonin LOD and Bulk Release Study**

To test the performance of the system and to calibrate the response, 0.14 nL of  $9 \times 10^{-7}$  M serotonin was injected, corresponding to an amount of 126 amol, or about 3% of the amount in a typical single rat peritoneal mast cell.<sup>6,25</sup> A detection limit of 1.7 amol (S/N = 3; rms) was achieved. The use of native fluorescence detection eliminates any uncertainties associated with reaction yields and kinetics when derivatization reagents are employed.

A bulk release study was performed, in which an aliquot of cells was centrifuged and the supernatant (without secretagogue exposure) was injected; the electropherogram revealed no peaks. Then, either 48/80 (10  $\mu\text{g/mL}$ ) or Pmx (50 U/mL) was added to the cells, allowed to react for about 5 min, and the cells were centrifuged again. The electropherograms of the ensuing supernatants revealed serotonin peaks for both Pmx and 48/80 induced secretion (data not shown). Pmx yielded only one small extra peak compared to two somewhat larger extra peaks with 48/80. Also, when 48/80 was tested with on-column release experiments (data not shown), we found excessive background disturbances which nearly obscured the release peak(s). For these reasons, we chose to use Pmx for the single-cell exocytosis measurements in this work.

### **Introduction of SDS for Cell Lysis**

The way in which SDS was introduced into the capillary to lyse the cell was critical. Initially, a 1-3 mm zone of SDS was injected hydrodynamically. Variations on this SDS injection procedure included immediately starting CE, as well as incorporating a ~20 s waiting period to ensure exposure of the cell to SDS. However, with this procedure, cell lysis was not always complete. In some cases, the degranulated cell could still be seen in the capillary even after the supposed lysis by SDS.

The SDS introduction procedure was thus modified to use the same set-up as for injecting individual cells. For SDS injection, a droplet of SDS solution was placed on the microscope slide, and the capillary was inserted such that the immobilized cell was in view under the microscope. Negative pressure either was present because of the height difference between the outlet reservoir and the capillary tip or was created by pulling slightly on the

syringe. The SDS solution entered the capillary, and when it reached the degranulated cell, lysis was confirmed visually. When the cell lysed, however, it did not disappear instantaneously. Instead, it was first dislodged from the capillary wall. Then, the plasma membrane disappeared while a region of granular-looking cell matter could still be seen. Within a few seconds, it gradually disappeared. The capillary was subsequently returned to the inlet buffer reservoir, and electrophoresis resumed. This visual verification of cell position in the capillary (following degranulation) as well as during cell lysis aided in the interpretation of the ensuing electropherograms. We also confirmed that the injection of similar lengths of SDS plugs does not interfere with the serotonin or protein signals from single mast cells.

### **Single-Cell Exocytosis**

While our bulk release experiments indicate that serotonin is released, single-cell studies may give new insights into intercellular differences involving exocytosis as well as the temporal dependence of these events. In our system, Pmx induces non-lytic degranulation of RPMCs. Multiple physiological stimuli<sup>26</sup> (e.g., foreign antigen, neuropeptides, complement C5a) trigger non-lytic degranulation by mast cells and basophils. Although its exact mechanism of action is unclear, Pmx is similar to these secretagogues in that it elicits release of granule constituents without causing cell death.<sup>26</sup> Pmx has been shown to cause ionic permeabilization of model cell membranes.<sup>27,28</sup>

Liu and Sweedler have demonstrated time-resolved monitoring of a derivatization reaction using rectangular electrophoresis channels.<sup>29</sup> However, to our knowledge, the present work is the first demonstration of CE being used to follow the evolution of a well-defined biological event at the single-cell level. Figure 2A shows a complete electropherogram of on-column exocytosis (and release of serotonin), followed by cell lysis, from a single RPMC. The serotonin peaks are seen around 3-5 min, whereas a band of protein peaks is evident around 8-12 min. The two major peaks correspond to release (3.8 min) and lysis (4.7 min) of the mast cell. In all experiments, there is 1.5 min of

Figure 2A. Electropherogram of individual RPMC (cell #4) in which the complete sequence is shown; full scale. See Table 1 for peak information.



# Relative Fluorescence

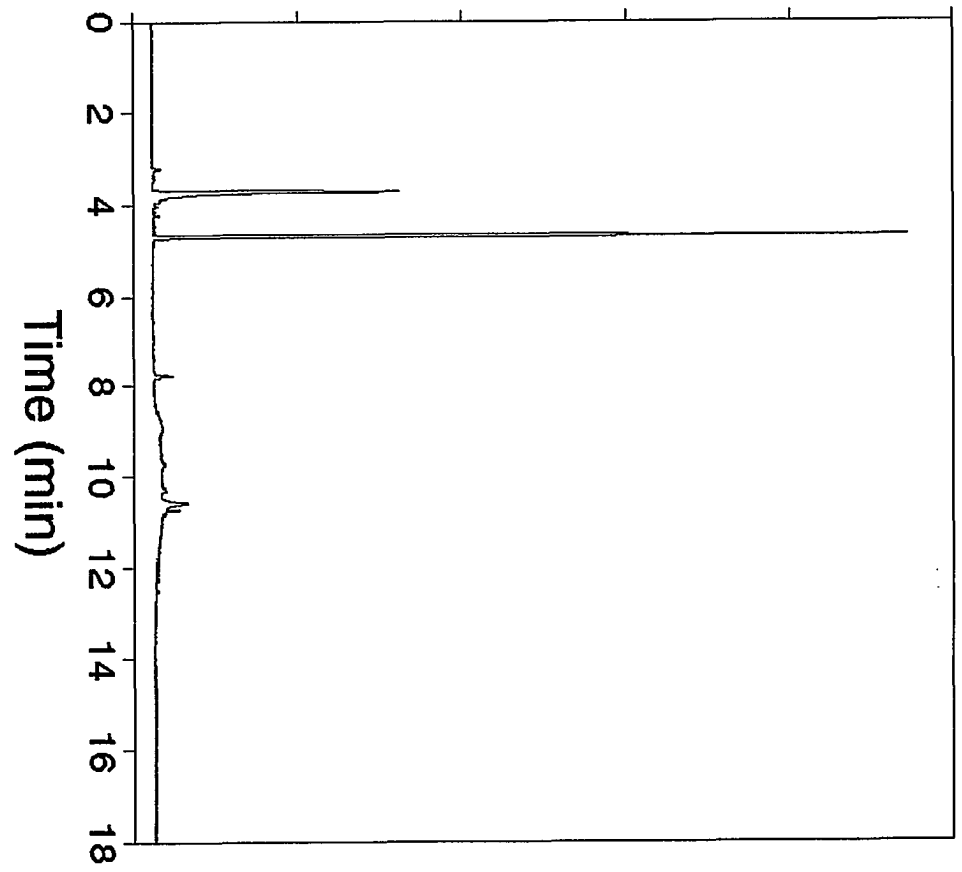


Figure 2B. Electropherogram of individual RPMC (cell #4); expanded region between release and lysis events. Each mark on the ordinate in 2B and 2C corresponds to an identical signal intensity. See Table 1 for peak information.

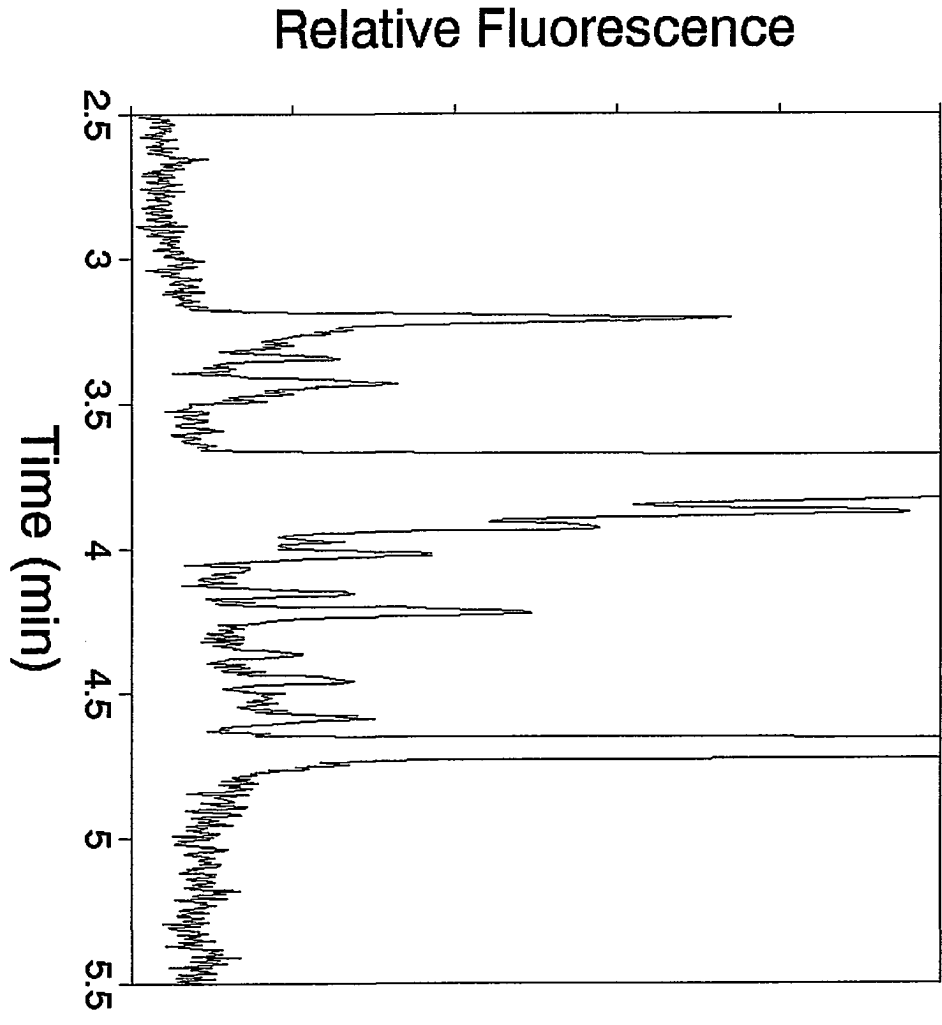
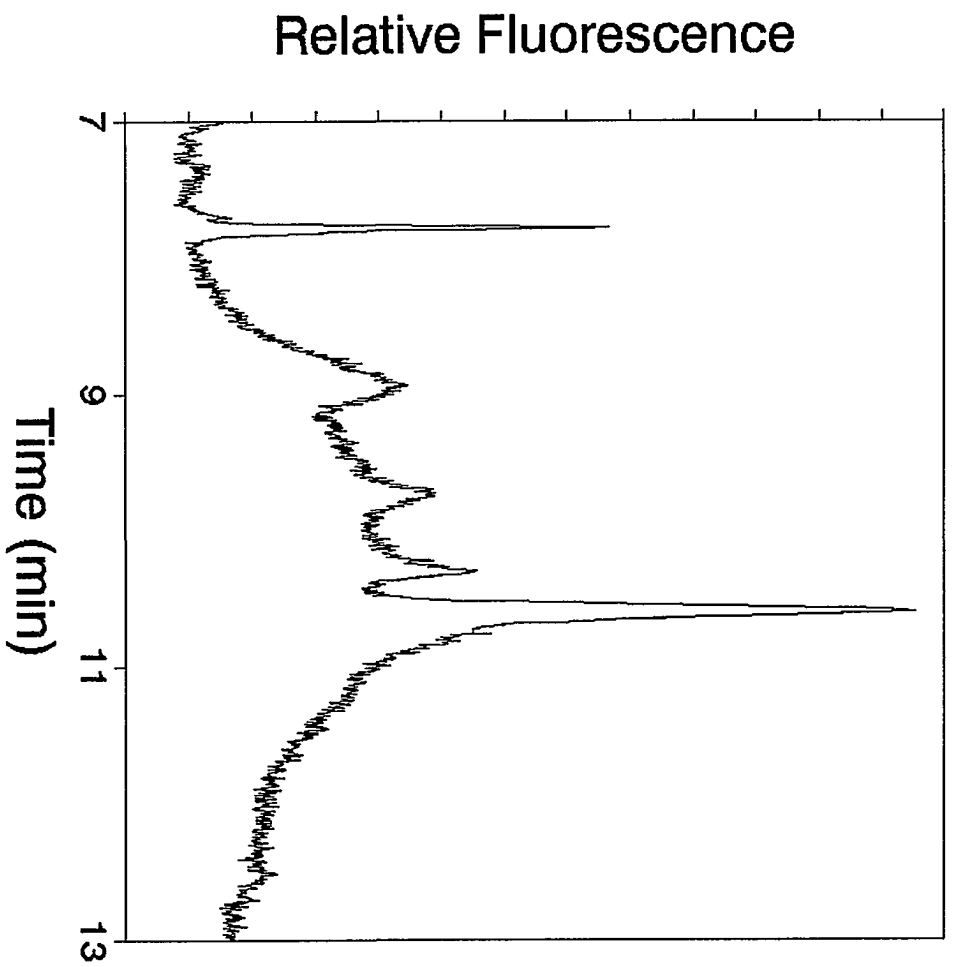


Figure 2C. Electropherogram of individual RPMC (cell #4); protein region. Each mark on the ordinate in 2B and 2C corresponds to an identical signal intensity. See Table 1 for peak information.



electrophoresis before the data are collected (i.e., data collection begins immediately following the lysis step). This is why the serotonin standard and the release peaks have different apparent migration times. Yet, the lysis peak and the serotonin standard have similar migration times. Since 1 min of this period corresponds to CE (with MCR running buffer) to migrate the released serotonin zone away from the cell, a separation between the release and lysis peaks of at least 1 min is expected. However, the 0.5 min migration time for introducing Pmx may not result in an additional 0.5 min separation. The additional time could be less than 0.5 min if exocytosis of a particular cell was delayed after contact with Pmx.

The separation of the release and lysis peaks also depends on cell movement during the initial 1.5 min of CE, and on the time required to introduce SDS for cell lysis. In the experiments involving Batch 1 (Fig. 2B and S3A-S10A), the cell did not move between exocytosis and lysis, as was visually confirmed. Because the cell remained close to the capillary inlet, only a relatively short plug of SDS needs to be introduced into the capillary to lyse the cell. These two factors explain why the separation between the two major peaks (Table 1) is relatively consistent.

Figures 2B and S3A-S10A are expanded plots of the region depicting the release and lysis peaks from individual RPMCs (Batch 1). All are plotted on the same scale, with the heights of the main release and lysis peaks (Table 1) measured according to the size of the divisions shown on the y-axes. The general patterns of these runs are consistent with one another, yet exhibit features which reveal intercellular differences in exocytosis. In every case the main release peak is broader than the lysis peak, which indicates that the exocytosis process occurs more slowly than cell lysis by SDS. The time course of these events is consistent with observation using a microscope (Fig. 1 and S1). The main release peak actually comprises many individual exocytotic events which, because of axial diffusion, are not resolved in the electropherograms. Even so, some features are clearly evident within each main peak, except for Fig. S6A. There, the release peak size is also small, which explains a more compact process (in time). In some runs (e.g., Fig. 2B and S3A, S7A, S9A, S10A), one main release peak is evident, which suggests that cell degranulation occurred essentially at

Table 1. Peak parameters for serotonin due to single-cell release and lysis

Cell #	Release			Lysis			% Release	
	migration time	width	height	migration time	width	height	(%) area	total
4	3.71	0.25	87	4.69	0.08	260	42	
6	2.90	0.23	5	4.36	0.07	180	12	
7	2.91	0.21	5.5	4.46	0.08	125	36	
	3.50	0.19	23					
8	3.00	0.13	6.5	4.45	0.11	360	5	
9	3.05	0.14	28	4.51	0.08	90	36	
10	2.97	0.20	23	4.48	0.08	220	33	
	3.49	0.15	13					
11	2.89	0.17	12	4.45	0.08	320	10	
12	3.12	0.18	21	4.64	0.11	53	47	
1	1.75	0.31	127	3.46	0.08	340	56	
2	3.78	0.17	26	5.05	0.11	190	19	
3	2.22	0.30	85	3.79	0.08	490	40	

Migration times (min) correspond to the peak maximum.

Width (min) corresponds to base width of the main peak.

Heights are in y-axis units as plotted in the figures.

Cells 4-12: Batch 1

Cells 1-3: Batch 2

Cell 4 corresponds to Figure 2: All other plots are included as Supporting Information.

once. In others (e.g., Fig. S4A, S5A, S8A), the presence of two main release peaks reveals different degranulation processes, which are presumably due to physiological differences between particular cells. Also evident in Fig. 2B and S3A-S10A are small peaks which are indicative of single-granular events (discussed in the next section in more detail). Again, intercellular variations are evident, with some cells showing more of these events (e.g., Fig. 2B and S3A, S7A, S8A) than others (e.g., Fig. S4A, S10A). Based on these data, it appears that the time profile for release consists of an initial burst of degranulation, followed by a substantially delayed release of a few more granules. It is significant that these small peaks are not found before the release event or after complete cell lysis. Vesicular membranes are clearly dissolved on contact with SDS, followed by displacement of all of the serotonin contained within the granules.

The amount of total serotonin per cell was calculated as the combined area of all release plus lysis peaks. The range of these values was between 0.8 and 2.6 fmol, with an average of  $1.6 \pm 0.6$  fmol. The average is low compared to the 4 fmol/cell previously reported,<sup>6</sup> and may be due to differences in the animals used. Eight individual RPMCs were analyzed, and the percentage of serotonin released via exocytosis was determined for each cell (Table 1). These values ranged from 5.4 to 47%, with an average of  $28 \pm 14\%$  released per cell. No trend is seen in these values with respect to run number, which confirms that this variation is not due to cell viability, changes in the capillary, or the detection system.

Figures S11-S13 show electropherograms from 3 individual RPMCs isolated on a different day (Batch 2). The general patterns of the electropherograms are similar between the two batches of cells, including the appearance of the presumed individual granular events. The data from Batch 2 are not pooled with those from Batch 1 since the cells came from different rats. However, the average percentage of released serotonin from these 3 cells in Batch 2 was  $38 \pm 15\%$ , which is within the range found with Batch 1.

Since the experimental procedure of Batches 1 and 2 were identical (i.e., 0.5 min electromigration of Pmx followed by 1 min CE with MCR only), the separation between the main release and lysis peaks should be consistent. However, when electropherograms from the two batches are compared, this is not found to be the case. For Batch 2, when the cell

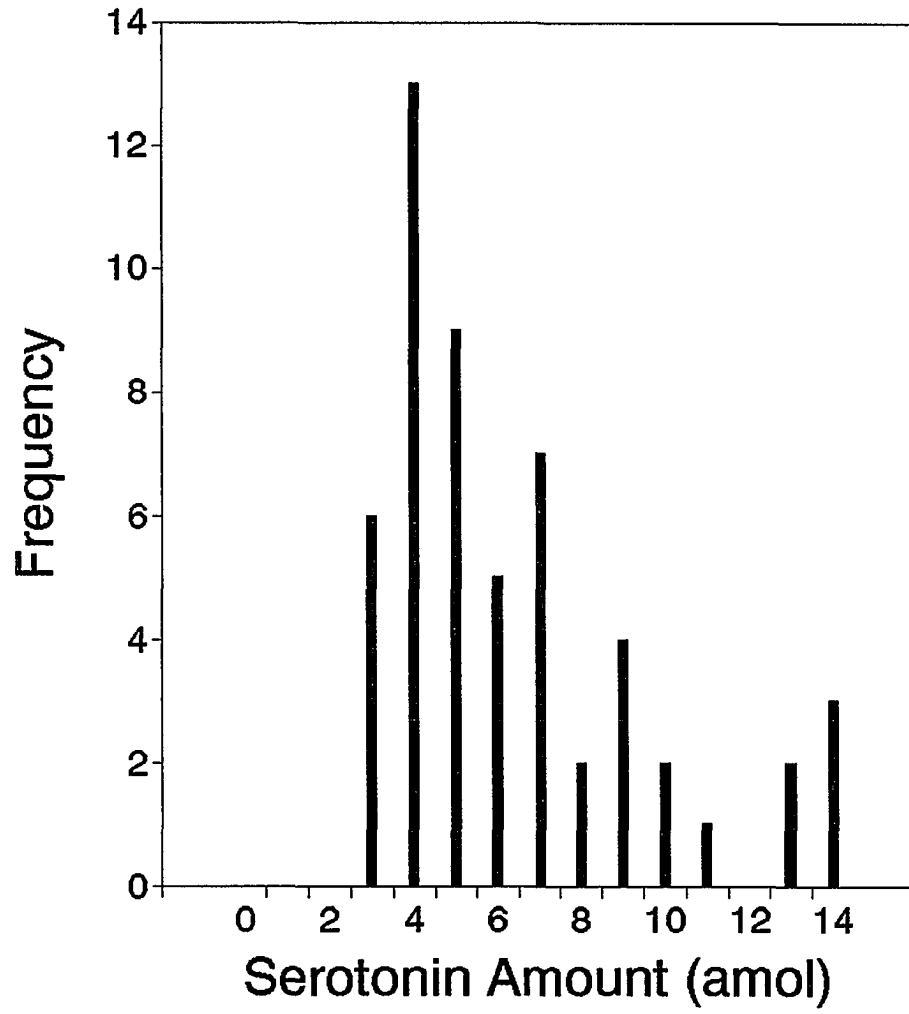


positions (inside the capillary) were visually determined between exocytosis and cell lysis, we found that the cells did not always remain in the same location as when they were injected. Usually, they had moved further inside the capillary (i.e., toward the detector). If the cell was further away from the capillary inlet, a longer injection plug was required for SDS to reach the cell. By pulling on the syringe for a longer time, the released serotonin zone was moved further toward the detector during the extra time it took for SDS to reach (and lyse) the cell. This results in the release peak or even the lysis peak eluting earlier than expected, in addition to a greater separation distance between the release and lysis peaks.

### **Single-Granule Detection**

The secretory vesicles of RPMCs are comprised of a granular core (i.e., granule) enclosed by a vesicular membrane.<sup>30</sup> The core consists mostly of heparin proteoglycan, to which serotonin, histamine and enzymes are attached. The mean diameter of RPMC granules has been determined by Helander and Bloom using electron microscopy to be  $0.777 \pm 0.090$   $\mu\text{m}$ , which corresponds to a volume of 246 attoliters.<sup>25</sup> The serotonin amounts of 54 peaks were determined from the 8 RPMCs (Batch 1) that were analyzed, and a distribution of the individual granular events is shown in Figure 3. By comparing the granular areas with the area and injected amount of serotonin standard, corresponding granular amounts were calculated. These correspond to an average amount of  $5.9 \pm 3.0$  (range = 2.2 to 13.6) amol per granular event (Fig. 3). These data show evidence of single granule detection following degranulation (via exocytosis) of individual RPMCs. Since these single granules elute slightly after the main peak, it is likely that they were released later than the initial burst. Even if these granules had remained tethered to the cell following exocytosis, exposure to the saline buffer should have caused the serotonin to be displaced without considerable delay. Another possibility is that some of these small peaks reveal serotonin released due to transient fusion.<sup>31</sup> In this process, the vesicle fuses with the plasma membrane briefly and releases only part of its contents before returning to the cytoplasm. In these experiments we cannot distinguish between transient and irreversible fusion. However, it is unlikely that transient fusion occurs (during the period between the main release peak and the lysis peak)

Figure 3. Histogram of amounts of serotonin released from individual granular events.



without being accompanied by the primary cellular response of exocytosis.

Statistically, all 54 of these events are not predicted to be from single granules. In Fig. 2B (and Fig. S3A-S13A), the base peakwidths of the small peaks are about 0.06 min, while the distance between the main release and the lysis peaks in Fig. 2B is 0.92 min. This means that approximately 1 out of 15 peaks will suffer complete overlap due to multiple events, or about 4 of the 54 total events arise from overlapping granules. Applying this to the histogram in Fig. 3, two groups of peaks are then apparent, consisting of the first 9 bars (49 events) and the next 2 (5 events). These have centroids at approximately 6 amol intervals, and are tentatively identified as 1- and 2-granule events, respectively.

A multiple event may be defined as follows. It is possible that when the cell degranulated, more than one individual granule (e.g., 2 or 3) was released into the same region of the capillary and their corresponding serotonin zones therefore overlapped. Another possibility is that the features of these electropherograms may be indicative of the exocytotic mechanism. It has been postulated by others that mast cell degranulation (hence, exocytosis) occurs by two mechanisms—compound and multigranular<sup>32</sup>—which account for single and aggregated granules, respectively, being released from the cell. Granule aggregates are the result of transient fusion, in which a vesicle fuses briefly with the plasma membrane, another granule fuses with it, and as an aggregate they return to the cytoplasm. Such an aggregate can later undergo irreversible fusion and exocytosis.<sup>32</sup> Some of the multiple events may reveal the multigranular portion of the exocytotic mechanism.

The integration technique used to calculate the areas of these peaks inherently incorporates baseline (i.e., noise) smoothing. However, the LOD calculation for serotonin was based on the peak height and rms noise, and did not involve any baseline smoothing. This explains why we can readily distinguish even the smallest single granule peaks with a  $S/N = 4$  (rms).

### **Protein Contents**

In addition to the release of serotonin by both exocytosis and cell lysis, proteins are also released by both processes. The two proteins present in the highest amounts (in RPMC granules) are a chymase (rat mast cell protease I, 24 pg/cell) and carboxypeptidase A (10 pg/cell).<sup>30</sup> Protein peaks are present in all electropherograms that were recorded, and these regions of the electropherograms are shown in Figures 2C and S3B-S13B. Since the release and lysis steps are typically only separated by ~1.5 min, the broad protein peaks coming from each event (at ~10 min) co-elute and are not well resolved. So, it is not possible to distinguish from which process the protein peaks originated. In Figure 4, the electropherogram of an individual RPMC (cell #5) is shown in which the exocytosis (i.e., release) step was deliberately separated from the lysis step by ~10 min. Fig. 4A and 4B correspond to the regions of the release and lysis events, respectively. The extended separation of these events was performed in order to confirm the peak identities, as well as to try to identify the source(s) of the protein peaks. In Fig. 4, a distinct band of protein is seen from each process, which means that at least part of the convoluted protein bands (Fig. S3B-S13B) originates from exocytosis. However, due to the extremely broad profiles of these peaks, deconvolution to determine the individual contributions was not possible. The protein peaks originating from cell lysis probably include membrane proteins, the granular proteins, as well as proteins from other cellular locations.

The presence of protein signal makes separation an important consideration in these experiments. Fortunately, the physiological buffer pH, column surface and column length selected provide clear separation of serotonin from the other fluorescent species. That is, the capillary here is more than a simple flow-sampling device.

### **CONCLUSIONS**

We have demonstrated the monitoring of the temporal development of exocytosis in individual mast cells using CE with native LIF. A low detection limit for serotonin, 1.7 amol, permitted determination of released and residual fractions from the same cell. Simultaneously, time dependent exocytotic release profiles, in which peaks with distinct

Figure 4A. Electropherogram of an individual RPMC (cell #5) in which the lysis step was delayed until all release peaks eluted; release caused by Pmx. The sharp peaks correspond to serotonin, the broad bands correspond to proteins, and the small peaks correspond to granules. Both A and B are plotted on the same scale.

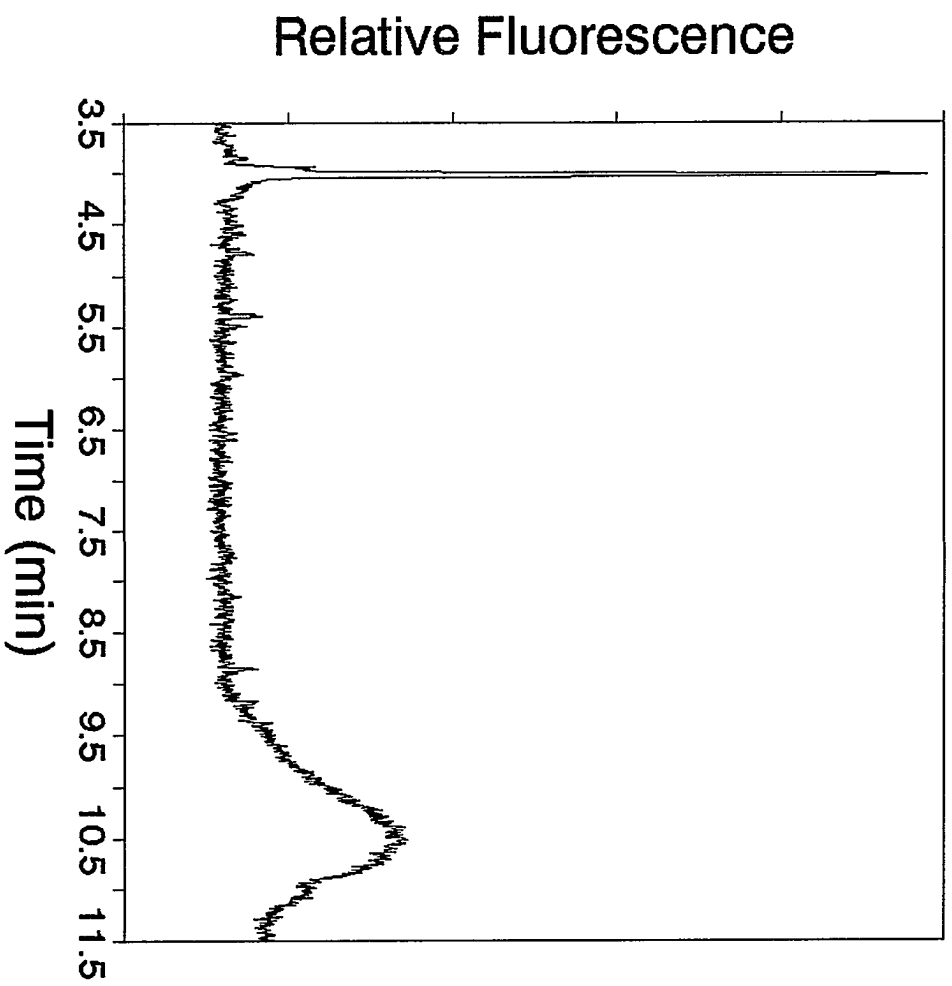
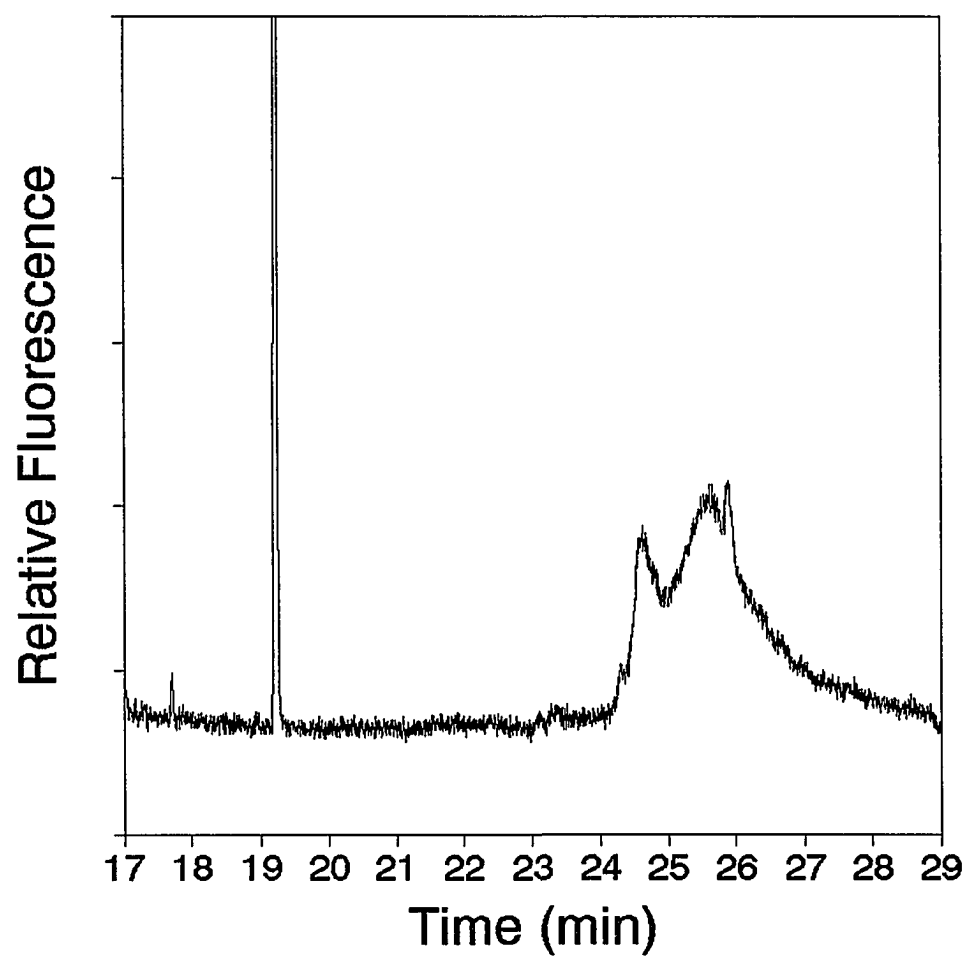


Figure 4B. Electropherogram of an individual RPMC (cell #5) in which the lysis step was delayed until all release peaks eluted; lysis caused by SDS 10 min after the release stimulation. The sharp peak corresponds to serotonin and the broad bands correspond to proteins. The lysis serotonin peak at 19.2 min has a peak height of 65 (y-axis divisions). Both A and B are plotted on the same scale.





features followed by individual granular events representing sub-micron entities are observed, have been characterized. Since sub-second CE separation has been demonstrated,<sup>33</sup> extension of the present scheme (e.g. by running at a higher voltage gradient) to study even faster biological processes or to resolve the envelope of release peaks should be feasible. In fact, we have here the ultimate microdialysis sampling probe—one that interrogates a 10- $\mu\text{m}$  sized mammalian cell immobilized at a well-defined location. From the analysis of 8 individual RPMCs, the average percentage of serotonin released was  $28 \pm 14\%$ . The features of the electropherograms that we have denoted as single exocytotic events reveal an average serotonin amount of  $5.9 \pm 3$  amol per event. At 250 aL each, these are the smallest “samples” ever studied by CE. In addition to the detection of serotonin, intracellular proteins originating from both exocytosis (i.e., from the granules) as well as from cell lysis were detected using native protein fluorescence.

#### ACKNOWLEDGMENTS

The Ames Laboratory is operated for the U.S. Department of Energy by Iowa State University under Contract No. W-7405-Eng-82. This work was supported by the Director of Energy Research, Office of Basic Energy Sciences, Division of Chemical Sciences, and by an NIH grant (GM48144) to M.A.M.

#### REFERENCES

1. Montgomery, S. A.; Fineberg, N. *British J. Psych.* **1989**, *155* (suppl. 8), 63-70.
2. Murphy, D. L.; Zohar, J.; Benkelfat, C.; Pato, M. T.; Pigott, T. A.; Insel, T. R. *British J. Psych.* **1989**, *155* (suppl. 8), 15-24.
3. Meltzer, H. *British J. Psych.* **1989**, *155* (suppl. 8), 25-31.
4. Man, J. J.; Arango, V.; Marzuk, P. N.; Theccanat, S.; Reis, D. J. *British J. Psych.* **1989**, *155* (suppl. 8), 7-14.
5. Hansen, M. B. *Pharmacol. and Toxicol.* **1995**, *77*, 3-39.
6. Pihel, K.; Showchien, H.; Jorgenson, J. W.; Wightman, R. M. *Anal. Chem.* **1995**, *67*, 4514-4521.

7. Tan, W; Parpura, V.; Haydon, P. G.; Yeung, E. S. *Anal. Chem.* **1995**, *67*, 2575-2579.
8. Kennedy, R. T.; Oates, M. D.; Cooper, B. R.; Nickerson, B.; Jorgenson, J. W. *Science* **1989**, *246*, 57-63.
9. Gilman, S. D.; Ewing, A. G. *Anal. Meth. Instrum.* **1995**, *2*, 133-141.
10. Shippy, S. A.; Jankowski, J. A.; Sweedler, J. V. *Anal. Chim. Acta* **1995**, *307*, 163-171.
11. Ewing, A. G.; Mesaro, J. M.; Gavin, P. F. *Anal. Chem.* **1994**, *66*, 527A-537A.
12. Kristensen, H. K.; Lau, Y. Y.; Ewing, A. G. *J. Neurosci. Methods* **1994**, *51*, 183-188.
13. Ewing, A. G. *J. Neurosci. Methods* **1993**, *48*, 215-224.
14. Olefirowicz, T. M.; Ewing, A. G. *Chimia* **1991**, *45*, 106-108.
15. Olefirowicz, T. M.; Ewing, A. G. *J. Neurosci. Methods* **1990**, *34*, 11-15.
16. Olefirowicz, T. M.; Ewing, A. G. *Anal. Chem.* **1990**, *62*, 1872-1876.
17. Hoyt Jr., A. M.; Beale, S. C.; Larmann Jr., J. P.; Jorgenson, J. W. *J. Microcol. Sep.* **1993**, *5*, 325-330.
18. Chang, H. T.; Yeung, E. S. *Anal. Chem.* **1995**, *67*, 1079-1083.
19. Tong, W; Yeung, E. S., submitted for publication.
20. Galli, S. J.; Dvorak, A. M.; Dvorak, H. F. in *Progress in Allergy; Mast Cell Activation and Mediator Release*, Volume 34, 1984, S. Karger, Basel, Switzerland, pp. 28-31.
21. Lillard, S. J.; Yeung, E. S.; Lautamo, R. M. A.; Mao, D. T. *J. Chromatogr.* **1995**, *718*, 397-404.
22. Rohlich, P.; Anderson, P.; Uvnas, B. *J. Cell Biol.* **1971**, *51*, 465-483.
23. Moran, N. C.; Uvnas, B.; Westerholm, B. *Acta Physiol. Scand.* **1962**, *56*, 26-41.
24. Foreman, J. C.; Mongar, J. L.; Gomperts, B. D. *Nature*, **1973**, *245*, 249-251.
25. Helander, H. F.; Bloom, G. D. *J. Microsc.* **1973**, *100*, 315-321.
26. Lagunoff, D.; Martin, T. W. *Ann. Rev. Pharmacol. Toxicol.* **1983**, *23*, 331-351.
27. Kubesch, P.; Boggs, J.; Luciano, L.; Maass, G.; Tummler, B. *Biochemistry* **1987**, *26*, 2139-2149.
28. Schroder, G.; Brandenburg, K.; Seydel, U. *Biochemistry* **1992**, *31*, 631-638.
29. Liu, Y.-M.; Sweedler, J. V. *J. Am. Chem. Soc.* **1995**, *117*, 8871-8872.

30. Schwartz, L. B.; Austen, K. F. in *Progress in Allergy; Mast Cell Activation and Mediator Release*, Volume 34, 1984, S. Karger, Basel, Switzerland, pp. 271-321.
31. Alvarez de Toledo, G.; Fernandez-Chacon, R.; Fernandez, J. M. *Nature* **1993**, *363*, 554-558.
32. Alvarez de Toledo, G.; Fernandez, J. M. *J. Gen. Physiol.* **1990**, *95*, 397-409.
33. Monnig, C. A.; Jorgenson, J. W. *Anal. Chem.* **1991**, *63*, 802-807.

**SUPPORTING INFORMATION**

Video images (Fig. S1 and S2) are available from Professor Edward S. Yeung, Department of Chemistry, Iowa State University, Ames, IA 50011.

**Figure S1.** Time evolution of exocytosis in mast cells stimulated by Pmx. Photos are taken at 0.5 s intervals. See text for details. (24 video images available as disk TIFF files only.)

**Figure S2.** Time evolution of exocytosis in mast cells stimulated by Pmx. Photos are taken at 1/15 s intervals. A granule can be seen being released from the top of the cell at the left and carried away by the wash solution. See text for details. (6 video images available as disk TIFF files only.)

Figure S3A. Electropherogram of an individual RPMC (cell #4); expanded region between release and lysis events. Each mark on the ordinate corresponds to an identical signal intensity. See Table 1 for peak information.

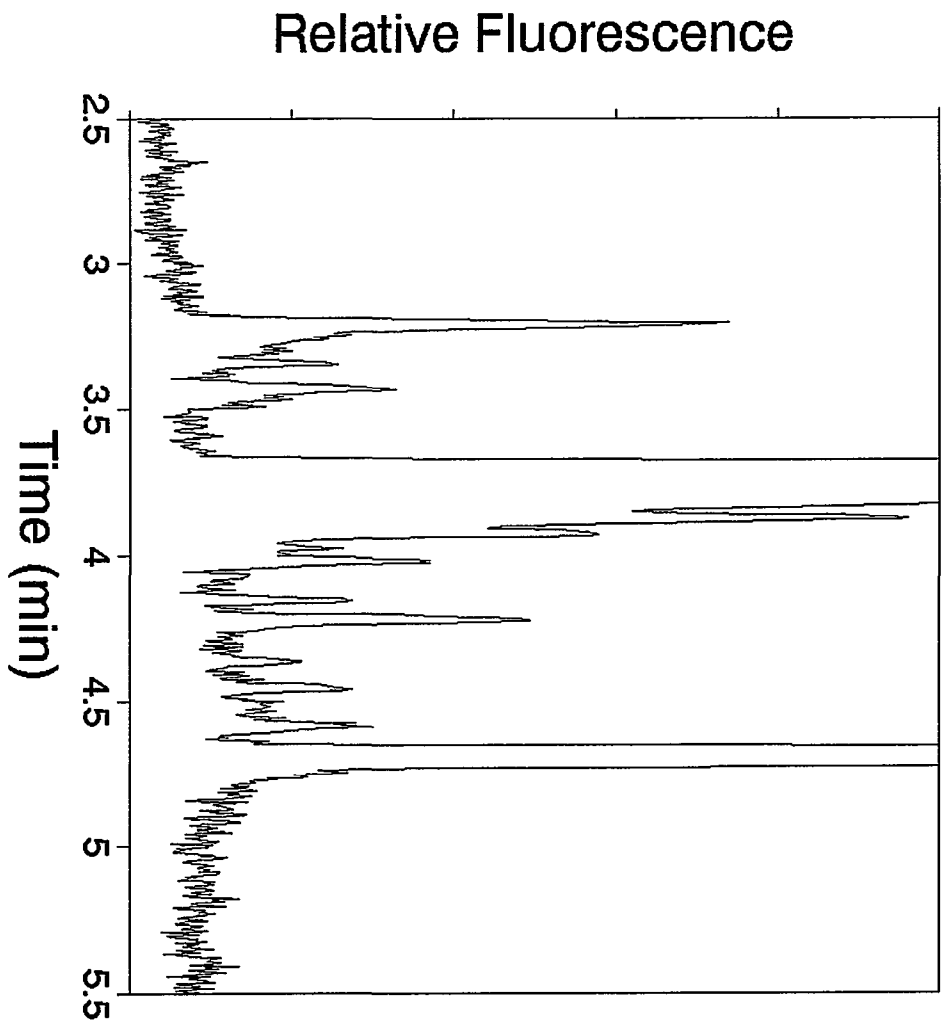


Figure S3B. Electropherogram of an individual RPMC (cell #4); protein region.



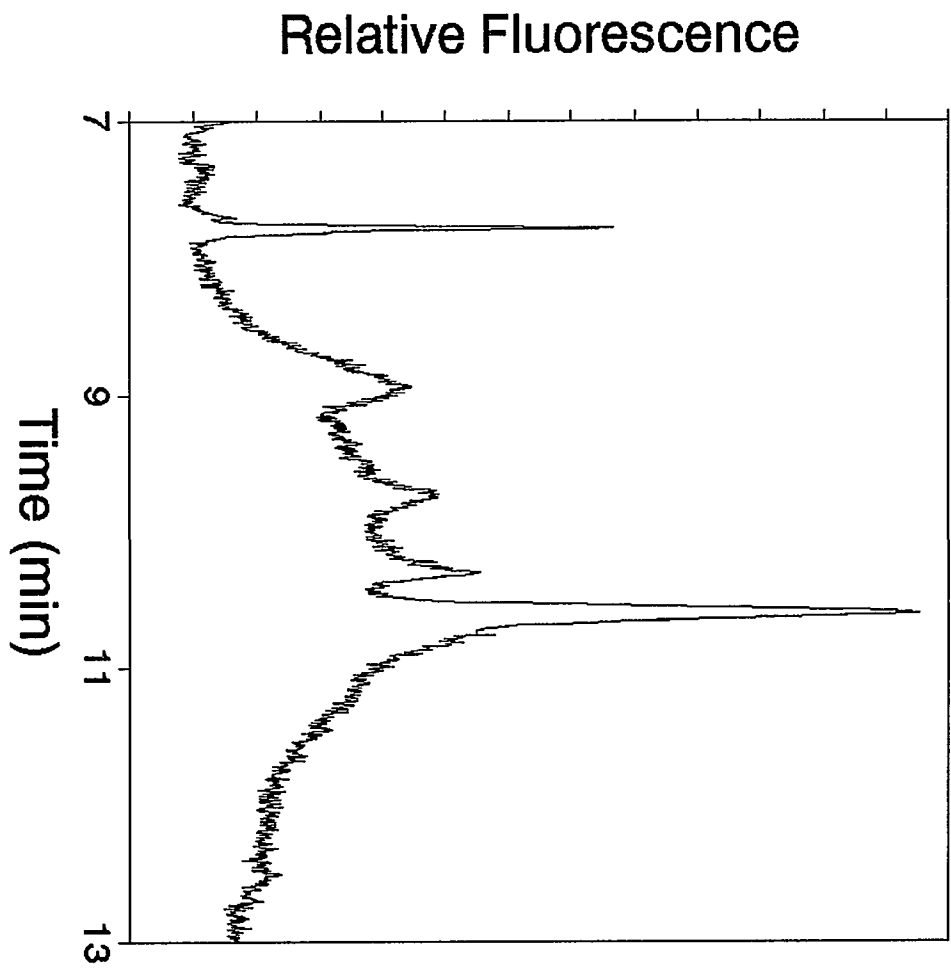


Figure S4A. Electropherogram of an individual RPMC (cell #6). See Fig. S3.

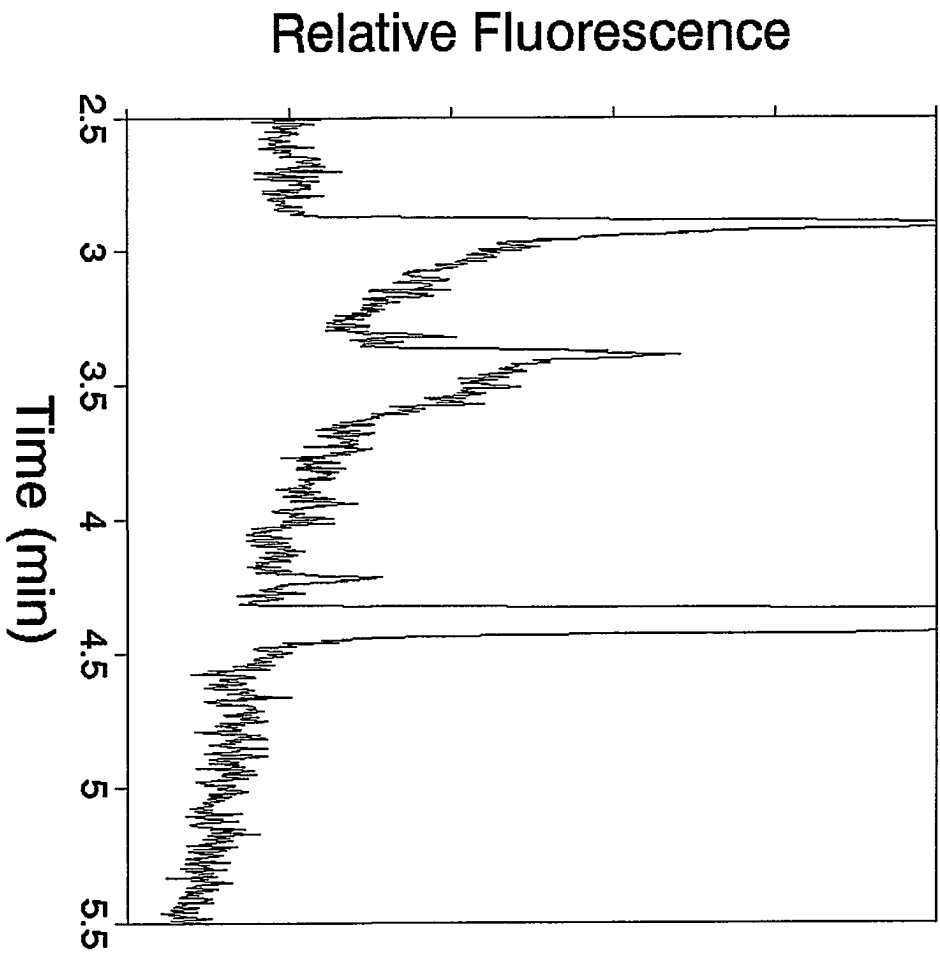


Figure S4B. Protein region (cell #6).

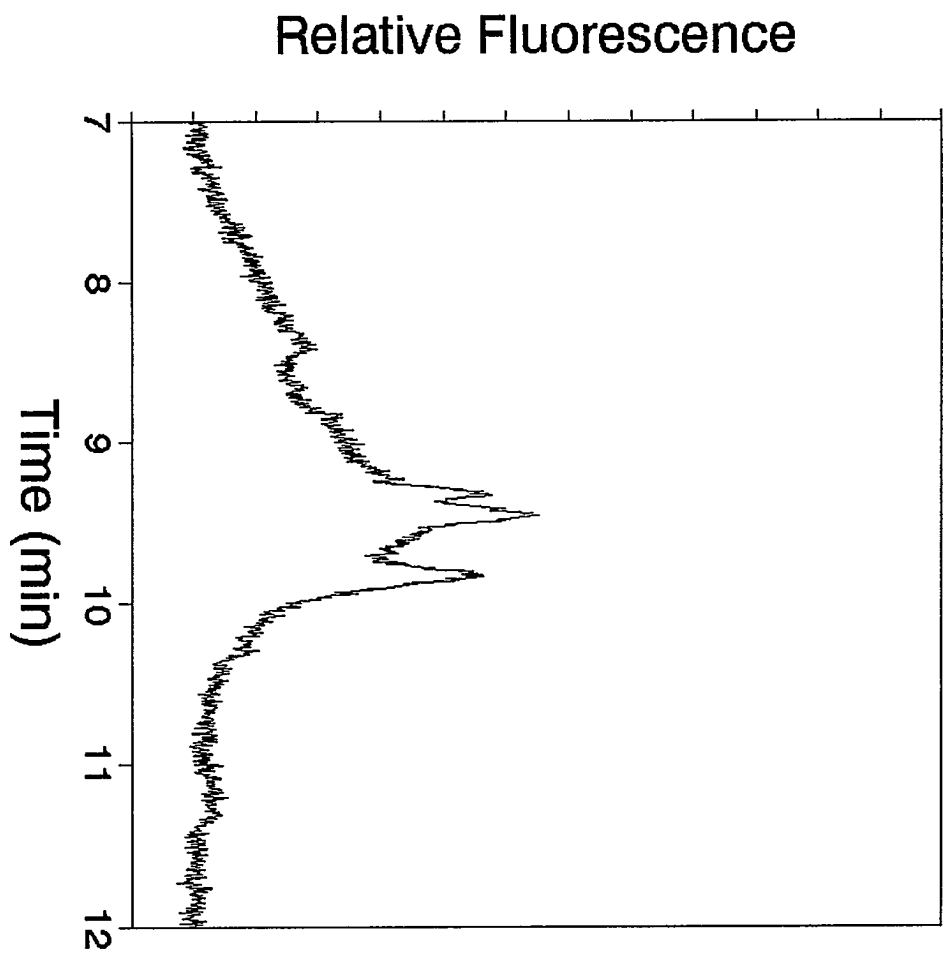


Figure S5A. Electropherogram of an individual RPMC (cell #7). See Fig. S3.

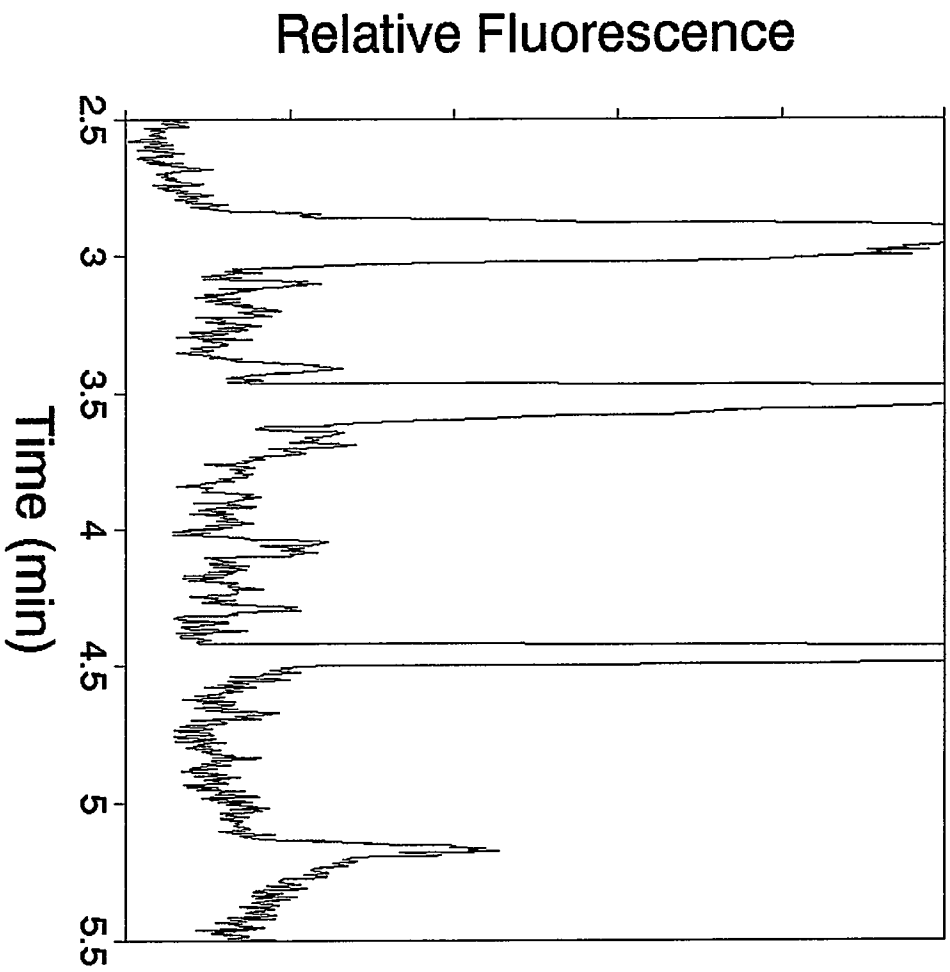


Figure S5B. Protein region (cell #7).



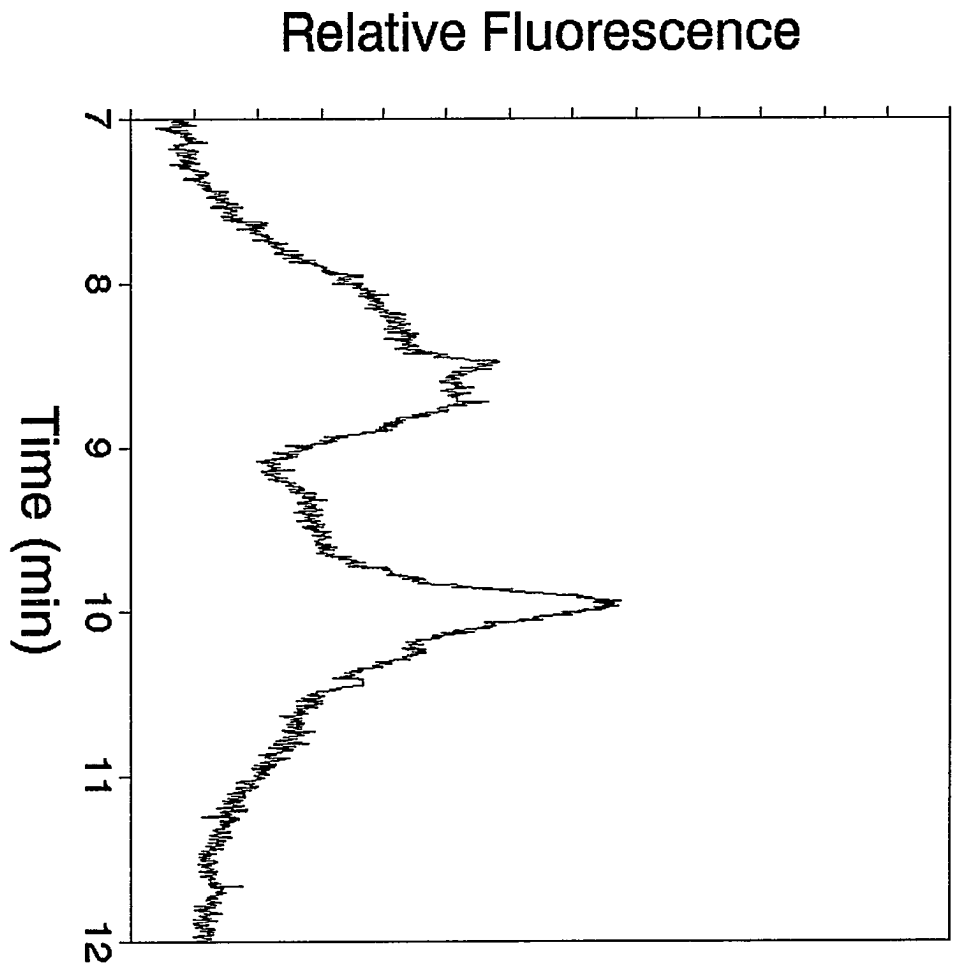


Figure S6A. Electropherogram of an individual RPMC (cell #8). See Fig. S3.

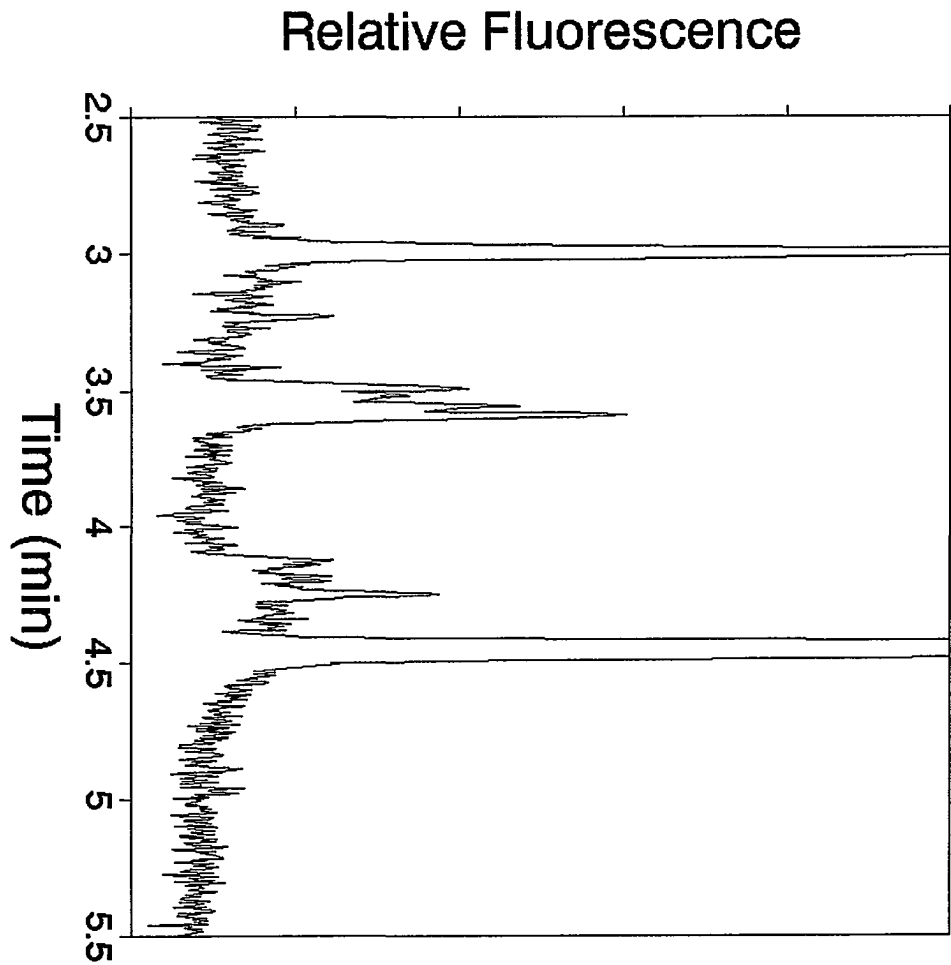


Figure S6B. Protein region (cell #8).

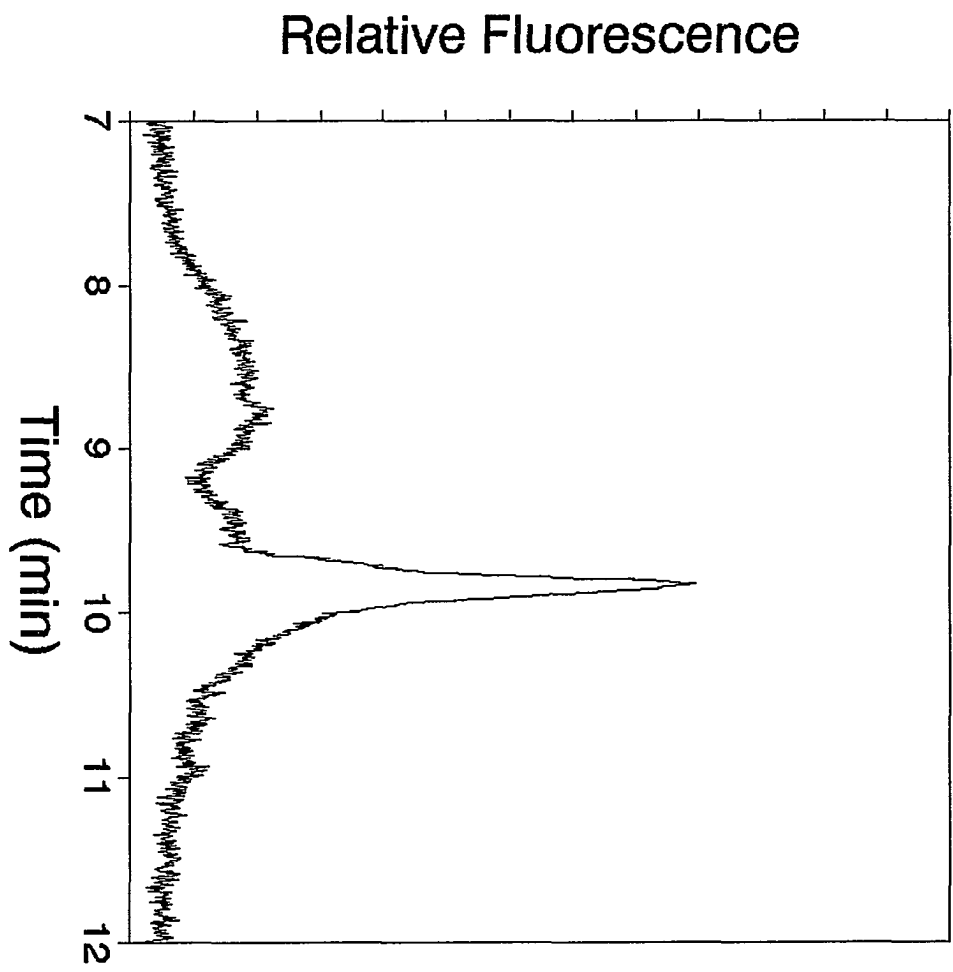


Figure S7A. Electropherogram of an individual RPMC (cell #9). See Fig. S3.

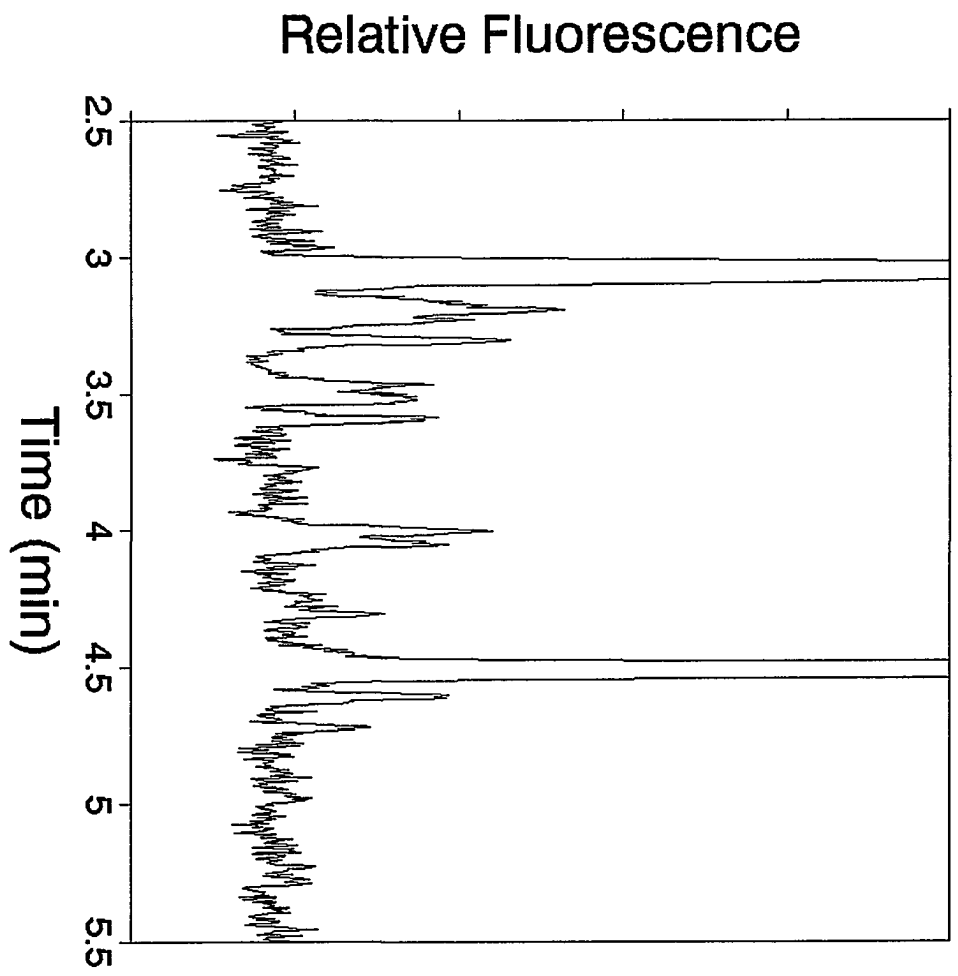


Figure S7B. Protein region (cell #9).



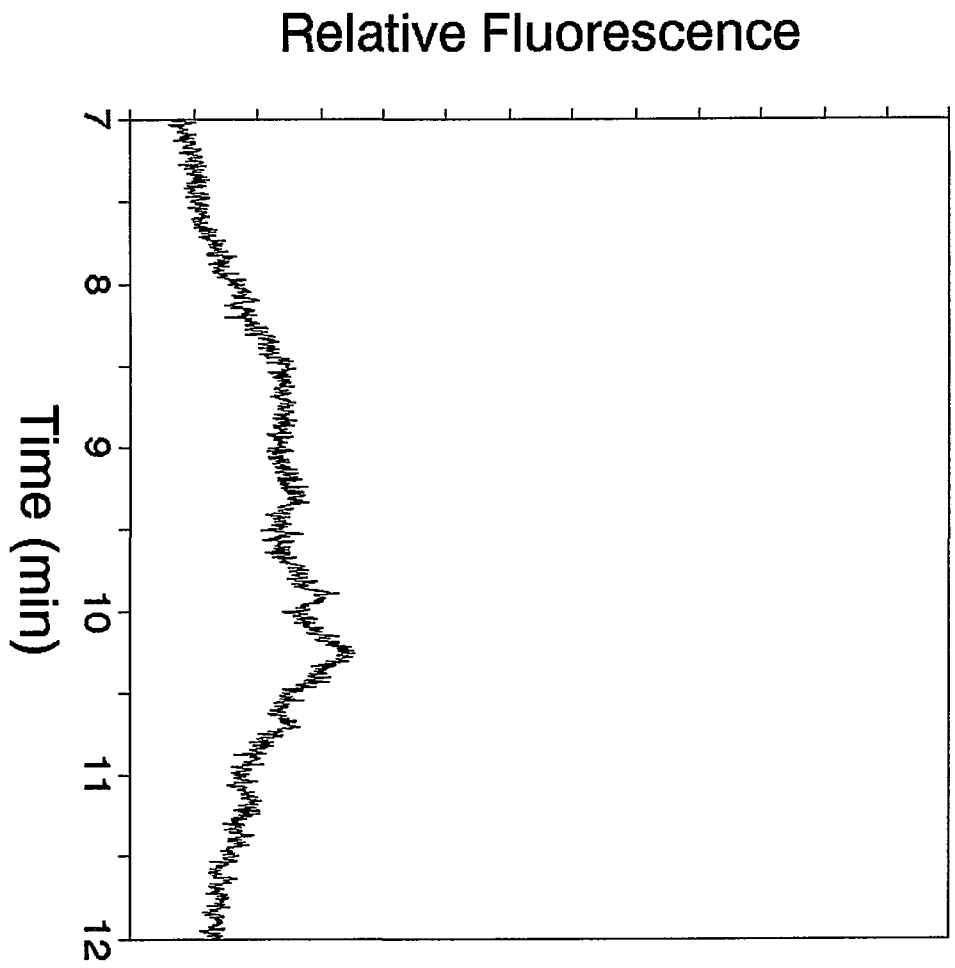


Figure S8A. Electropherogram of an individual RPMC (cell #10). See Fig. S3.

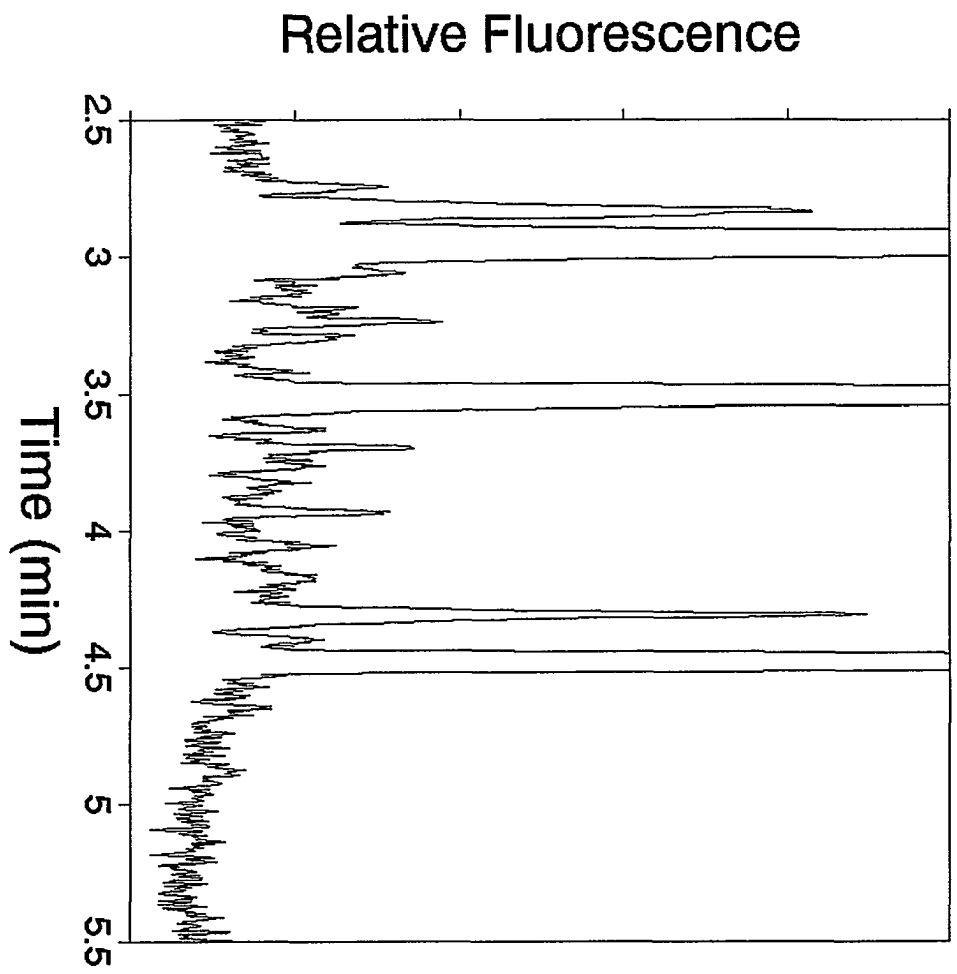


Figure S8B. Protein region (cell #10).

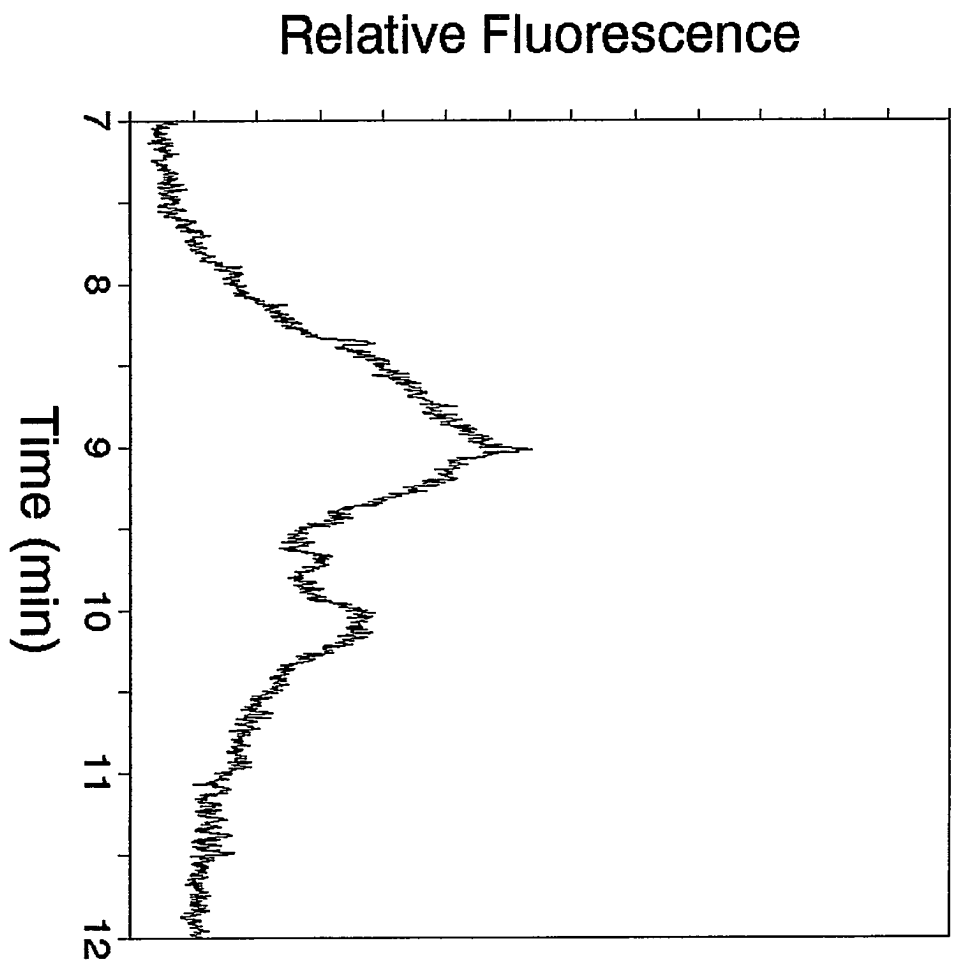


Figure S9A. Electropherogram of an individual RPMC (cell #11). See Fig. S3.

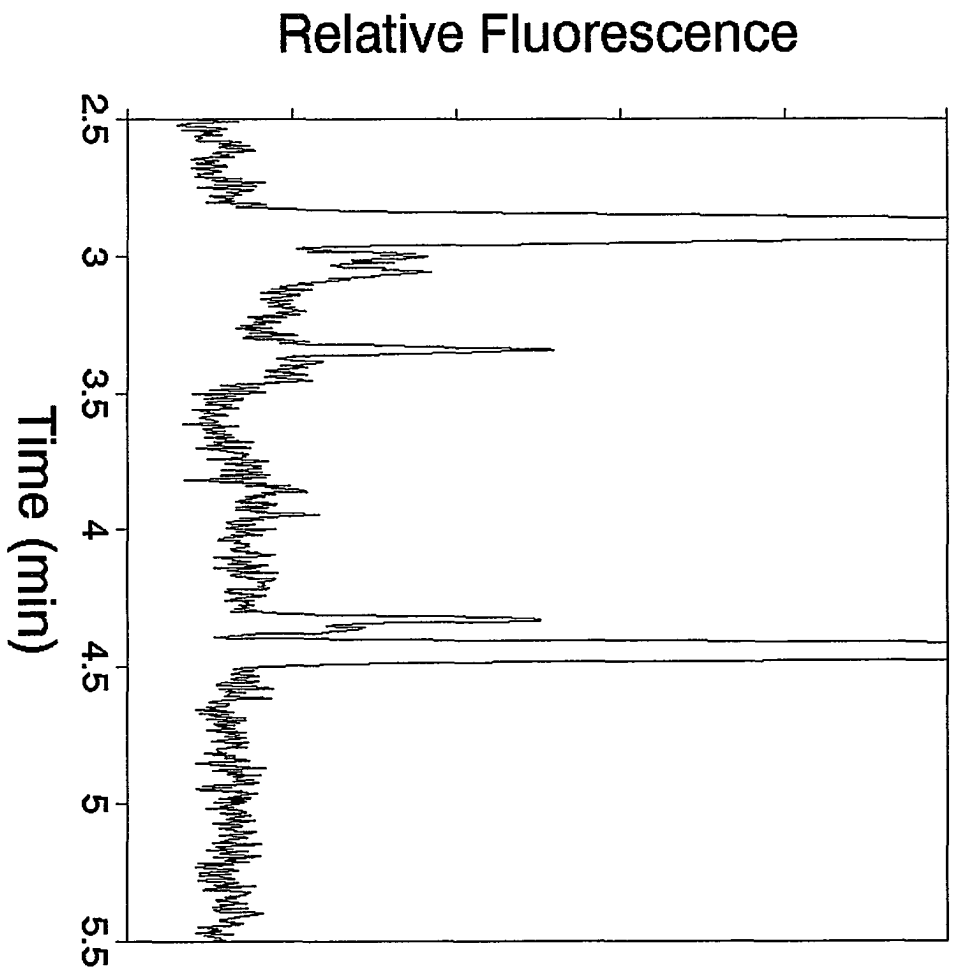


Figure S9B. Protein region (cell #11).



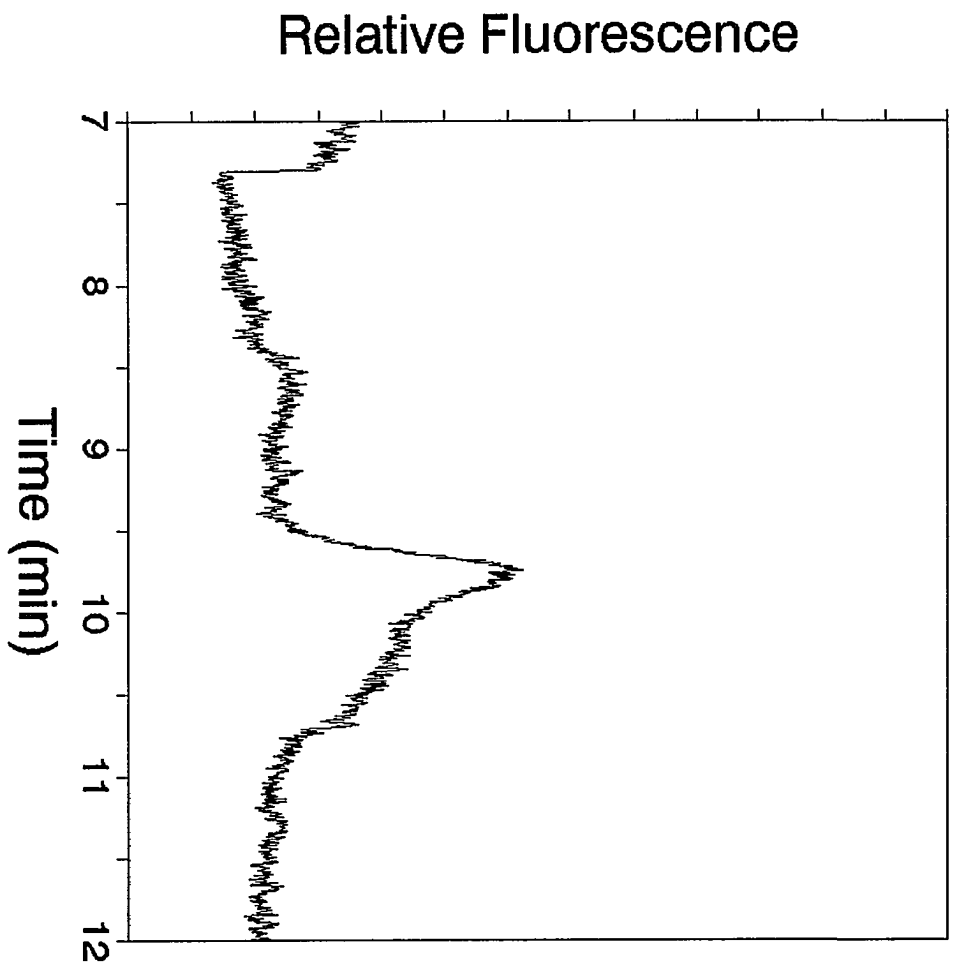


Figure S10A. Electropherogram of an individual RPMC (cell #12). See Fig. S3.

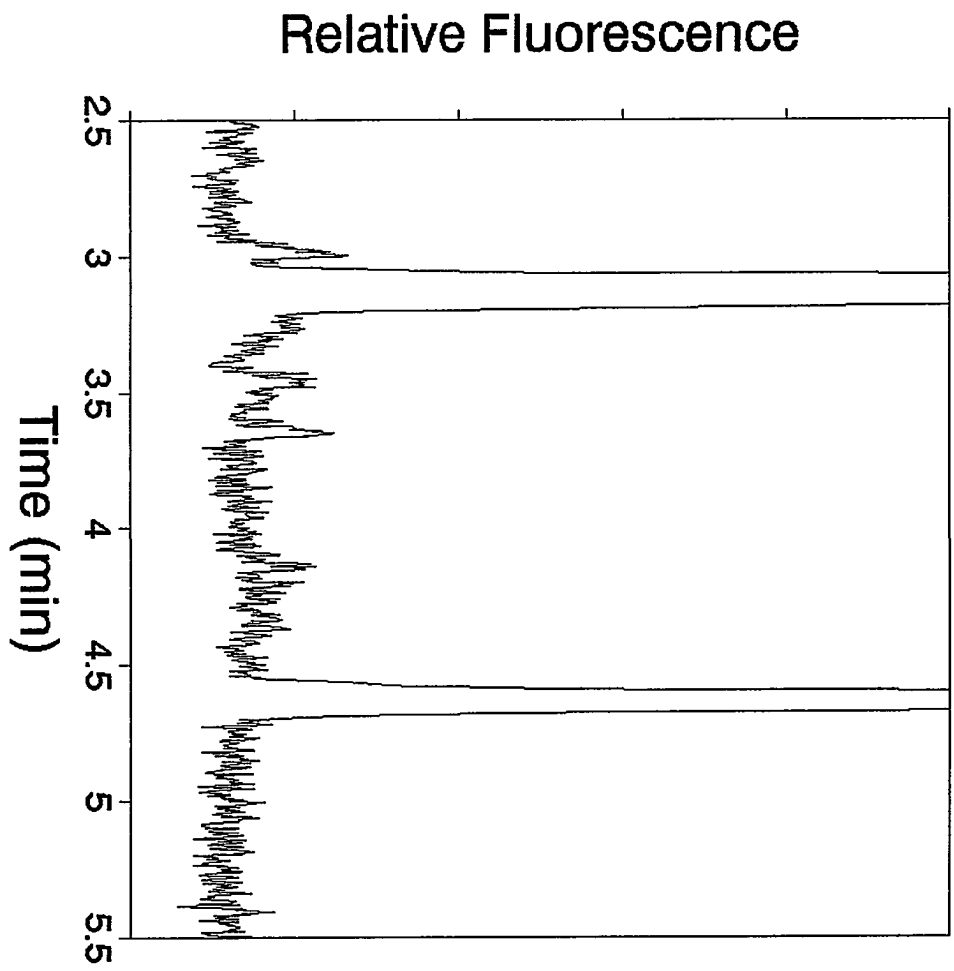


Figure S10B. Protein region (cell #12).

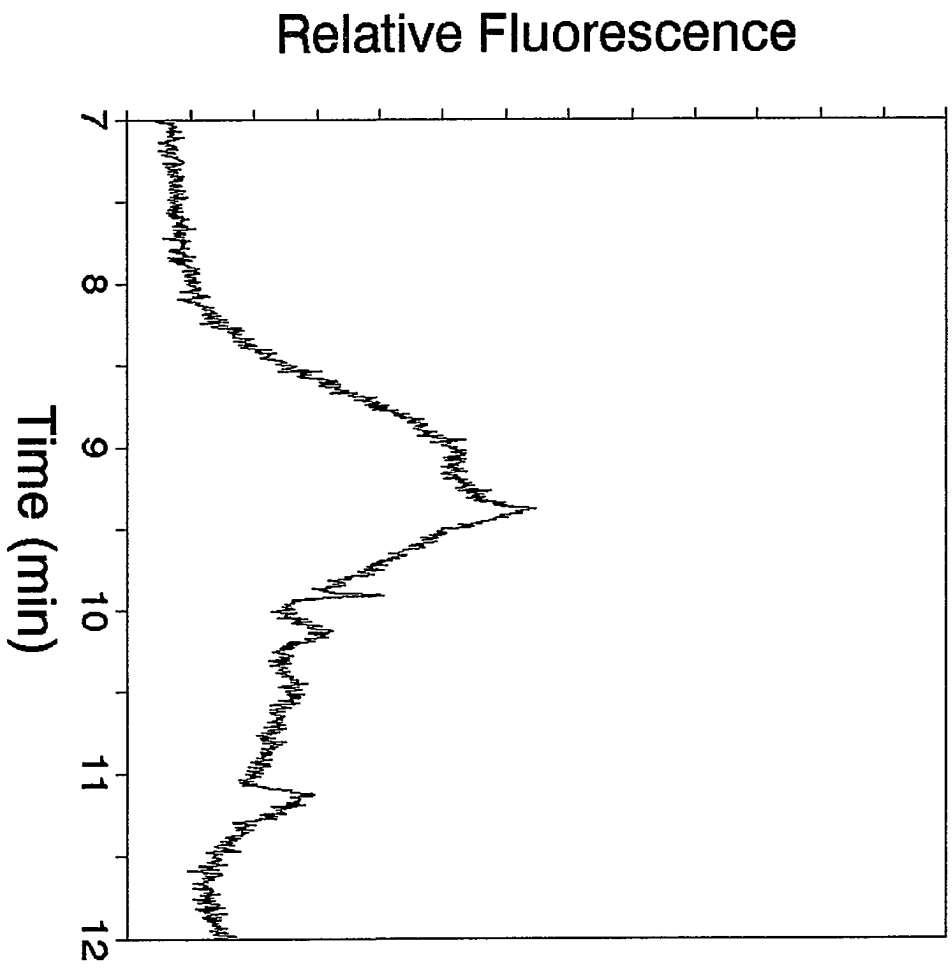


Figure S11A. Electropherogram of an individual RPMC (cell #1, Batch 2). See Fig. S3.

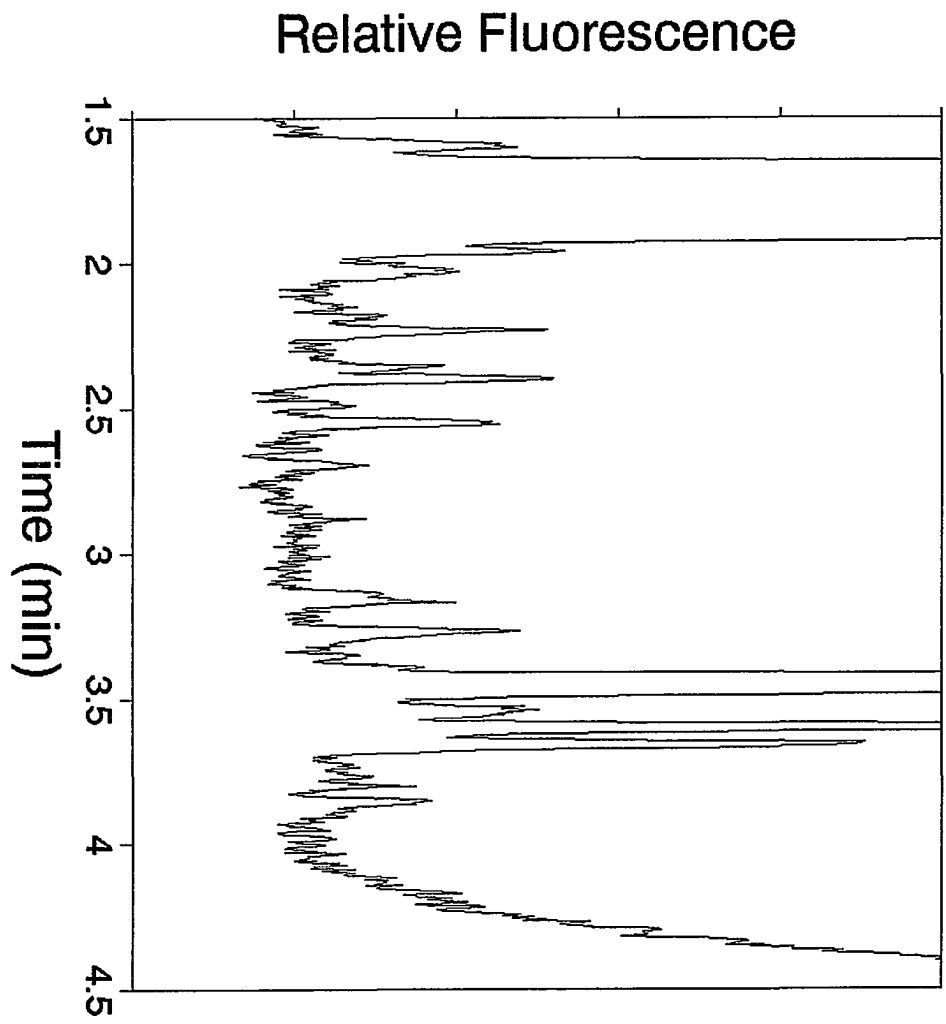


Figure S11B. Protein region (cell #1, Batch 2).



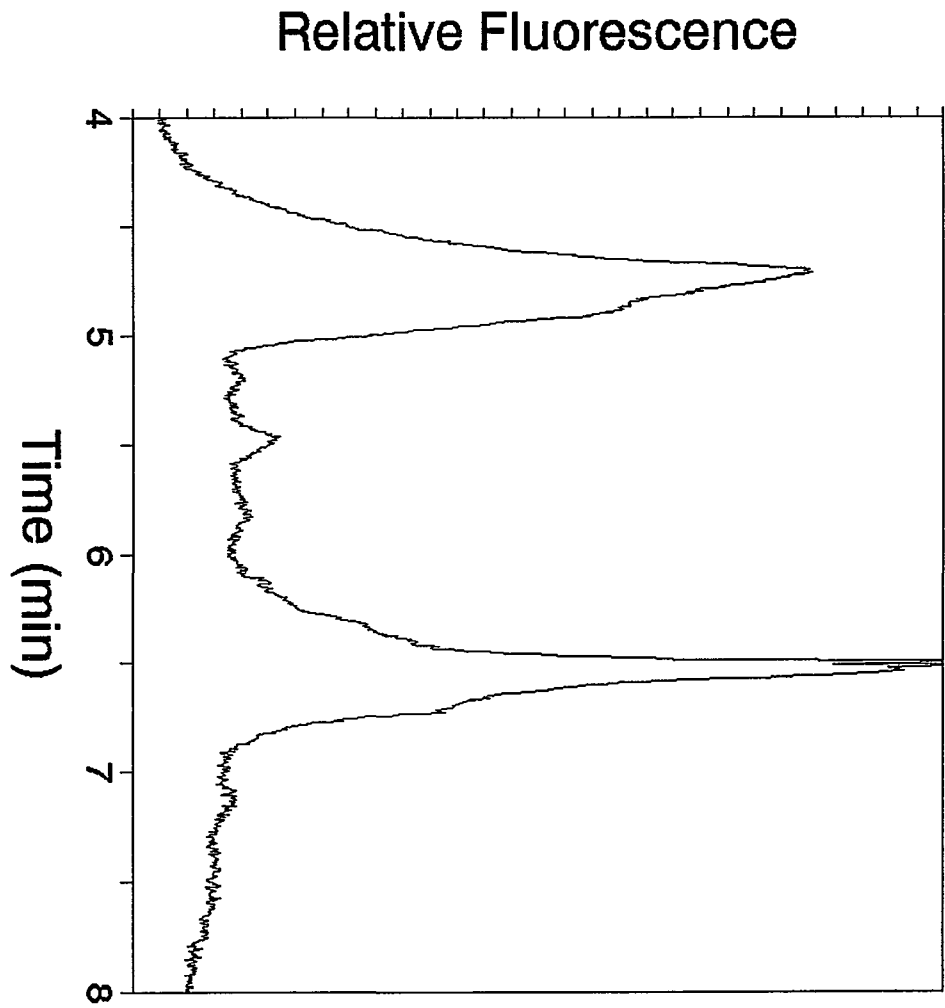


Figure S12A. Electropherogram of an individual RPMC (cell #2, Batch 2). See Fig. S3.

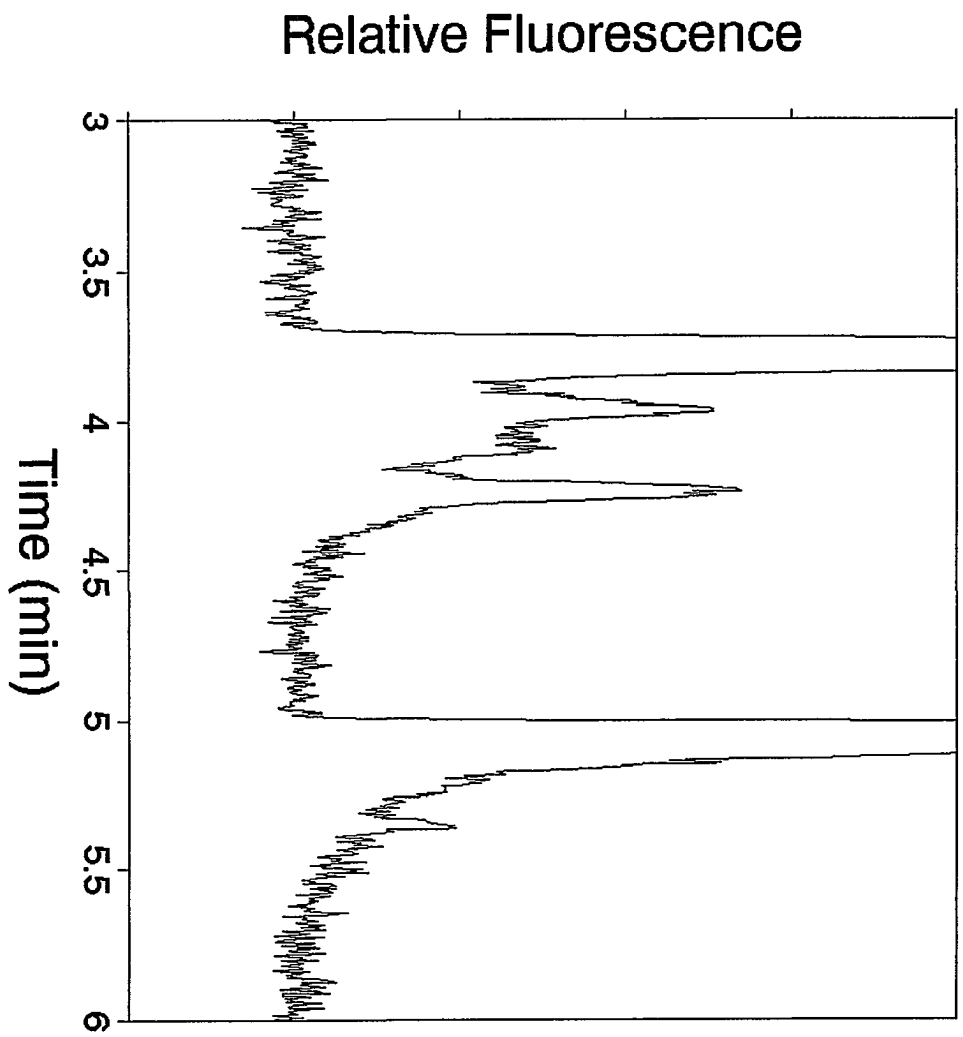


Figure S12B. Protein region (cell #2, Batch 2).

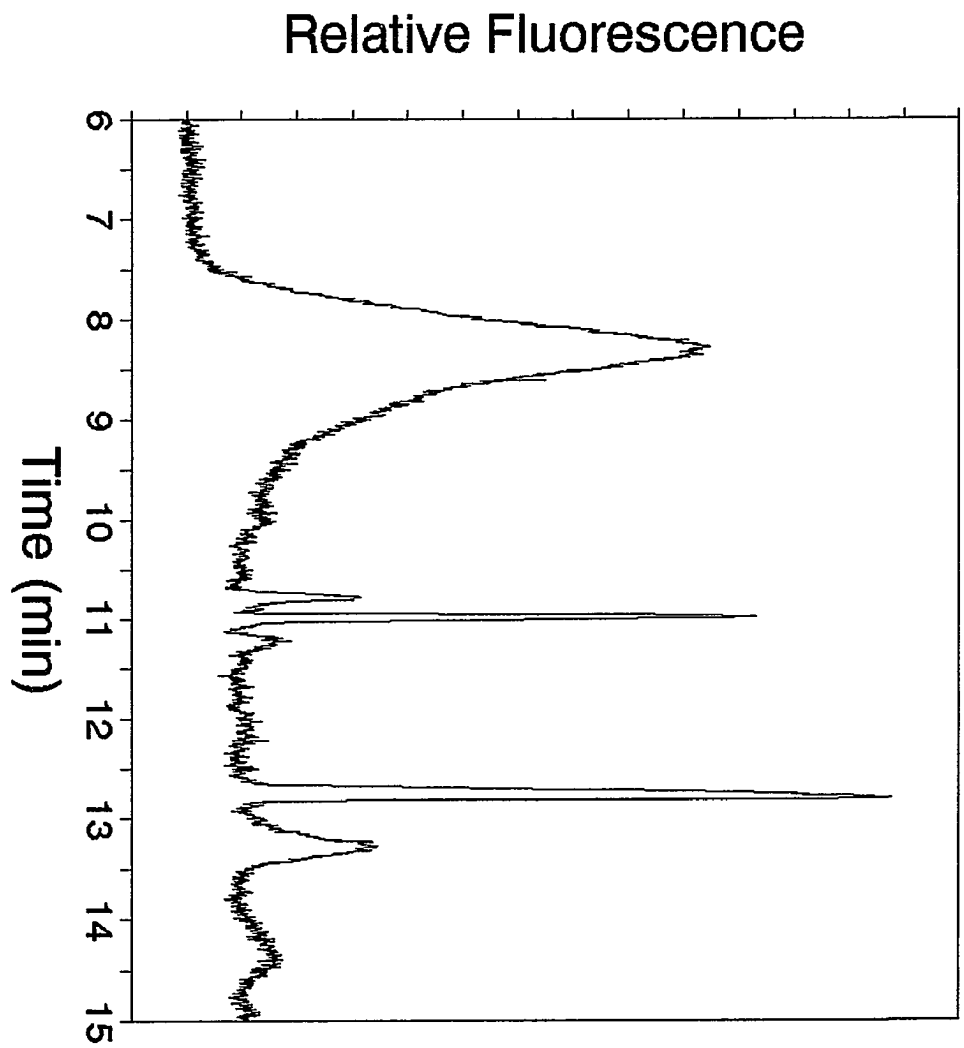


Figure S13A. Electropherogram of an individual RPMC (cell #3, Batch 2). See Fig. S3.

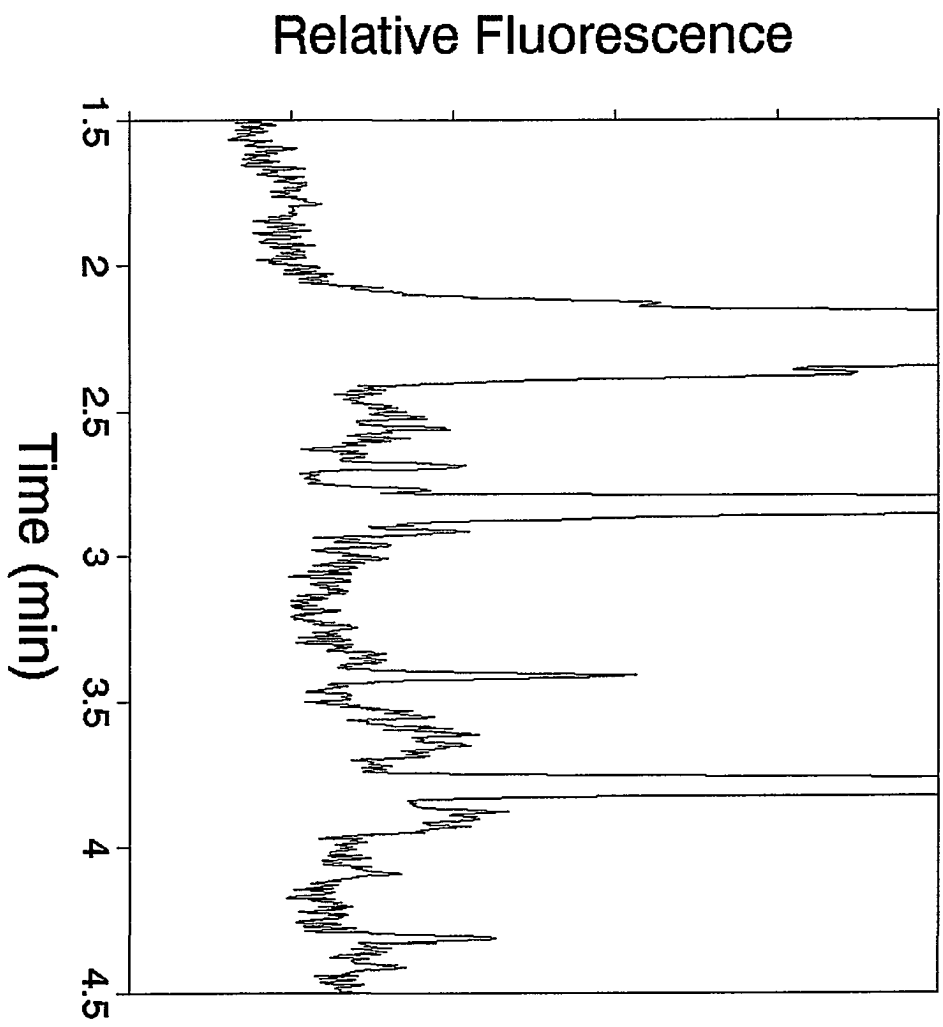
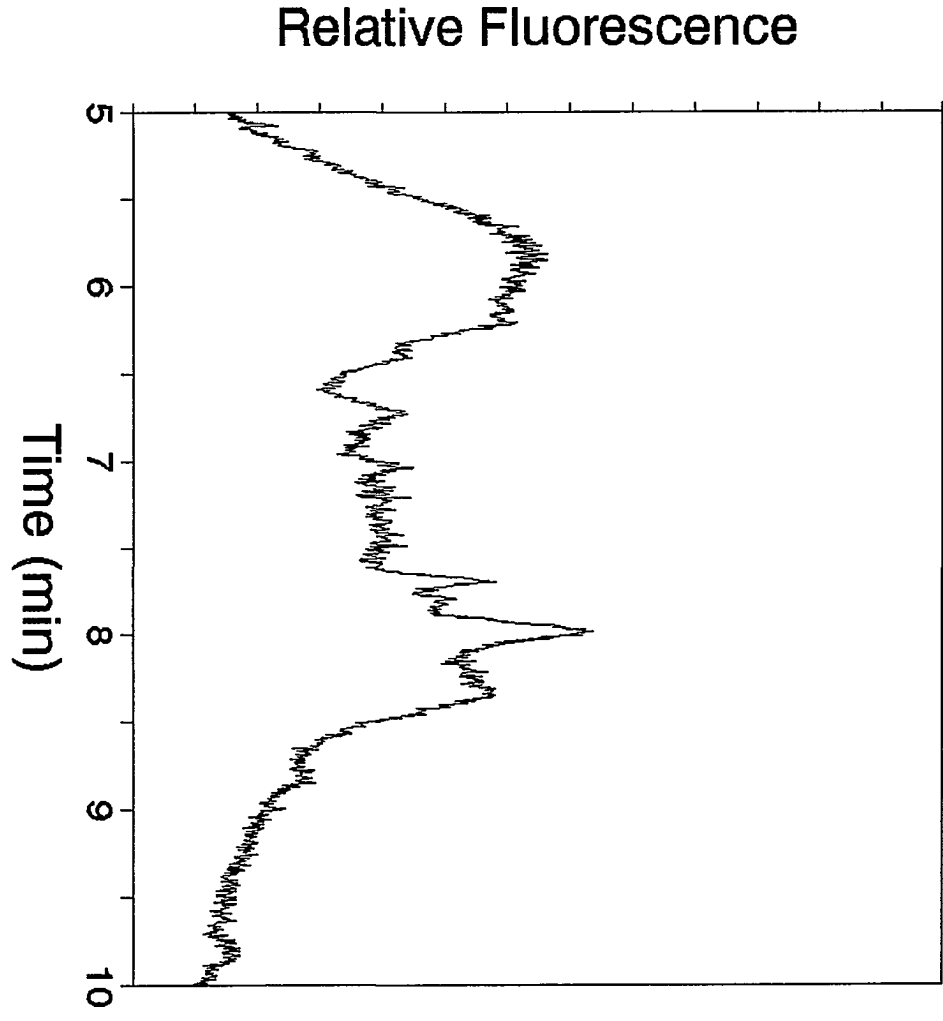


Figure S13B. Protein region (cell #3, Batch 2).





### GENERAL SUMMARY

The study of individual cells by capillary electrophoresis has emerged as a powerful technique by which important biochemical information can be obtained. There are certain requirements of any method used to analyze individual cells, and these are met by CE simply due to the nature of the technique. Parameters such as very low sample volumes, sensitive detection and high separation efficiencies are most notable when considering single cell analyses. There is no doubt that CE is a highly effective tool for this application, but what are the practical expectations and limitations of this method? How does its versatility fit into the needs of the biochemical community?

This dissertation has approached single cell analysis in a couple different ways. First, we have demonstrated variations of separation mode, thus showing that the separation step of analysis is not limited simply to capillary zone electrophoresis. We have shown that determining the amount of an intracellular component may be useful in early disease diagnosis--possibly as a complement to genetic analysis. Also, we can monitor exocytosis, which has important implications in the areas of neurochemistry and cell signaling.

Although single cell analysis by CE is still relatively new, in recent years it has been shown to be sufficiently versatile. Many different cell types, intracellular constituents, and detection schemes have been developed (as discussed in Chapter 1). Also, one can see the trend shifting, from simply detecting components in giant invertebrate cells, to quantitation of smaller mammalian intracellular components, to monitoring cellular dynamics. Novel detection methods--either completely new ones or creative variations of existing detectors--will continue to emerge and influence the types of cells that can be studied. Increasing cell throughput, by multiplexing or automation, will be a key step in obtaining the necessary statistics to demonstrate clearly early disease diagnosis based on a few abnormal cells. Along with this, incorporating biophysical measurements with the mentioned applications and improvements, will further expand the realm of single cell analysis. It will not be long before this technique shifts again from one which research labs can demonstrate, to one on which clinical labs rely.